

Calculations with spectroscopic accuracy: energies and transition rates in the nitrogen isoelectronic sequence from Ar XII to Zn XXIV

K. Wang^{1,2,3}, R. Si^{3,4}, W. Dang¹, P. Jönsson⁵, X.L. Guo^{3,4}, S. Li^{2,3,4}, Z.B. Chen⁶, H. Zhang², F. Y. Long², H.T. Liu², D.F. Li², R. Hutton^{3,4}, C.Y. Chen^{3,4}, and J. Yan^{2,7,8}

chychen@fudan.edu.cn

yan_jun@iapcm.ac.cn

¹*Hebei Key Lab of Optic-electronic Information and Materials, The College of Physics Science and Technology, Hebei University, Baoding 071002, China*

²*Institute of Applied Physics and Computational Mathematics, Beijing 100088, China*

³*Applied Ion Beam Physics Laboratory, Fudan University, Key Laboratory of the Ministry of Education, China*

⁴*Shanghai EBIT Lab, Institute of Modern Physics, Department of Nuclear Science and Technology, Fudan University, Shanghai 200433, China*

⁵*Group for Materials Science and Applied Mathematics, Malmö University, S-20506, Malmö, Sweden*

⁶*College of Science, National University of Defense Technology, Changsha 410073, China*

⁷*Center for Applied Physics and Technology, Peking University, Beijing 100871, China*

⁸*Collaborative Innovation Center of IFSA (CICIFSA), Shanghai Jiao Tong University, Shanghai 200240, China*

ABSTRACT

Combined relativistic configuration interaction and many-body perturbation calculations are performed for the 359 fine-structure levels of the $2s^22p^3$, $2s2p^4$, $2p^5$, $2s^22p^23l$, $2s2p^33l$, $2p^43l$, and $2s^22p^24l$ configurations in N-like ions from Ar XII to Zn XXIV. A complete and consistent data set of energies, wavelengths, radiative rates, oscillator strengths, and line strengths for all possible electric dipole, magnetic dipole, electric quadrupole, and magnetic quadrupole transitions among the 359 levels are given for each ion. The present work significantly increases the amount of accurate data for ions in the nitrogen-like sequence, and the accuracy of the energy levels is high enough to serve identification and interpretation of observed spectra involving the $n = 3, 4$ levels, for which the experimental values are largely scarce. Meanwhile, the results should be of great help in modeling and diagnosing astrophysical and fusion plasmas.

Subject headings: atomic data - atomic processes

1. INTRODUCTION

Spectra from L-shell ions, in a wide wavelength range from the X-ray to the ultraviolet, have been obtained from the solar atmosphere, stars, and other astronomical objects by many astrophysical missions, such as the *Solar and Heliospheric Observatory*, *Hinode*, *Chandra*, and *Solar Dynamics Observatory* (Brinkman et al. 2000; Landi et al.

2002; Raassen et al. 2002; Curdt et al. 2004; Ishibashi et al. 2006; Brown et al. 2008; Del Zanna 2008, 2012; Warren et al. 2008; Del Zanna & Andretta 2011; Del Zanna & Woods 2013; Beiersdorfer et al. 2014; Träbert et al. 2014a,b). The analysis of the observed spectra provides information on the structure, chemical abundances, evolution, and physical conditions of the astrophysical objects. Such an analysis requires a wide range of atomic

parameters, such as energy levels and radiative transition properties (Kallman & Palmeri 2007; Massacrier & Artru 2012; Del Zanna & Woods 2013; Beiersdorfer et al. 2014; Nave et al. 2015). In view of this, we have already reported the systematic and highly accurate calculations for the beryllium and carbon isoelectronic sequences (Wang et al. 2014, 2015). This work presents our effort on the nitrogen isoelectronic sequence from Ar XII to Zn XXIV. Numerous lines of the above N-like ions have been observed in astrophysical plasmas, as well as in laboratory plasmas (Feldman et al. 1980, 1997; McKenzie et al. 1980b; Doschek et al. 1981; Eidelsberg et al. 1981; Phillips et al. 1982, 1983; Doschek & Cowan 1984; Lawson & Peacock 1984; Acton et al. 1985; Seely et al. 1986; Doyle 1987; Fawcett et al. 1987; Lippmann et al. 1987; Brosius et al. 1998; Feldman et al. 2000; Mewe et al. 2001; Curdt et al. 2001; Behar et al. 2001; Brown et al. 2002; Kaastra et al. 2002; Ko et al. 2002; Lepson et al. 2003; Mohan et al. 2003; Ness et al. 2003; Curdt et al. 2004; Feldman et al. 2004; Landi & Phillips 2005, 2006; Parenti et al. 2005; Chen et al. 2007; Del Zanna 2008, 2012; Gu et al. 2007; Shestov et al. 2008; Beiersdorfer et al. 2014; Träbert et al. 2014a,b).

Many theoretical efforts have been devoted to studying energy levels and transition characteristics in N-like ions. Most of the systematic calculations, such as Godefroid & Fischer (1984); Becker et al. (1989); Merkelis et al. (1997, 1999); Gu (2005a) and Rynkun et al. (2014), were limited to a few transitions among the 15 fine-structure levels of the $(1s^2)2s^22p^3$, $2s2p^4$, and $2p^5$ configurations (the $n = 2$ complex).

To our knowledge, there were no systematic calculations beyond the $n = 2$ states along the isoelectronic sequence, except for one calculation performed by Tachiev & Froese Fischer (2002). Using the multiconfiguration Hartree-Fock method with relativistic corrections in the Breit-Pauli approximation (MCHF-BP), they computed energies and transition data for the levels up to $2s^22p^23d$ in N-like ions with $Z = 7 - 17$. However, a few calculations have been carried out for selected individual ions. Bhatia et al. (1989); Eissner et al. (2005) and Landi & Bhatia (2005) reported both the $n = 2$ and $n = 3$ results of Ar XII, Ca XIV, Ti XVI, Fe XX, Zn XXIV, and Kr XXX using the SUPERSTRUCTURE (SS) code (Eissner et al. 1974). The energy levels and radiative decay

rates for the transitions involving the $n \geq 3$ levels in Fe XX were calculated using various methods. The calculations include the BreitPauli R-matrix (BPRM) calculations and the configuration interaction calculations using the SS code by Nahar (2004), the multiconfiguration Dirac-Hartree-Fock (MCDHF) calculations by Jonauskas et al. (2005), the results of Witthoef et al. (2007) using the AUTOSTRUCTURE (AS) code (Badnell 1986). Dong et al. (2012) employed the MCDHF method in the GRASP package (Dyall et al. 1989) to calculate level energies and radiative rates among the transitions for the 272 levels of the $n = 2, 3$ levels in Ca XIV. Energy levels and radiative data for the transitions up to the $n = 10$ levels in Sc XV were provided by Massacrier & Artru (2012) using the FAC code (Gu 2003, 2008). A combined relativistic configuration interaction (RCI) and many-body perturbation theory (MBPT) approach was used by Gu (2005b) to obtain the level energies for the $2l^5$ and $2l^43l'$ configurations in Fe XX and Ni XXII with high accuracy.

Among the above calculations for N-like ions, the results for the $n = 2$ states reported by Rynkun et al. (2014) and Gu (2005a), and the data for the $n = 2, 3$ levels obtained by Gu (2005b) in Fe XX and Ni XXII are so far the most accurate. In contrast with the accurate values (Rynkun et al. 2014; Gu 2005a,b), all the other mentioned calculations involving the $n \geq 3$ complexes for highly charged N-like ions from Ar XII to Zn XXIV are quite inaccurate due to limited configuration interaction effects included in their works. For instance, the energies of the SS calculations (Bhatia et al. 1989; Eissner et al. 2005; Landi & Bhatia 2005) for five ions from Ar XII to Zn XXIV deviate from the corresponding observations by up to 5%, which may be outdated for line identification and plasma diagnostics. In terms of theoretical works, Fe XX is currently the most studied ion in the nitrogen isoelectronic sequence so far. The deviations from the observed energies are up to 3.4% for the BPRM calculations (Nahar 2004), 2.2% for the MCDHF values (Jonauskas et al. 2005), and 4.3% for the AS results (Witthoef et al. 2007), which are far from the spectroscopic accuracy. Therefore, systematic calculations of high quality involving states beyond the $n = 2$ configurations are greatly desired, because of their im-

portance in modeling and diagnosing of astrophysical plasmas (Phillips et al. 1982; Acton et al. 1985; Del Zanna 2008; Beiersdorfer et al. 2014) and laboratory plasmas (Fawcett & Hayes 1975). Databases such as CHIANTI (Dere et al. 1997; Landi et al. 2013) also demand complete and consistent data sets of high accuracy, with the view of offering the astrophysical community tools and data to carry out accurate plasma diagnostics.

Recently, Radžiūtė et al. (2015) reported calculated energies and radiative transition properties for the 272 states of the $2s^22p^3$, $2s2p^4$, $2p^5$, $2s^22p^23l$, $2s2p^33l$, and $2p^43l$ ($l = 0, 1, 2$) configurations in N-like ions Cr XVIII, Fe XX, Ni XXII and Zn XXIV by using the MCDHF and RCI method implemented in the GRASP2K code (Jönsson et al. 2013; Jönsson et al. 2007). Comparing with the calculations of Rynkun et al. (2014) who used the same method while only reported the results for the $n = 2$ complex, Radžiūtė et al. (2015) adopted much larger configuration state function expansions and considered the electron correlation effects elaborately for both the $n = 2$ and $n = 3$ levels. Therefore, high accuracy was achieved in their calculations, which was in general at the same level with the accuracy of the calculations performed by Rynkun et al. (2014) and Gu (2005a,b), and the data can be used to identify observed spectral lines.

In the present work, we report energy levels and transition properties for all possible electric dipole (E1), magnetic dipole (M1), electric quadrupole (E2), and magnetic quadrupole (M2) transitions among the 359 levels of the $2s^22p^3$, $2s2p^4$, $2p^5$, $2s^22p^23l$, $2s2p^33l$, $2p^43l$, and $2s^22p^24l$ configurations in the N-like ions with $18 \leq Z \leq 30$, in an effort to offer complete and consistent data sets of high accuracy. A combined RCI and MBPT approach implemented in the FAC code (Gu 2003, 2005a,b; Gu et al. 2006) is used, in which both dynamic and nondynamic electron correlation effects could be well accounted for. For the purpose of assessing the present MBPT results, extensive MCDHF and RCI calculations (hereafter referred to as MCDHF/RCI) for Fe XX have been carried out using the latest version of GRASP2K code (Jönsson et al. 2013). Comparisons are made between the present MCDHF/RCI and MBPT results, as well as with available observed data and theoretical values. The MBPT

calculated energies agree well with the observed values from the Atomic Spectra Database (ASD) of the National Institute of Standards and Technology (NIST) (Kramida et al. 2014), i.e., a difference is within 0.2% for all levels. The present calculations are generally more accurate than existing systematic calculations, and stand for a significant extension of the MBPT work reported by Gu (2005b) and the MCDHF/RCI results performed by Radžiūtė et al. (2015) to include data for the other nine ions in the range of Ar XII to Zn XXIV. We hope that the present data should be of great help in analyzing older experiments and planning new ones. Meanwhile, complete data sets will be useful in the identification of observed spectra, as well as in modeling and diagnosing of astrophysical and fusion plasmas.

2. Calculations and Results

A combined RCI and MBPT approach (Lindgren 1974; Safronova et al. 1996; Vilkas et al. 1999) was implemented within the FAC code by Gu (2005a,b). In the present work, we employ the improved implementation by Gu et al. (2006), in which the Hamiltonian is taken to be the no-pair Dirac–Coulomb–Breit Hamiltonian H_{DCB} . The key feature of the RCI and MBPT approach is to partition the Hilbert space of the system into two subspaces, i.e., a model space M and an orthogonal space N . The true eigenvalues of H_{DCB} can be obtained through solving the eigenvalue problem of a non-Hermitian effective Hamiltonian in the model space M . The first-order perturbation expansion of the effective Hamiltonian within the Rayleigh–Schrödinger scheme consists of two parts: one is the exact H_{DCB} matrix in the model space M , and the other includes perturbations from the configurations in the N space up to the second order for the level energies of interest. In the present calculations, the model space M contains all of the configurations $2l^4nl'$ ($2 \leq n \leq 3$ and $l' \leq n - 1$) and $2s^22p^24l'$ ($l' = 0 - 3$). The N space contains all configurations formed by single and double virtual excitations of the M space. For single excitations, configurations with $n \leq 200$ and $l \leq \min(n - 1, 25)$ are included. For double excitations, configurations with the inner electron promotion up to $n = 65$ and promotion of the outer electron up to $n' = 200$ are considered.

We start the energy structure calculations for N-like ions using an optimized local central potential, which is derived from a Dirac–Fock–Slater self-consistent field calculation with the $(2s, 2p)^5$ configurations. We then perform the MBPT calculations to obtain level energies and radiative transition properties, such as transition wavelengths, line strengths, oscillator strengths and radiative rates of all E1, M1, E2, and M2 transitions among the states in the M space using the length form. In addition to the Hamiltonian H_{DCB} , several high-order corrections, such as the finite nuclear size, nuclear recoil, vacuum polarization (VP), and electron self-energy (SE), are also taken into account in the calculations.

Table 1 lists our energies (in eV) of the 359 levels for each ion, as well as the observed results from the NIST ASD (Kramida et al. 2014). Also listed in Table 1 is the symmetry J^π of the state, i.e., the parity π and total angular momentum J . For each state in each ion, an index number j/i is assigned, which can be used in Table 2 to represent the upper (j) or lower (i) levels of the radiative transition. The wavelength (λ_{ji} in Å), line strength (S_{ji} in atomic units, $1 \text{ AU} = 6.460 \times 10^{-36} \text{ cm}^2 \text{ esu}^2$), oscillator strength (f_{ji} dimensionless) and radiative rate (A_{ji} in s^{-1}) for all possible E1, M1, E2, and M2 transitions among the 359 levels, are listed in Table 2.

In a large-scale calculation, it is difficult to label unambiguously all of the states. Using the LSJ - or jj coupling schemes, the identifications and the corresponding configurations can be determined clearly for a majority of the states listed in Table 1. However, in the symmetry of $3/2^\circ$ in $2s^2 2p^2 np$ configurations and $3/2^\circ$ in $2s^2 2p^2 nd$ configurations, the identifications of some states are not unique. The dominant components of the configuration basis for each state in both the LSJ - and jj coupling schemes are also given for each state in Table 1 to help to remove these ambiguities. The jj notation is given directly by the MBPT calculations, and the LSJ - notation is obtained using the $jj \rightarrow LSJ$ - transformation presented by Gaigalas et al. (2004).

For assessing the accuracy of the MBPT results, extensive MCDHF and subsequent RCI calculations are performed for Fe XX using the GRASP2K code (Jönsson et al. 2013). In the MCDHF method, the Hamiltonian is taken to be

Dirac–Coulomb Hamiltonian H_{DC} . The atomic state functions (ASFs) are approximated by expansions over jj -coupled configuration state functions (CSFs). Based on equal level weights of several states, the so called extended optimal level (EOL) scheme (Dyall et al. 1989), both the radial parts of the Dirac orbitals and the expansion coefficients were optimized to self-consistency in the relativistic self-consistent field procedure. In the subsequent RCI calculation (McKenzie et al. 1980a), the Breit interaction is computed in the low-frequency limit by multiplying the frequency with a scale factor of 10^{-6} , and the other small corrections such as finite nuclear size, nuclear recoil, VP and SE, are also included.

In the present MCDHF/RCI calculations, the configurations in the M space of the above MBPT calculations are split up into the even and odd groups, and are chosen as the reference configurations. Then the multi-configuration expansions are obtained through single and double excitations of the orbitals in the reference configurations with orbitals in an active set with principal quantum numbers $n = 3, \dots, 7$ and angular symmetries s, p, d, f, g , and h . To monitor the convergence of the calculated energies and transition parameters, the active sets were increased in a systematic way by adding layers of orbitals. For the $n = 7$ expansion this resulted in 1182541 CSFs with odd parity and 1150043 CSFs with even parity. The self-consistent field calculations for each layer of orbitals are followed by the RCI calculations. A more detailed description of the calculation procedure could be found in our very recent work for Mg-like Cu XVIII and Kr XXV (Si et al. 2015a,b).

3. Comparisons

Employing the MBPT approach, we have carried out systematic and highly accurate calculations for energy levels and transition rates of the beryllium and carbon isoelectronic sequences (Wang et al. 2014, 2015). We now focus our attention on the nitrogen isoelectronic sequence, and our work greatly increases accurate results for nitrogen-like ions in quantity. The accuracy of our MBPT results will be accessed, in the following, by comparing with available observed values, as well as with other elaborate/systematic calculations.

3.1. Energy Levels

Our MBPT values agree well with the NIST observations for all the 182 $n = 2$ states of the thirteen ions considered here, i.e., the differences are within 0.1% for 157 levels, and are between 0.1% and 0.2% for the remaining 25 levels. The previous theoretical results, including the MBPT calculations reported by Gu (2005a, hereafter referred to as MBPT2) and the MCDHF and RCI calculations performed by Rynkun et al. (2014, MCDHF/RCI2), are so far the most accurate in the sequence, when compared with the observed values. The relative differences between calculations and observations are within 0.1% for 150 levels in MBPT2, and 138 levels in MCDHF/RCI2. The deviations are larger than 0.2% for 7 levels (up to 0.3% for $2s^2 2p^3 \ ^2P_{3/2}$ in Ar XII) in MBPT2, and 14 levels (up to 0.34% for $2s^2 2p^3 \ ^2D_{3/2}$ in Ca XIV) in MCDHF/RCI2. Comparing with the MBPT2 and MCDHF/RCI2 calculations, a general better agreement of the NIST values and our results is attained due to more effectively electron correlation effects included within our work by considering more configurations in both the N and M spaces.

Recently, using the MCDHF and RCI method Radziūtė et al. (2015) reported the energies and transition rates for the 272 states of the $(2s, 2p)^5$ and $(2s, 2p)^4 3l$ ($l = 0, 1, 2$) configurations in N-like ions Cr XVIII, Fe XX, Ni XXII, and Zn XXIV (MCDHF/RCI3). Since effective configuration interaction effects have been taken into account, their data of high accuracy can be used to identify the observed spectra. Comparisons of the NIST and CHIANTI experimental results, the present calculations, and the MCDHF/RCI3 values for the $n = 2$ states in Fe XX show good agreements among them, i.e., the mean relative deviations from NIST & CHIANTI experimental values are 0.021% & 0.021% for this work, 0.041% & 0.046% for the MCDHF/RCI3 results; plus the mean (with standard deviation) of the relative differences between the two sets of calculated values is $0.015\% \pm 0.015\%$ for all 272 states of the $n = 2, 3$ configurations, which, again, is highly satisfactory.

The experimental values are sparse for the $n = 3, 4$ levels of N-like ions. To confirm the accuracy of the present $n \geq 3$ results and show the importance of the electron correlation effects, we

have performed another independent calculation for Fe XX using the MCDHF and RCI method. In Table 3, energies for the 344 levels of the $n = 3, 4$ complexes in Fe XX from the MBPT and MCDHF/RCI calculations in this work are compared with calculated values from a previous calculation using the AS code by Witthoef et al. (2007). Collected in Table 3 are also experimental values from the NIST and CHIANTI databases. The deviations of the MCDHF/RCI and MBPT energies are plotted in Figure 1. It can be seen that the agreement between the two calculations is better than 0.08% for all the 344 levels. The mean (with standard deviation) of the relative differences between the two sets of energy values is $0.023\% \pm 0.012\%$, which is highly satisfactory.

As shown in Table 3, experimental observations are largely missing, i.e., the NIST & CHIANTI databases list the energies for 27 & 37 out of the 344 $n = 3, 4$ levels in Fe XX. Furthermore, the identification of these levels becomes problematic in some cases. For example, the $2s^2 2p^2(^3P)3d \ ^4P_{5/2}$ (967.32 eV) level (Sugar & Corliss 1985) from the NIST ASD is observed at a considerably higher energy (>2.1 eV) than from the CHIANTI database and the present MBPT and MCDHF/RCI calculations. The $2s^2 2p^2(^3P)3d \ ^2D_{3/2}$ (974.39 eV), $2s^2 2p^2(^1D)3d \ ^2F_{5/2}$ (989.77 eV), $2s^2 2p^2(^3P)4d \ ^2D_{3/2}$ (1245.17 eV), and $2s^2 2p^2(^1S)4d \ ^2D_{5/2}$ (1275.67 eV) levels in the NIST ASD are also higher than the present MBPT and MCDHF/RCI calculations by over 2-3 eV. The misidentification for these five levels from the NIST ASD cannot be ruled out, as suggested by Radziūtė et al. (2015). The relative differences between the NIST observations and the MBPT calculations (or the MCDHF/RCI calculations) are within 0.2% for the remaining 22 $n = 3, 4$ levels in Fe XX. The agreement with the CHIANTI observed values is better. Deviations of the CHIANTI values relative to the MBPT results (or the MCDHF/RCI results) are less than 0.2% for 33 levels, except for the $2s2p^3(^3S)3p \ ^4P_{5/2}$ level. The CHIANTI value is 1056.17 eV for the $^4P_{5/2}$ level, which is very close to our MBPT and MCDHF/RCI results for the $2s2p^3(^1D)3p \ ^2F_{5/2}$ level, 1056.83 and 1056.99 eV. This indicates that the CHIANTI results should perhaps be designated as the $2s2p^3(^1D)3p \ ^2F_{5/2}$ level. The mean differences with the CHIANTI values are both

0.05% for the MBPT and MCDHF/RCI calculations. The other theoretical energies shown in Table 3, i.e., the AS results, differ from the CHIANTI values significantly. The deviations of the AS results from the CHIANTI values are up to 0.42% for the $2s^2 2p^2 ({}^3P) 3s {}^4P_{5/2}$ levels. The mean deviation relative to the CHIANTI values is 0.24%, being larger by over one order of magnitude than the present MBPT (MCDHF/RCI) results.

The NIST ASD only includes 108 levels of the total 4472 $n \geq 3$ levels in the 13 N-like ions considered here. The relative deviations between the MBPT and NIST values are less than 0.2% for 85 levels. The remaining 23 states for which the differences are larger than 0.2% are listed in Table 4. First, we look at the states for which the differences between the MBPT and NIST values exceed 0.5%. The NIST energy 404.004 eV for the $2s^2 2p^2 ({}^1D) 3d {}^2G_{7/2}$ level is very close to our MBPT result for the $2s^2 2p^2 ({}^1D) 3d {}^2F_{7/2}$ level, 403.552 eV, which suggests that it might be mislabeled and should be designated as the ${}^2F_{7/2}$ level. Figure 2(a) display the deviations for two representative states ($2s^2 2p^2 ({}^1D) 3d {}^2D_{5/2}$ and $2s^2 2p^2 ({}^1S) 3d {}^2D_{5/2}$), as well as the differences for the same states but in other N-like ions so as to aid in comparisons. The deviations are 0.39%, 0.45%, and 0.65% for the $2s^2 2p^2 ({}^1D) 3d {}^2D_{5/2}$ level in K XIII, Ca XIV, and V XVII, respectively. Whereas the MBPT results agree well with the observations for the same level in Sc XV and Fe XX. In fact, the NIST energy for the $2s^2 2p^2 ({}^1D) 3d {}^2D_{5/2}$ level in K XIII is 463.2 eV, and the observed wavelengths 27.53 ($2s^2 2p^3 {}^2D_{5/2} - 2s^2 2p^2 ({}^1D) 3d {}^2D_{5/2}$) and 28.012 ($2s^2 2p^3 {}^2P_{3/2} - 2s^2 2p^2 ({}^1D) 3d {}^2D_{5/2}$) Å are used to deduce the energy for $2s^2 2p^2 ({}^1D) 3d {}^2D_{5/2}$ with the aid of the known energies of $2s^2 2p^3 {}^2D_{5/2}$ and ${}^2P_{3/2}$ (Fawcett & Hayes 1975). The MBPT wavelengths, respectively, are 27.656 and 28.142 Å for the above two transitions, which deviate from the observed values (27.53 and 28.012 Å) up to 0.46% and 0.47%, but agree well (0.08% and 0.15%) with the more recent experimental values 27.63 and 28.10 Å in the revised identification recommended by the same group (Bromage & Fawcett 1977). Using the above revised observations, the experimental data for $2s^2 2p^3 {}^2D_{5/2}$ should be corrected as 461.8 and 462.1 eV, respectively, with

the aid of the known energies of $2s^2 2p^3 {}^2D_{5/2}$ and ${}^2P_{3/2}$, which agree with our MBPT value of 461.403 eV to within 0.15%. The NIST values of the $2s^2 2p^3 {}^2D_{5/2}$ level in Ca XIV, and V XVII are also determined using the observations given by Fawcett & Hayes (1975). We consider that the observation uncertainty should be relatively large according to similar arguments for K XIII used above. Furthermore, our MBPT energies of the $2s^2 2p^2 ({}^1D) 3d {}^2D_{5/2}$ level in eight ions (from K XII to Fe XX) agree well (within 0.1%) with the calculated values recommended by Bromage & Fawcett (1977). Thus, we can state with confidence that the observation uncertainty for the $2s^2 2p^2 ({}^1D) 3d {}^2D_{5/2}$ level in K XIII, Ca XIV, and V XVII in the NIST ASD exceeds the "uncertainty" of the MBPT calculations. As also shown in Figure 2(a), the NIST and MBPT values agree within 0.01% for the same level in Fe XX, but the NIST compiled energy of 605.0 eV for the $2s^2 2p^2 ({}^1S) 3d {}^2D_{5/2}$ state in Sc XV is 0.58% higher than the MBPT values. This is quite strange because the unified treatment is adopted for each ion in the present MBPT calculations, which implies that the calculated results of Sc XV may only be slightly less accurate than those of Fe XX because of more important effects of the electron correlation in the relatively *lower-Z* system in principle (Wang et al. 2015). In addition, Sugar & Corliss (1985) said that the $2s^2 2p^2 ({}^1S) 3d {}^2D_{5/2}$ state in Sc XV was from the interpretation by Fawcett & Hayes (1975) and Bromage & Fawcett (1977). We look over the above two papers, but do not find the measurement regarding the $2s^2 2p^2 ({}^1S) 3d {}^2D_{5/2}$ state. Therefore, the NIST value for the $2s^2 2p^2 ({}^1S) 3d {}^2D_{5/2}$ level in Sc XV may not be determined by the measurement, and we argue that the uncertainty might be large for this level.

In Table 4, there are 17 levels for which the differences between the MBPT and NIST values are in the range of 0.2%–0.5%. In Figure 2(b) we show the comparison of some representative cases. In order to discuss the Z-dependent behavior, Figure 2(b) also displays the energy deviations ($< 0.2\%$) for levels in other ions along the sequence. The NIST and MBPT values agree within 0.2% for most levels, and large differences happen at the *higher-Z* end ($2s^2 2p^2 ({}^1D) 3d {}^2F_{5/2}$ and $2s^2 2p^2 ({}^3P) 3d {}^2D_{3/2}$ and ${}^4P_{5/2}$) and/or in the mid-

dle of the isoelectric sequence ($2s^22p^2(^3P)3d^2D_{3/2}$ and $^2P_{3/2}$). Theoretically, this is not reasonable because the electron correlation effects are usually more significant for *lower-Z* ions. Furthermore, the present MBPT and MCDHF/RCI results agree well within 0.05% for the $2s^22p^2(^1D)3d^2F_{5/2}$ and $2s^22p^2(^3P)3d^2D_{3/2}$ and $^4P_{5/2}$ levels in Fe XX. Therefore, we consider that the large deviations for the 23 $n = 3, 4$ levels listed in Table 4 should be mainly caused by relatively large observation uncertainty.

3.2. Radiative rates

In Figure 3, we compare the present MBPT line strengths (S values) with the MCDHF/RCI2 results (Rynkun et al. 2014) for all of 637 E1 transitions among the $n = 2$ levels in N-like ions with $18 \leq Z \leq 30$. The transitions for which the S values $< 10^{-6}$ are not displayed in Figure 3, because there are only five transitions in this range. For most of the transitions (except for 6 relatively weak transitions with the S values $< 10^{-5}$), the agreement of the two sets of results is within 5%, which is highly satisfactory. The differences of two data sets result from different electron correlation effects considered in the calculations. Weak transitions are generally very sensitive to the electron correlation effects considered in the calculations, and sometimes are even sensitive to the high-order relativistic effects which might be necessary to describe the coupling conditions very accurately.

The NIST ASD lists the S values for 337 out of the total 637 transitions among the $n = 2$ complex. Figure 4 compares the present MBPT S values with those included in the NIST ASD. The NIST values differ from the MBPT results by over 10% for 74% out of the 337 E1 transitions. Even for many very strong transitions with the S values $\geq 10^{-2}$, the differences are also larger than 10%. Table 5 lists all the E1 transitions for which the deviations between the NIST and MBPT S values exceed 10%. We notice that these transitions belong to the ions with 21–28, and the source of the NIST data is from Cheng et al. (1979), which may be out of date. In their calculations, the MCDHF technique was used to calculate energy levels and wave functions for the $n = 2$ levels. Only the configurations within the $n = 2$ complex were included to account for electron correlations and intermediate coupling. As shown in Figure 4 and

Table 5, there is a good agreement (within 2%) between the present MBPT S values and those from Rynkun et al. (2014). The present MBPT calculations, as well as the MCDHF/RCI2 results, should be more accurate and reliable than those values recommended by the NIST ASD.

Of the large number of the E1 transitions involving the higher excited levels of the $n = 3, 4$ complexes in the 13 N-like ions, the NIST ASD only lists the S values for 26 one-photon-one-electron transitions in Fe XX. These NIST values are included in Table 6, as well as the present MBPT and MCDHF/RCI results. Even for the one electron transitions, the differences of the NIST values relative to the MBPT results (or the MCDHF/RCI results) are over 20% (up to a factor of 7 for $2s^22p^2(^1D)3d^2D_{5/2} \rightarrow 2s^22p^3^4S_{3/2}$ for which $\Delta S = 1$ and $\Delta L = 2$) in six cases. As seen from Table 6, the agreement between the present MBPT and MCDHF/RCI S values is satisfactory, being within 4% for all 26 E1 transitions. To further assess the accuracy of the present transitions properties, in Figure 5 the MCDHF/RCI S values are plotted against the MBPT results for 2307 strong transitions (S values $\geq 10^{-2}$) in Fe XX. For 83% of these strong transitions, our MBPT and MCDHF/RCI S values agree to within 5%, while they differ from each other by over 20% (but no more than a factor of 3.5) for 67 transitions. Many of these transitions are intercombination E1 transitions, for which cancellation effects often decrease the accuracy considerably. Nevertheless, except for those 67 transitions, the average difference (with standard deviation) between our MBPT and MCDHF/RCI S values for the remaining 2240 strong transitions is only $2\% \pm 4\%$.

The NIST ASD lists the S values for the total 129 M1 and E2 transitions in the 13 ions considered here, which are all within the $n = 2$ states. The NIST values for these 129 transitions are compared with the MBPT results in Table 7. The MCDHF/RCI2 results are also collected in Table 7 for comparison. The deviations of the NIST S values relative to the present MBPT results are less than 10% for 109 transitions, are between 10% and 30% for 20 transitions. The largest discrepancy is about 27% for the $2s2p^4^2D_{3/2} \rightarrow ^4P_{1/2}$ transition in Ti XVI. The MBPT and MCDHF/RCI2 values agree well (1%) for this transition. The MCDHF/RCI2 calcula-

tions reported the S values for 107 out of the total 129 transitions. The MBPT and MCDHF/RCI2 values agree within 2% for all the transitions. The MBPT and MCDHF/RCI2 calculations are also more accurate and reliable than the NIST values for the M1 and E2 transitions.

4. SUMMARY

Using the combined RCI and MBPT approach, we have performed the systematic calculations of the energies and radiative transition properties for highly charged N-like ions from Ar XII to Zn XXIV. A complete and consistent data set of energies, wavelengths, line strengths, oscillator strengths, and transition rates for all possible E1, M1, E2, and M2 transitions among the 359 levels of the $2s^22p^3$, $2s2p^4$, $2p^5$, $2s^22p^23l$, $2s2p^33l$, $2p^43l$, and $2s^22p^24l$ configurations, is provided for all the 13 ions. By comparing with available observations, the present MCDHF/RCI values and other elaborate/systematic theoretical calculations, high accuracy of the present MBPT results is verified, i.e., the accuracy of level energies is assessed to be within 0.1% for most states, and is less than 0.2% for all states; the accuracy of the line strengths is estimated to be better than 5% for most transitions among the $n = 2$ states, and for a majority of strong transitions in Fe XX. In view of the fact that our calculations are systematic and consistent, which means the unified treatment thus unified quality of data, we anticipated that the accuracy of the line strengths is within 5% for a majority of transitions involving the $n \geq 3$ levels, especially for the strong transitions. We consider that the observation uncertainty should be large for the $n \geq 3$ states included in Table 4, and precise experimental investigations are expected. The elaborate calculations involving higher excited states, especially for the $n = 4$ states, are also expected to further assess the accuracy of the existing experimental and theoretical data.

Since more sufficient correlation effects have been taken into account by considering more configurations in both the N and M spaces, the present MBPT energies reveal an improvement in accuracy compared with the elaborate systematic calculations, such as the MCDHF/RCI work (Rynkun et al. 2014) and the MBPT re-

sults (Gu 2005a). The present MBPT calculations agree well with the MCDHF/RCI results of Radziūtė et al. (2015), i.e., the mean energy deviation for Fe XXI is 0.015%. Meanwhile, the present calculations have significantly increased accurate data for nitrogen-like ions in quantity, and may be considered as the benchmark for other calculations. The accuracy of the energy data is high enough to serve identification and interpretation of observed spectra involving the $n = 3, 4$ levels, for which the experimental values are largely missing. We expect that the present data sets of high accuracy will be useful in the identification and interpretation of observed spectra, and in modeling and diagnosing of astrophysical and fusion plasmas.

The authors express our gratitude to Dr. MingFeng Gu for offering guidance in using his FAC code. We acknowledge the support from the National Natural Science Foundation of China (Grant No. 21503066, No. 11504421, No. 11105015, No. 11205019, No. 11371218, No. 11274001, and No. 11474034) and the support from the Foundation for the Development of Science and Technology of Chinese Academy of Engineering Physics (Grant No. 2012B0102012). This work is also supported by NSAF under Grant No. 11076009, the Chinese Association of Atomic and Molecular Data, the Chinese National Fusion Project for ITER No. 2015GB117000, and the Swedish research council. One of the authors (KW) express his gratefully gratitude to the support from the visiting researcher program at the Fudan University.

REFERENCES

- Acton, L. W., Bruner, M. E., Brown, W. A., Fawcett, B. C., Schweizer, W., & Speer, R. J. 1985, *ApJ*, 291, 865
- Badnell, N. R. 1986, *JPhB*, 19, 3827
- Becker, S. R., Butler, K., & Zeppen, C. J. 1989, *A&A*, 221, 375
- Behar, E., Cottam, J., & Kahn, S. M. 2001, *ApJ*, 548, 966
- Beiersdorfer, P., Träbert, E., Lepson, J. K., Brickhouse, N. S., & Golub, L. 2014, *ApJ*, 788, 25
- Bhatia, A. K., Seely, J. F., & Feldman, U. 1989, *ADNDT*, 43, 99
- Brinkman, A. C., et al. 2000, *ApJ*, 530, L111
- Bromage, G. E., & Fawcett, B. C. 1977, *MNRAS*, 179, 683
- Brosius, J. W., Davila, J. M., & Thomas, R. J. 1998, *ApJS*, 119, 255
- Brown, C. M., Feldman, U., Seely, J. F., Kordyke, C. M., & Hara, H. 2008, *ApJS*, 176, 511
- Brown, G. V., Beiersdorfer, P., Liedahl, D. A., Widmann, K., Kahn, S. M., & Clothiaux, E. J. 2002, *ApJS*, 140, 589
- Chen, H., Gu, M. F., Behar, E., Brown, G. V., Kahn, S. M., & Beiersdorfer, P. 2007, *ApJS*, 168, 319
- Cheng, K., Kim, Y. K., & Desclaux, J. 1979, *ADNDT*, 24, 111
- Curdt, W., Brekke, P., Feldman, U., Wilhelm, K., Dwivedi, B. N., Schühle, U., & Lemaire, P. 2001, *A&A*, 375, 591
- Curdt, W., Landi, E., & Feldman, U. 2004, *A&A*, 427, 1045
- Del Zanna, G. 2008, *A&A*, 481, L69
- . 2012, *A&A*, 537, A38
- Del Zanna, G., & Andretta, V. 2011, *A&A*, 528, A139
- Del Zanna, G., & Woods, T. N. 2013, *A&A*, 555, A59
- Dere, K. P., Landi, E., Mason, H. E., Monsignori Fossi, B. C., & Young, P. R. 1997, *A&AS*, 125, 149
- Dong, F., Wang, F., Zhong, J., Liang, G., & Zhao, G. 2012, *PASJ*, 64, 131
- Doschek, G. A., & Cowan, R. D. 1984, *ApJS*, 56, 67
- Doschek, G. A., Feldman, U., & Cowan, R. D. 1981, *ApJ*, 245, 315
- Doyle, J. G. 1987, *A&A*, 173, 408
- Dyall, K., Grant, I., Johnson, C., Parpia, F., & Plummer, E. 1989, *CoPhC*, 55, 425
- Eidelsberg, M., Crifo-Magnant, F., & Zeppen, C. J. 1981, *A&AS*, 43, 455
- Eissner, W., Jones, M., & Nussbaumer, H. 1974, *CoPhC*, 8, 270
- Eissner, W., Landi, E., & Bhatia, A. K. 2005, *ADNDT*, 89, 139
- Fawcett, B. C., & Hayes, R. W. 1975, *MNRAS*, 170, 185
- Fawcett, B. C., Phillips, K. J. H., Jordan, C., & Lemen, J. R. 1987, *MNRAS*, 225, 1013
- Feldman, U., Behring, W. E., Curdt, W., Schühle, U., Wilhelm, K., Lemaire, P., & Moran, T. M. 1997, *ApJS*, 113, 195
- Feldman, U., Curdt, W., Landi, E., & Wilhelm, K. 2000, *ApJ*, 544, 508
- Feldman, U., Doschek, G. A., & Kreplin, R. W. 1980, *ApJ*, 238, 365
- Feldman, U., Landi, E., & Curdt, W. 2004, *ApJ*, 607, 1039
- Gaigalas, G., Zalandauskas, T., & Fritzsche, S. 2004, *CoPhC*, 157, 239
- Godefroid, M., & Fischer, C. F. 1984, *JPhB*, 17, 681
- Gu, M. F. 2003, *ApJ*, 582, 1241

- Gu, M. F. 2005a, *ADNDT*, 89, 267
- . 2005b, *ApJS*, 156, 105
- Gu, M. F. 2008, *CaJPh*, 86, 675
- Gu, M. F., Beiersdorfer, P., Brown, G. V., Chen, H., Thorn, D. B., & Kahn, S. M. 2007, *ApJ*, 657, 1172
- Gu, M. F., Holczer, T., Behar, E., & Kahn, S. M. 2006, *ApJ*, 641, 1227
- Ishibashi, K., Dewey, D., Huenemoerder, D. P., & Testa, P. 2006, *ApJ*, 644, L117
- Jonauskas, V., et al. 2005, *A&A*, 433, 745
- Jönsson, P., Gaigalas, G., Bieroń, J., Fischer, C. F., & Grant, I. P. 2013, *CoPhC*, 184, 2197
- Jönsson, P., He, X., Fischer, C. F., & Grant, I. 2007, *CoPhC*, 177, 597
- Kaastra, J. S., Steenbrugge, K. C., Raassen, A. J. J., van der Meer, R. L. J., Brinkman, A. C., Liedahl, D. A., Behar, E., & de Rosa, A. 2002, *A&A*, 386, 427
- Kallman, T. R., & Palmeri, P. 2007, *RvMP*, 79, 79
- Ko, Y. K., Raymond, J. C., Li, J., Ciaravella, A., Michels, J., Fineschi, S., & Wu, R. 2002, *ApJ*, 578, 979
- Kramida, A., Yu. Ralchenko, Reader, J., & and NIST ASD Team. 2014, *NIST Atomic Spectra Database (ver. 5.2)*, [Online]. Available: <http://physics.nist.gov/asd> [2015, May 19]. National Institute of Standards and Technology, Gaithersburg, MD.
- Landi, E., & Bhatia, A. K. 2005, *ADNDT*, 90, 177
- Landi, E., Feldman, U., & Dere, K. P. 2002, *ApJS*, 139, 281
- Landi, E., & Phillips, K. J. H. 2005, *ApJS*, 160, 286
- . 2006, *ApJS*, 166, 421
- Landi, E., Young, P. R., Dere, K. P., Del Zanna, G., & Mason, H. E. 2013, *ApJ*, 763, 86
- Lawson, K. D., & Peacock, N. J. 1984, *A&AS*, 58, 475
- Lepson, J. K., Beiersdorfer, P., Behar, E., & Kahn, S. M. 2003, *ApJ*, 590, 604
- Lindgren, I. 1974, *JPhB*, 7, 2441
- Lippmann, S., Finkenthal, M., Huang, L. K., Moos, H. W., Stratton, B. C., Yu, T. L., & Bhatia, A. K. 1987, *ApJ*, 316, 819
- Massacrier, G., & Artru, M. C. 2012, *A&A*, 538, A52
- McKenzie, B. J., Grant, I. P., & Norrington, P. H. 1980a, *CoPhC*, 21, 233
- McKenzie, D. L., Landecker, P. B., Broussard, R. M., Rugge, H. R., Young, R. M., Feldman, U., & Doschek, G. A. 1980b, *ApJ*, 241, 409
- Merkelis, G., Martinson, I., Kisielius, R., & Vilkas, M. J. 1999, *PhyS*, 59, 122
- Merkelis, G., Vilkas, M. J., Kisielius, R., Gaigalas, G., & Martinson, I. 1997, *PhyS*, 56, 41
- Mewe, R., Raassen, A. J. J., Drake, J. J., Kaastra, J. S., van der Meer, R. L. J., & Porquet, D. 2001, *A&A*, 368, 888
- Mohan, A., Landi, E., & Dwivedi, B. N. 2003, *ApJ*, 582, 1162
- Nahar, S. N. 2004, *A&A*, 413, 779
- Nave, G., Nahar, S., & Zhao, G. 2015, *ArXiv e-prints*
- Ness, J.-U., Brickhouse, N. S., Drake, J. J., & Huenemoerder, D. P. 2003, *ApJ*, 598, 1277
- Parenti, S., Vial, J.-C., & Lemaire, P. 2005, *A&A*, 443, 679
- Phillips, K. J. H., Lemen, J. R., Cowan, R. D., Doschek, G. A., & Leibacher, J. W. 1983, *ApJ*, 265, 1120
- Phillips, K. J. H., et al. 1982, *ApJ*, 256, 774
- Raassen, A. J. J., et al. 2002, *A&A*, 389, 228
- Radziūtė, L., Ekman, J., Jönsson, P., & Gaigalas, G. 2015, *A&A*, 582, A61

- Rynkun, P., Jönsson, P., Gaigalas, G., & Froese Fischer, C. 2014, ADNDT, 100, 315
- Safronova, M. S., Johnson, W. R., & Safronova, U. I. 1996, PhRvA, 53, 4036
- Seely, J. F., Feldman, U., & Safronova, U. I. 1986, ApJ, 304, 838
- Shestov, S. V., Bozhenkov, S. A., Zhitnik, I. A., Kuzin, S. V., Urnov, A. M., Beigman, I. L., Goryaev, F. F., & Tolstikhina, I. Y. 2008, Astrophys. Lett., 34, 33
- Si, R., Guo, X. L., Yan, J., Li, C. Y., Li, S., Huang, M., Chen, C. Y., & Zou, Y. M. 2015a, JPhB, 48, 175004
- Si, R., et al. 2015b, JQSRT, 163, 7
- Sugar, J., & Corliss, C. 1985, JPCRD, 14, 1
- Tachiev, G. I., & Froese Fischer, C. 2002, A&A, 385, 716
- Träbert, E., Beiersdorfer, P., Brickhouse, N. S., & Golub, L. 2014a, ApJS, 215, 6
- . 2014b, ApJS, 211, 14
- Vilkas, M. J., Ishikawa, Y., & Koc, K. 1999, PhRvA, 60, 2808
- Wang, K., et al. 2014, ApJS, 215, 26
- . 2015, ApJS, 218, 16
- Warren, H. P., Feldman, U., & Brown, C. M. 2008, ApJ, 685, 1277
- Witthoef, M. C., Del Zanna, G., & Badnell, N. R. 2007, A&A, 466, 763

Figure and Table

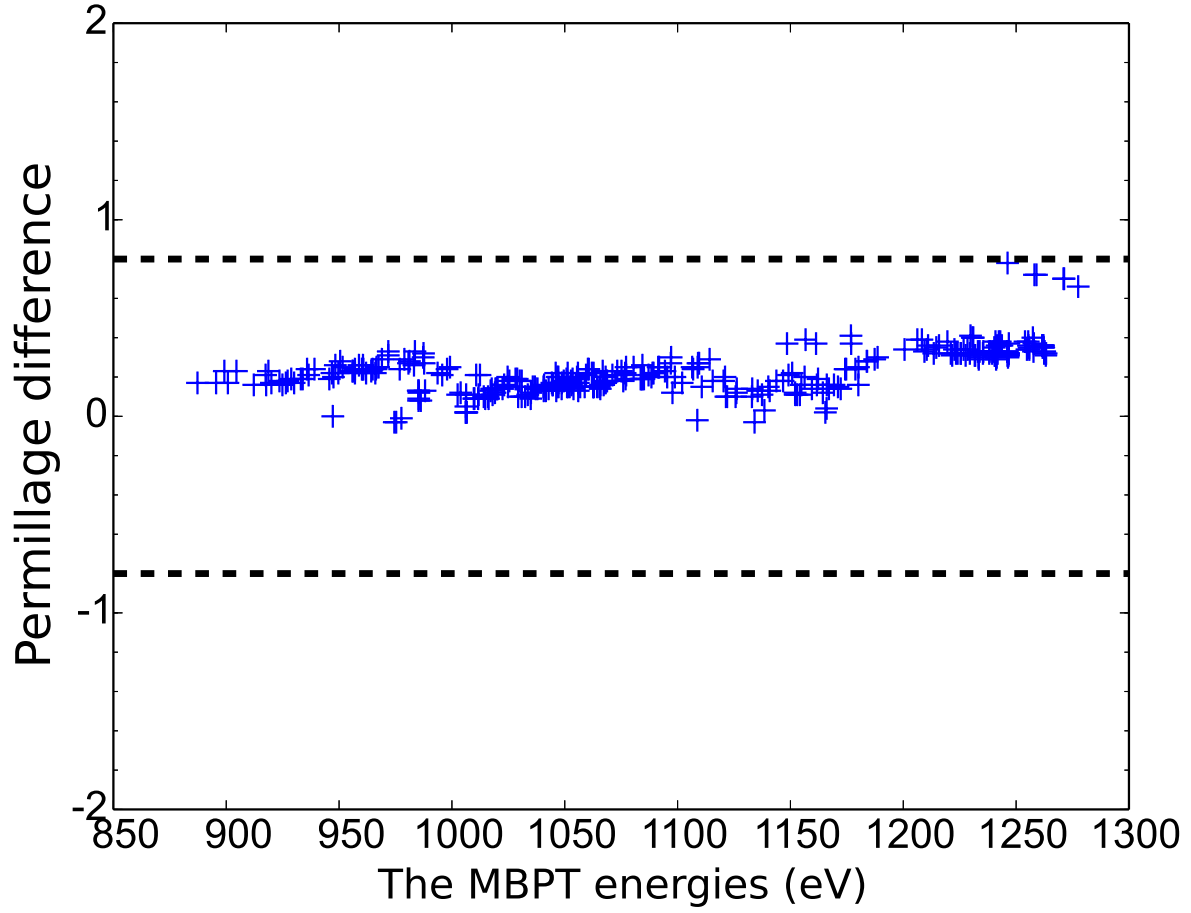


Fig. 1.— Permillage differences of the MCDHF/RCI values relative to the MBPT energies for the $n = 3, 4$ levels in Fe XX. Dashed lines indicate the differences of $\pm 0.08\%$.

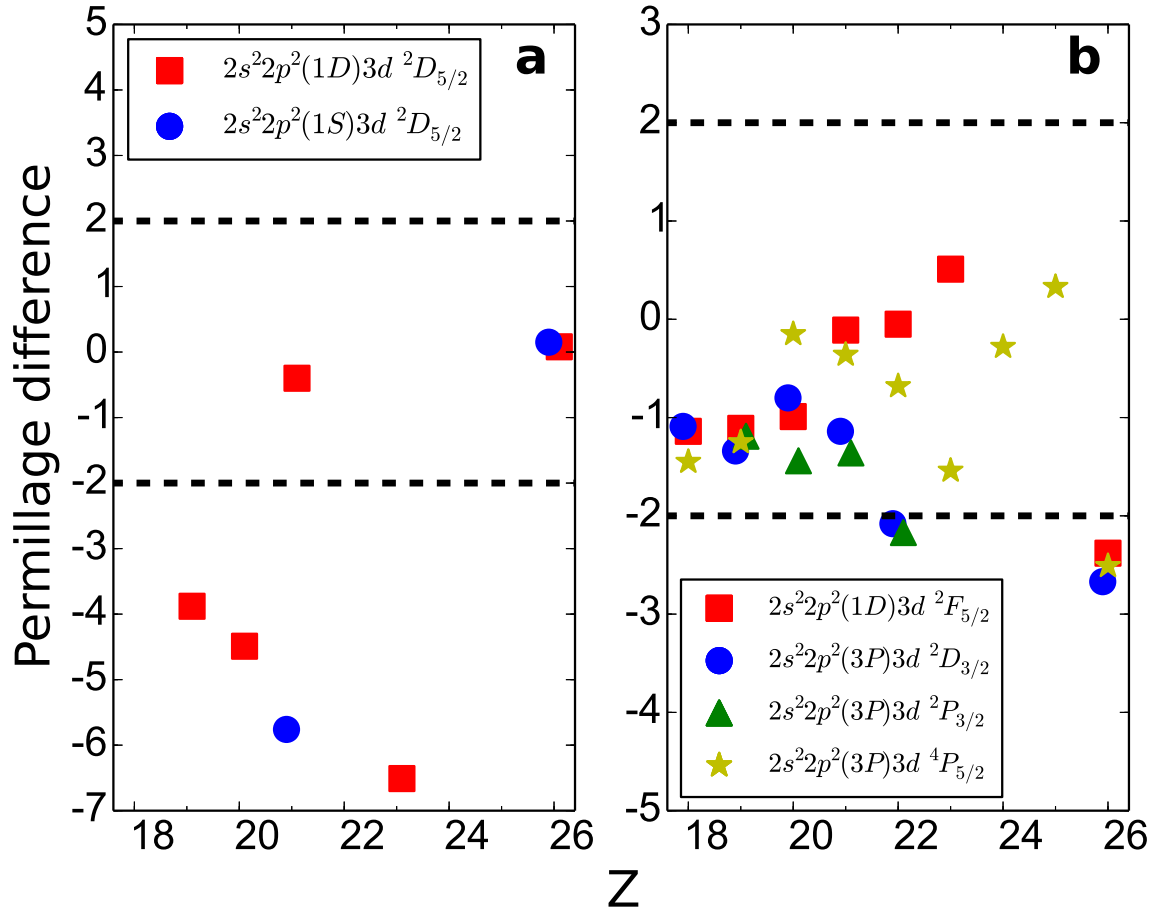


Fig. 2.— Permillage differences of the present MBPT energies relative to the NIST observations (a) for the $2s^2 2p^2 (1D) 3d \ ^2D_{5/2}$ and $2s^2 2p^2 (1S) 3d \ ^2D_{5/2}$ levels, and (b) for the $2s^2 2p^2 (1D) 3d \ ^2F_{5/2}$ and $2s^2 2p^2 (3P) 3d \ ^2D_{3/2}$ and $^4P_{5/2}$ levels along the sequence.

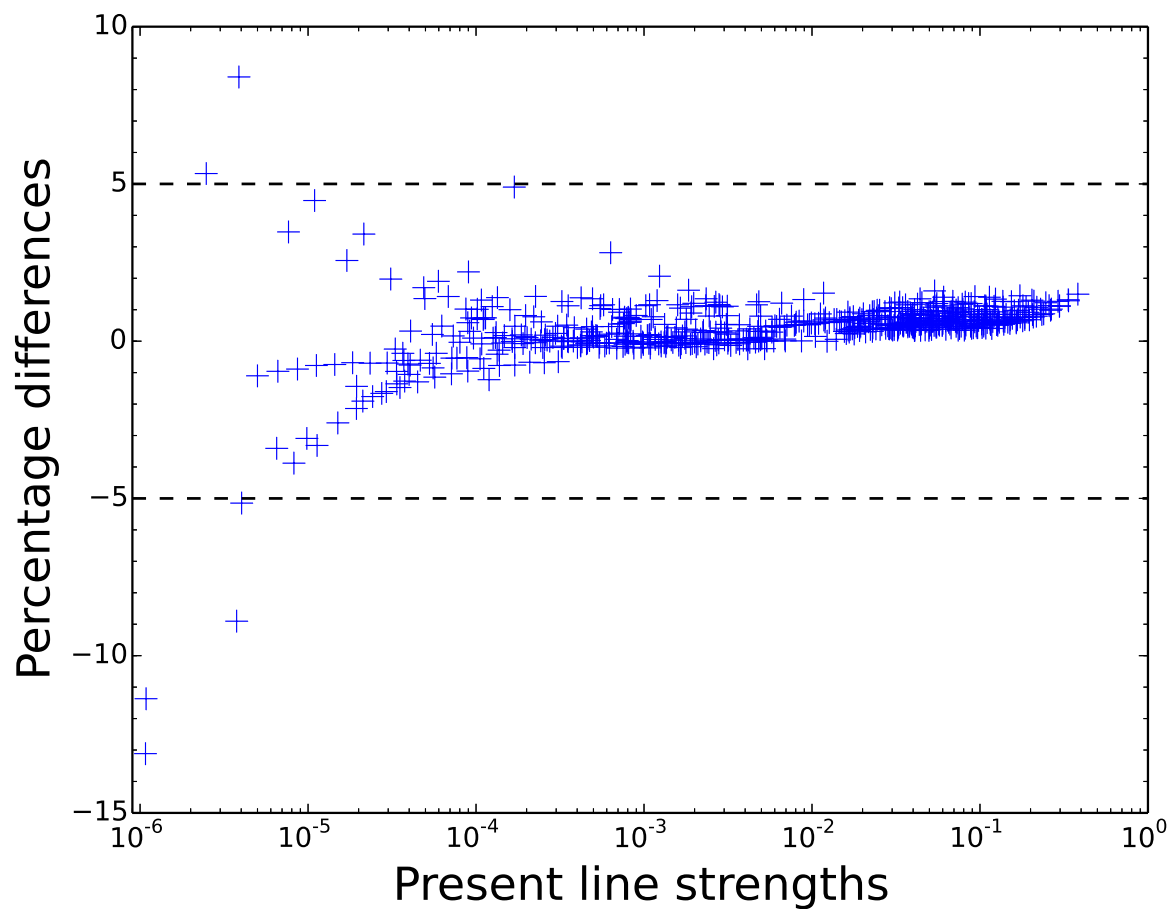


Fig. 3.— Percentage differences between the present MBPT line strengths and the MCDHF/RCI results for the E1 transitions among the $n = 2$ levels. Dashed lines indicate the differences of $\pm 5\%$.

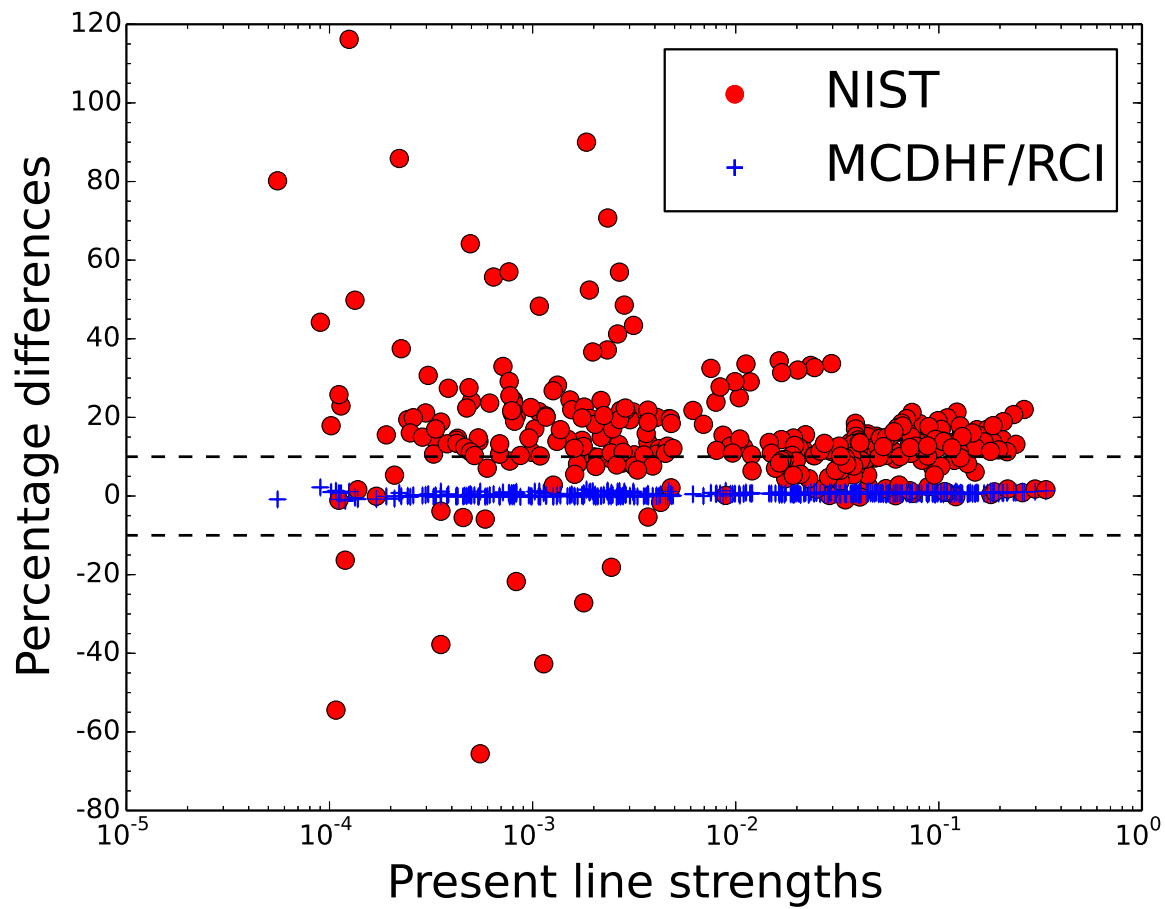


Fig. 4.— Percentage differences of the NIST and MCDHF/RCI2 line strengths relative to the present MBPT results for the E1 transitions among the $n = 2$ levels given by the NIST ASD. Dashed lines indicate the differences of $\pm 10\%$.

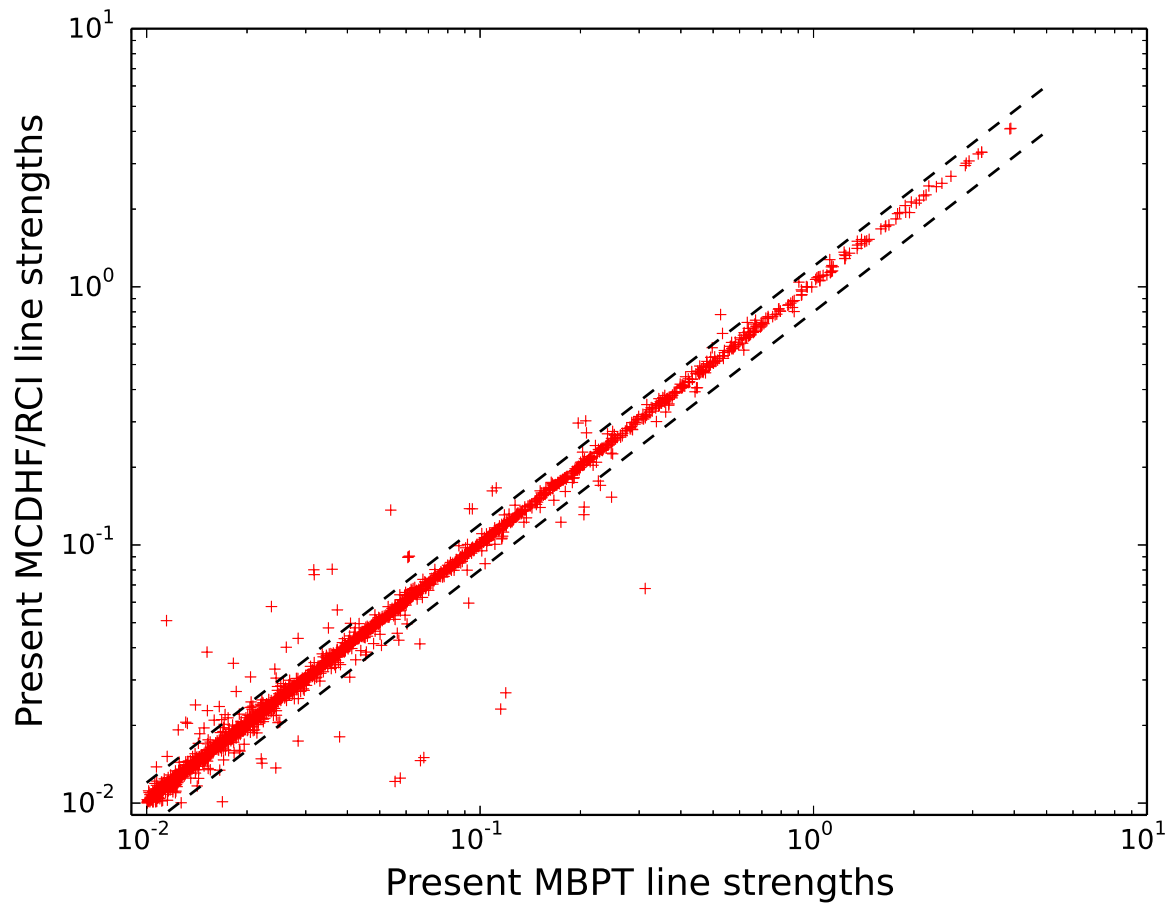


Fig. 5.— Comparison of the present MBPT line strengths with the MCDHF/RCI results for the strong E1 transitions involving the $n = 3, 4$ levels in Fe XX. Dashed lines indicate the differences of $\pm 20\%$.

TABLE 1

Level energies (in eV) of the states in N-like ions with $Z = 18 - 30$, as well as level designations in both the LSJ - and jj coupling schemes, and the dominant mixing coefficients of the LSJ basis.

Z	Key	Conf	LSJ	$jj^{a,b,c}$	J^π	Energy		Mixing coefficients
						NIST ^d	MBPT ^e	LSJ ^f
26	1	$2s^2 2p^3$	$4S_{3/2}$	$2p + 1(3)3$	$3/2^o$	0.00000E+00	0.00000E+00	-0.94(1)
26	2	$2s^2 2p^3$	$2D_{3/2}$	$2p - 1(1)1 2p + 2(4)3$	$3/2^o$	1.71867E+01	1.71795E+01	0.86(2) - 0.42(5)
26	3	$2s^2 2p^3$	$2D_{5/2}$	$2p - 1(1)1 2p + 2(4)5$	$5/2^o$	2.18373E+01	2.18329E+01	1.00(3)
26	4	$2s^2 2p^3$	$2F_{1/2}$	$2p - 1(1)1 2p + 2(0)1$	$1/2^o$	3.22694E+01	3.22817E+01	0.99(4)
26	5	$2s^2 2p^3$	$2F_{3/2}$	$2p + 3(3)3$	$3/2^o$	4.00890E+01	4.01007E+01	-0.84(5) - 0.48(2)
26	6	$2s^2 2p^4$	$4F_{5/2}$	$2s + 1(1)1 2p + 2(4)5$	$5/2^e$	9.33266E+01	9.33152E+01	-0.99(6)
26	7	$2s^2 2p^4$	$4F_{3/2}$	$2s + 1(1)1 2p - 1(1)0 2p + 3(3)3$	$3/2^e$	1.01745E+02	1.01741E+02	-0.99(7)
26	8	$2s^2 2p^4$	$4F_{1/2}$	$2s + 1(1)1 2p + 2(0)1$	$1/2^e$	1.04454E+02	1.04450E+02	-0.97(8)
26	9	$2s^2 2p^4$	$2D_{3/2}$	$2s + 1(1)1 2p + 2(4)3$	$3/2^e$	1.29262E+02	1.29225E+02	-0.97(9)
26	10	$2s^2 2p^4$	$2D_{5/2}$	$2s + 1(1)1 2p - 1(1)2 2p + 3(3)5$	$5/2^e$	1.31220E+02	1.31187E+02	-0.98(10)
26	11	$2s^2 2p^4$	$2S_{1/2}$	$2s + 1(1)1 2p + 2(0)1$	$1/2^e$	1.48193E+02	1.48170E+02	0.85(11)0.49(13)
26	12	$2s^2 2p^4$	$2F_{3/2}$	$2s + 1(1)1 2p - 1(1)2 2p + 3(3)3$	$3/2^e$	1.54042E+02	1.54031E+02	0.97(12)
26	13	$2s^2 2p^4$	$2F_{1/2}$	$2s + 1(1)1$	$1/2^e$	1.66144E+02	1.66140E+02	-0.87(13)0.48(11)
26	14	$2p^5$	$2P_{3/2}$	$2p + 3(3)3$	$3/2^o$	2.42304E+02	2.42209E+02	-0.99(14)
26	15	$2p^5$	$2F_{1/2}$	$2p - 1(1)1$	$1/2^o$	2.55654E+02	2.55574E+02	-0.99(15)
26	16	$2s^2 2p^2 (3P)3s$	$4P_{1/2}$	$3s + 1(1)1$	$1/2^e$...	8.87256E+02	0.88(16)
26	17	$2s^2 2p^2 (3P)3s$	$4P_{3/2}$	$2p - 1(1)1 2p + 1(3)2 3s + 1(1)3$	$3/2^e$...	8.95508E+02	0.97(17)
26	18	$2s^2 2p^2 (3P)3s$	$2F_{1/2}$	$2p - 1(1)1 2p + 1(3)2 3s + 1(1)1$	$1/2^e$...	8.99163E+02	-0.91(18) - 0.40(16)
26	19	$2s^2 2p^2 (3P)3s$	$4F_{5/2}$	$2p - 1(1)1 2p + 1(3)4 3s + 1(1)5$	$5/2^e$...	9.00731E+02	-0.89(19)0.44(22)
26	20	$2s^2 2p^2 (3P)3s$	$2F_{3/2}$	$2p - 1(1)1 2p + 1(3)4 3s + 1(1)3$	$3/2^e$...	9.04521E+02	-0.81(20)0.56(24)
26	21	$2s^2 2p^2 (3P)3p$	$4D_{1/2}$	$3p - 1(1)1$	$1/2^o$...	9.12215E+02	0.76(21)0.45(25)
26	22	$2s^2 2p^2 (1D)3s$	$2D_{5/2}$	$2p + 2(4)4 3s + 1(1)5$	$5/2^e$...	9.17442E+02	0.89(22)0.44(19)
26	23	$2s^2 2p^2 (3P)3p$	$4D_{3/2}$	$3p + 1(3)3$	$3/2^o$...	9.17687E+02	-0.80(23) - 0.48(26)
26	24	$2s^2 2p^2 (1D)3s$	$2D_{3/2}$	$2p + 2(4)4 3s + 1(1)3$	$3/2^e$...	9.18679E+02	-0.82(24) - 0.53(20)
26	25	$2s^2 2p^2 (3P)3p$	$2S_{1/2}$	$2p - 1(1)1 2p + 1(3)2 3p - 1(1)1$	$1/2^o$...	9.20003E+02	0.66(25) - 0.60(21)0.44(28)
26	26	$2s^2 2p^2 (3P)3p$	$4P_{3/2}$	$2p - 1(1)1 2p + 1(3)2 3p - 1(1)3$	$3/2^o$...	9.23572E+02	-0.59(23)0.56(26) - 0.48(30)
26	27	$2s^2 2p^2 (3P)3p$	$4D_{5/2}$	$2p - 1(1)1 2p + 1(3)2 3p + 1(3)5$	$5/2^o$...	9.24893E+02	0.93(27)
26	28	$2s^2 2p^2 (3P)3p$	$4F_{1/2}$	$2p - 1(1)1 2p + 1(3)2 3p + 1(3)1$	$1/2^o$...	9.26421E+02	-0.82(28)0.45(25)
26	29	$2s^2 2p^2 (3P)3p$	$4F_{5/2}$	$2p - 1(1)1 2p + 1(3)4 3p - 1(1)5$	$5/2^o$...	9.27206E+02	0.69(29) - 0.48(35) - 0.45(43)
26	30	$2s^2 2p^2 (3P)3p$	$2D_{3/2}$	$2p - 1(1)1 2p + 1(3)2 3p + 1(3)3$	$3/2^o$...	9.28803E+02	0.70(30)0.52(26)
26	31	$2s^2 2p^2 (3P)3p$	$4D_{7/2}$	$2p - 1(1)1 2p + 1(3)4 3p + 1(3)7$	$7/2^o$...	9.30078E+02	0.90(31) - 0.42(40)
26	32	$2s^2 2p^2 (3P)3p$	$4S_{3/2}$	$2p - 1(1)1 2p + 1(3)4 3p + 1(3)3$	$3/2^o$...	9.33058E+02	0.79(32) - 0.46(49)
26	33	$2s^2 2p^2 (1S)3s$	$2S_{1/2}$	$2p + 2(0)0 3s + 1(1)1$	$1/2^e$...	9.33892E+02	0.94(33)
26	34	$2s^2 2p^2 (3P)3p$	$2F_{3/2}$	$2p - 1(1)1 2p + 1(3)4 3p + 1(3)3$	$3/2^o$...	9.35816E+02	-0.82(34)
26	35	$2s^2 2p^2 (3P)3p$	$2D_{5/2}$	$2p - 1(1)1 2p + 1(3)4 3p + 1(3)5$	$5/2^o$...	9.36508E+02	-0.58(35) - 0.56(29)0.53(37)
26	36	$2s^2 2p^2 (3P)3p$	$2F_{1/2}$	$2p + 2(4)4 3p + 1(3)1$	$1/2^o$...	9.39099E+02	0.83(36) - 0.40(25)
26	37	$2s^2 2p^2 (1D)3p$	$2F_{5/2}$	$2p + 2(4)4 3p + 1(3)5$	$5/2^o$...	9.45675E+02	0.73(37)0.52(43)
26	38	$2s^2 2p^2 (3P)3d$	$4F_{3/2}$	$3d - 1(3)3$	$3/2^e$...	9.46845E+02	-0.82(38)
26	39	$2s^2 2p^3 (5S)3s$	$6S_{5/2}$	$2s + 1(1)1 2p + 1(3)4 3s + 1(1)5$	$5/2^o$...	9.47222E+02	0.97(39)
26	40	$2s^2 2p^2 (1D)3p$	$2F_{7/2}$	$2p + 2(4)4 3p + 1(3)7$	$7/2^o$...	9.47512E+02	-0.90(40) - 0.41(31)
26	41	$2s^2 2p^2 (1D)3p$	$2D_{3/2}$	$2p + 2(4)4 3p - 1(1)3$	$3/2^o$...	9.48346E+02	0.73(41) - 0.52(49)
26	42	$2s^2 2p^2 (3P)3d$	$4D_{5/2}$	$3d + 1(5)5$	$5/2^e$...	9.49663E+02	-0.73(47) - 0.54(42)
26	43	$2s^2 2p^2 (1D)3p$	$2D_{5/2}$	$2p + 2(4)4 3p - 1(1)5$	$5/2^o$...	9.50483E+02	-0.74(43)0.57(35)
26	44	$2s^2 2p^2 (1D)3p$	$2F_{1/2}$	$2p - 1(1)1 2p + 1(3)4 3p + 1(3)1$	$1/2^o$...	9.51568E+02	0.96(44)
26	45	$2s^2 2p^2 (3P)3d$	$2F_{3/2}$	$2p - 1(1)1 2p + 1(3)2 3d - 1(3)3$	$3/2^e$...	9.55961E+02	0.67(45) - 0.55(38)0.45(50)
26	46	$2s^2 2p^2 (3P)3d$	$4F_{7/2}$	$2p - 1(1)1 2p + 1(3)2 3d + 1(5)7$	$7/2^e$...	9.56098E+02	-0.85(46) - 0.49(51)
26	47	$2s^2 2p^2 (3P)3d$	$4F_{5/2}$	$2p - 1(1)1 2p + 1(3)2 3d - 1(3)5$	$5/2^e$...	9.57029E+02	-0.68(47) - 0.49(52) - 0.41(80)
26	48	$2s^2 2p^2 (3P)3d$	$4D_{1/2}$	$2p - 1(1)1 2p + 1(3)2 3d - 1(3)1$	$1/2^e$...	9.57031E+02	0.91(48)
26	49	$2s^2 2p^2 (1D)3p$	$2F_{3/2}$	$2p + 2(4)4 3p + 1(3)3$	$3/2^o$...	9.58815E+02	-0.61(49) - 0.53(34) - 0.46(54)
26	50	$2s^2 2p^2 (3P)3d$	$4D_{3/2}$	$2p - 1(1)1 2p + 1(3)2 3d + 1(5)3$	$3/2^e$...	9.60139E+02	0.74(50) - 0.56(45)
26	51	$2s^2 2p^2 (3P)3d$	$4D_{7/2}$	$2p - 1(1)1 2p + 1(3)4 3d - 1(3)7$	$7/2^e$...	9.60413E+02	0.64(51) - 0.49(72) - 0.44(46)
26	52	$2s^2 2p^2 (3P)3d$	$2F_{5/2}$	$2p - 1(1)1 2p + 1(3)2 3d + 1(5)5$	$5/2^e$...	9.60594E+02	-0.64(52) - 0.53(56)
26	53	$2s^2 2p^2 (3P)3d$	$4F_{9/2}$	$2p - 1(1)1 2p + 1(3)4 3d + 1(5)9$	$9/2^e$...	9.60748E+02	-0.91(53)0.40(68)
26	54	$2s^2 2p^3 (5S)3s$	$4S_{3/2}$	$2s + 1(1)1 2p + 1(3)4 3s + 1(1)3$	$3/2^o$...	9.61962E+02	-0.84(54)
26	55	$2s^2 2p^2 (1S)3p$	$2F_{1/2}$	$2p + 2(0)0 3p - 1(1)1$	$1/2^o$...	9.64255E+02	0.90(55)
26	56	$2s^2 2p^2 (3P)3d$	$4F_{5/2}$	$2p - 1(1)1 2p + 1(3)4 3d + 1(5)5$	$5/2^e$	9.67320E+02	9.64894E+02	0.66(56) - 0.61(42) - 0.40(70)
26	57	$2s^2 2p^2 (1S)3p$	$2F_{3/2}$	$2p + 2(0)0 3p + 1(3)3$	$3/2^o$...	9.66050E+02	0.93(57)
26	58	$2s^2 2p^2 (3P)3d$	$4F_{3/2}$	$2p - 1(1)1 2p + 1(3)4 3d - 1(3)3$	$3/2^e$	9.67320E+02	9.66340E+02	0.85(58)
26	59	$2s^2 2p^2 (3P)3d$	$2F_{1/2}$	$2p - 1(1)1 2p + 1(3)4 3d + 1(5)1$	$1/2^e$...	9.66610E+02	-0.75(59)0.52(60)
26	60	$2s^2 2p^2 (3P)3d$	$4F_{1/2}$	$2p - 1(1)1 2p + 1(3)4 3d - 1(3)1$	$1/2^e$...	9.67502E+02	-0.76(60) - 0.51(59)

TABLE 1—Continued

Z	Key	Conf	LSJ	$j_j^{a,b,c}$	J^π	Energy		Mixing coefficients
						NIST ^d	MBPT ^e	LSJ ^f
26	61	$2s^2 2p^2 ({}^3P)3d$	$2F_{7/2}$	$2p + 2(4)4 3d + 1(5)7$	$7/2^e$	9.69600E+02	9.68982E+02	0.67(61)0.51(51) - 0.49(66)
26	62	$2s^2 2p^2 ({}^3P)3d$	$2D_{3/2}$	$2p - 1(1)1 2p + 1(3)4 3d + 1(5)3$	$3/2^e$	9.74390E+02	9.71784E+02	- 0.87(62)
26	63	$2s^2 2p^2 ({}^3P)3d$	$2D_{5/2}$	$2p - 1(1)1 2p + 1(3)4 3d + 1(5)5$	$5/2^e$	9.72410E+02	9.71812E+02	0.81(63) - 0.40(80)
26	64	$2s2p^3 ({}^5S)3p$	$6F_{3/2}$	$2s + 1(1)1 2p + 1(3)4 3p - 1(1)3$	$3/2^e$...	9.74484E+02	- 0.97(64)
26	65	$2s2p^3 ({}^5S)3p$	$6F_{5/2}$	$2s + 1(1)1 2p + 1(3)4 3p - 1(1)5$	$5/2^e$...	9.75301E+02	- 0.95(65)
26	66	$2s^2 2p^2 ({}^1D)3d$	$2G_{7/2}$	$2p + 2(4)4 3d + 1(5)7$	$7/2^e$...	9.76874E+02	- 0.67(66) - 0.64(72)
26	67	$2s2p^3 ({}^5S)3p$	$6F_{7/2}$	$2s + 1(1)1 2p + 1(3)4 3p + 1(3)7$	$7/2^e$...	9.77608E+02	0.96(67)
26	68	$2s^2 2p^2 ({}^1D)3d$	$2G_{9/2}$	$2p + 2(4)4 3d + 1(5)9$	$9/2^e$...	9.78936E+02	0.91(68)
26	69	$2s^2 2p^2 ({}^1D)3d$	$2D_{3/2}$	$2p + 2(4)4 3d - 1(3)3$	$3/2^e$	9.81830E+02	9.80739E+02	0.92(69)
26	70	$2s^2 2p^2 ({}^1D)3d$	$2D_{5/2}$	$2p + 2(4)4 3d - 1(3)5$	$5/2^e$	9.81090E+02	9.81172E+02	0.75(70) - 0.52(80)
26	71	$2s^2 2p^2 ({}^1D)3d$	$2F_{1/2}$	$2p - 1(1)1 2p + 1(3)4 3d + 1(5)1$	$1/2^e$...	9.83193E+02	- 0.95(71)
26	72	$2s^2 2p^2 ({}^1D)3d$	$2F_{7/2}$	$2p + 2(4)4 3d - 1(3)7$	$7/2^e$	9.83810E+02	9.83605E+02	0.60(61) - 0.60(72)0.49(66)
26	73	$2s2p^3 ({}^3D)3s$	$4D_{3/2}$	$2s + 1(1)1 2p + 1(3)2 3s + 1(1)3$	$3/2^o$...	9.85101E+02	- 0.93(73)
26	74	$2s2p^3 ({}^5S)3p$	$4F_{3/2}$	$2s + 1(1)1 2p + 1(3)4 3p + 1(3)3$	$3/2^e$...	9.85218E+02	- 0.95(74)
26	75	$2s2p^3 ({}^5S)3p$	$4F_{5/2}$	$2s + 1(1)1 2p - 1(1)2 2p + 2(4)4 3p + 1(3)5$	$5/2^e$...	9.85272E+02	0.93(75)
26	76	$2s2p^3 ({}^3D)3s$	$4D_{1/2}$	$2s + 1(1)1 2p + 1(3)2 3s + 1(1)1$	$1/2^o$...	9.85295E+02	0.95(76)
26	77	$2s2p^3 ({}^3D)3s$	$4D_{5/2}$	$2s + 1(1)1 2p - 1(1)0 2p + 2(4)4 3s + 1(1)5$	$5/2^o$...	9.85360E+02	0.91(77)
26	78	$2s2p^3 ({}^5S)3p$	$4F_{1/2}$	$2s + 1(1)1 2p + 1(3)4 3p + 1(3)1$	$1/2^e$...	9.86208E+02	0.97(78)
26	79	$2s^2 2p^2 ({}^1D)3d$	$2S_{1/2}$	$2p + 2(4)4 3d - 1(3)1$	$1/2^e$...	9.87258E+02	- 0.91(79)
26	80	$2s^2 2p^2 ({}^1D)3d$	$2F_{5/2}$	$2p + 2(4)4 3d + 1(5)5$	$5/2^e$	9.89770E+02	9.87413E+02	- 0.59(63) - 0.54(80) - 0.49(70)
26	81	$2s^2 2p^2 ({}^1D)3d$	$2F_{3/2}$	$2p + 2(4)4 3d + 1(5)3$	$3/2^e$	9.87780E+02	9.87692E+02	- 0.87(81)
26	82	$2s2p^3 ({}^3D)3s$	$4D_{7/2}$	$2s + 1(1)1 2p - 1(1)2 2p + 2(4)6 3s + 1(1)7$	$7/2^o$...	9.88095E+02	0.99(82)
26	83	$2s2p^3 ({}^3D)3s$	$2D_{3/2}$	$2s + 1(1)1 2p - 1(1)0 2p + 2(4)4 3s + 1(1)3$	$3/2^o$...	9.93651E+02	0.90(83)
26	84	$2s2p^3 ({}^3D)3s$	$2D_{5/2}$	$2s + 1(1)1 2p - 1(1)2 2p + 2(4)6 3s + 1(1)5$	$5/2^o$...	9.95696E+02	0.91(84)
26	85	$2s^2 2p^2 ({}^1S)3d$	$2D_{5/2}$	$2p + 2(0)0 3d + 1(5)5$	$5/2^e$	9.97700E+02	9.97849E+02	- 0.94(85)
26	86	$2s^2 2p^2 ({}^1S)3d$	$2D_{3/2}$	$2p + 2(0)0 3d - 1(3)3$	$3/2^e$...	9.99148E+02	0.90(86)
26	87	$2s2p^3 ({}^3P)3s$	$4P_{1/2}$	$2s + 1(1)1 2p - 1(1)0 2p + 2(0)0 3s + 1(1)1$	$1/2^o$...	1.00253E+03	- 0.97(87)
26	88	$2s2p^3 ({}^3P)3s$	$4F_{3/2}$	$2s + 1(1)1 2p - 1(1)2 2p + 2(0)2 3s + 1(1)3$	$3/2^o$...	1.00387E+03	- 0.90(88)
26	89	$2s2p^3 ({}^5S)3d$	$6D_{1/2}$	$2s + 1(1)1 2p + 1(3)4 3d - 1(3)1$	$1/2^o$...	1.00616E+03	0.98(89)
26	90	$2s2p^3 ({}^5S)3d$	$6D_{3/2}$	$2s + 1(1)1 2p + 1(3)4 3d - 1(3)3$	$3/2^o$...	1.00619E+03	- 0.98(90)
26	91	$2s2p^3 ({}^5S)3d$	$6D_{5/2}$	$2s + 1(1)1 2p + 3(3)4 3s + 1(1)5$	$5/2^o$...	1.00620E+03	- 0.80(91) - 0.51(92)
26	92	$2s2p^3 ({}^3P)3s$	$4F_{5/2}$	$2s + 1(1)1 2p + 1(3)2 3s + 1(1)5$	$5/2^o$...	1.00630E+03	- 0.67(92)0.62(91)
26	93	$2s2p^3 ({}^5S)3d$	$6D_{7/2}$	$2s + 1(1)1 2p + 1(3)4 3d + 1(5)7$	$7/2^o$...	1.00633E+03	0.98(93)
26	94	$2s2p^3 ({}^5S)3d$	$6D_{9/2}$	$2s + 1(1)1 2p + 1(3)4 3d + 1(5)9$	$9/2^o$...	1.00660E+03	0.98(94)
26	95	$2s2p^3 ({}^3D)3p$	$4D_{1/2}$	$2s + 1(1)1 2p + 1(3)2 3p - 1(1)1$	$1/2^e$...	1.00969E+03	- 0.85(95) - 0.40(105)
26	96	$2s2p^3 ({}^3D)3p$	$4D_{3/2}$	$2s + 1(1)1 2p - 1(1)0 2p + 2(4)4 3p - 1(1)3$	$3/2^e$...	1.00997E+03	- 0.79(96) - 0.45(103)
26	97	$2s2p^3 ({}^3P)3s$	$2P_{1/2}$	$2s + 1(1)1 2p - 1(1)2 2p + 2(0)2 3s + 1(1)1$	$1/2^o$...	1.01075E+03	- 0.95(97)
26	98	$2s2p^3 ({}^3D)3p$	$4F_{5/2}$	$2s + 1(1)1 2p - 1(1)0 2p + 2(4)4 3p - 1(1)5$	$5/2^e$...	1.01162E+03	0.74(98) - 0.56(102)
26	99	$2s2p^3 ({}^3D)3p$	$4F_{3/2}$	$2s + 1(1)1 2p + 1(3)2 3p - 1(1)3$	$3/2^e$...	1.01182E+03	0.84(99)0.40(103)
26	100	$2s2p^3 ({}^3P)3s$	$2F_{3/2}$	$2s + 1(1)1 2p + 3(3)4 3s + 1(1)3$	$3/2^o$...	1.01243E+03	- 0.86(100)
26	101	$2s2p^3 ({}^3D)3p$	$4F_{7/2}$	$2s + 1(1)1 2p - 1(1)2 2p + 2(4)6 3p - 1(1)7$	$7/2^e$...	1.01411E+03	0.82(101) - 0.49(104)
26	102	$2s2p^3 ({}^3D)3p$	$4D_{5/2}$	$2s + 1(1)1 2p - 1(1)0 2p + 2(4)4 3p + 1(3)5$	$5/2^e$...	1.01475E+03	0.80(102)0.54(98)
26	103	$2s2p^3 ({}^3D)3p$	$2F_{3/2}$	$2s + 1(1)1 2p - 1(1)2 2p + 2(4)6 3p + 1(3)3$	$3/2^e$...	1.01599E+03	0.62(96) - 0.62(103)0.42(99)
26	104	$2s2p^3 ({}^3D)3p$	$4D_{7/2}$	$2s + 1(1)1 2p - 1(1)0 2p + 2(4)4 3p + 1(3)7$	$7/2^e$...	1.01625E+03	0.78(104)0.44(101)
26	105	$2s2p^3 ({}^3D)3p$	$2F_{1/2}$	$2s + 1(1)1 2p - 1(1)0 2p + 2(4)4 3p + 1(3)1$	$1/2^e$...	1.01715E+03	0.88(105) - 0.40(95)
26	106	$2s2p^3 ({}^3D)3p$	$2F_{5/2}$	$2s + 1(1)1 2p + 1(3)2 3p + 1(3)5$	$5/2^e$...	1.01763E+03	- 0.92(106)
26	107	$2s2p^3 ({}^3D)3p$	$4F_{9/2}$	$2s + 1(1)1 2p - 1(1)2 2p + 2(4)6 3p + 1(3)9$	$9/2^e$...	1.01802E+03	1.00(107)
26	108	$2s2p^3 ({}^3D)3p$	$2F_{7/2}$	$2s + 1(1)1 2p - 1(1)2 2p + 2(4)6 3p + 1(3)7$	$7/2^e$...	1.01907E+03	0.88(108)0.41(104)
26	109	$2s2p^3 ({}^5S)3d$	$4D_{5/2}$	$2s + 1(1)1 2p + 1(3)4 3d + 1(5)5$	$5/2^o$...	1.01928E+03	0.95(109)
26	110	$2s2p^3 ({}^5S)3d$	$4D_{3/2}$	$2s + 1(1)1 2p + 1(3)4 3d + 1(5)3$	$3/2^o$...	1.01963E+03	- 0.96(110)
26	111	$2s2p^3 ({}^5S)3d$	$4D_{7/2}$	$2s + 1(1)1 2p + 1(3)4 3d - 1(3)7$	$7/2^o$...	1.02008E+03	0.96(111)
26	112	$2s2p^3 ({}^5S)3d$	$4D_{1/2}$	$2s + 1(1)1 2p + 1(3)4 3d + 1(5)1$	$1/2^o$...	1.02020E+03	0.96(112)
26	113	$2s2p^3 ({}^3D)3p$	$4F_{3/2}$	$2s + 1(1)1 2p - 1(1)0 2p + 2(4)4 3p + 1(3)3$	$3/2^e$...	1.02243E+03	0.77(113) - 0.53(125)
26	114	$2s2p^3 ({}^3D)3p$	$4P_{1/2}$	$2s + 1(1)1 2p + 1(3)2 3p + 1(3)1$	$1/2^e$...	1.02314E+03	- 0.89(114) - 0.42(128)
26	115	$2s2p^3 ({}^3D)3p$	$4F_{5/2}$	$2s + 1(1)1 2p - 1(1)2 2p + 2(4)6 3p - 1(1)5$	$5/2^e$...	1.02468E+03	- 0.90(115)
26	116	$2s2p^3 ({}^3S)3s$	$4S_{3/2}$	$2s + 1(1)1 2p - 1(1)2 2p + 2(4)2 3s + 1(1)3$	$3/2^o$...	1.02487E+03	- 0.90(116)
26	117	$2s2p^3 ({}^3D)3p$	$2D_{3/2}$	$2s + 1(1)1 2p - 1(1)2 2p + 2(4)6 3p + 1(3)3$	$3/2^e$...	1.02545E+03	0.80(117) - 0.43(103)
26	118	$2s2p^3 ({}^3D)3p$	$2D_{5/2}$	$2s + 1(1)1 2p - 1(1)2 2p + 2(4)6 3p + 1(3)5$	$5/2^e$...	1.02819E+03	0.88(118)
26	119	$2s2p^3 ({}^3S)3s$	$2S_{1/2}$	$2s + 1(1)1 2p - 1(1)2 2p + 2(4)2 3s + 1(1)1$	$1/2^o$...	1.02892E+03	- 0.86(119) - 0.45(144)
26	120	$2s2p^3 ({}^3P)3p$	$4D_{1/2}$	$2s + 1(1)1 2p - 1(1)0 2p + 2(0)0 3p - 1(1)1$	$1/2^e$...	1.02935E+03	- 0.83(120) - 0.50(127)

TABLE 1—Continued

Z	Key	Conf	LSJ	$jj^{a,b,c}$	J^π	Energy		Mixing coefficients
						NIST ^d	MBPT ^e	LSJ ^f
26	121	$2s2p^3(^1D)3s$	$2^2D_{5/2}$	$2s + 1(1)1\ 2p - 1(1)2\ 2p + 2(4)4\ 3s + 1(1)5$	$5/2^o$...	1.03004E+03	-0.96(121)
26	122	$2s2p^3(^3P)3p$	$4^2D_{3/2}$	$2s + 1(1)1\ 2p - 1(1)2\ 2p + 2(0)2\ 3p - 1(1)3$	$3/2^e$...	1.03091E+03	-0.91(122)
26	123	$2s2p^3(^1D)3s$	$2^2D_{3/2}$	$2s + 1(1)1\ 2p - 1(1)2\ 2p + 2(4)4\ 3s + 1(1)3$	$3/2^o$...	1.03093E+03	0.93(123)
26	124	$2s2p^3(^3P)3p$	$4^2D_{5/2}$	$2s + 1(1)1\ 2p - 1(1)2\ 2p + 2(0)2\ 3p + 1(3)5$	$5/2^e$...	1.03242E+03	0.90(124)
26	125	$2s2p^3(^3P)3p$	$4^2S_{3/2}$	$2s + 1(1)1\ 2p - 1(1)0\ 2p + 2(0)0\ 3p + 1(3)3$	$3/2^e$...	1.03361E+03	0.79(125)0.52(113)
26	126	$2s2p^3(^3P)3p$	$4^2D_{7/2}$	$2s + 1(1)1\ 2p + 3(3)4\ 3p + 1(3)7$	$7/2^e$...	1.03492E+03	-0.87(126)
26	127	$2s2p^3(^3P)3p$	$2^2P_{1/2}$	$2s + 1(1)1\ 2p - 1(1)2\ 2p + 2(0)2\ 3p + 1(3)1$	$1/2^e$...	1.03502E+03	-0.75(127)0.45(120)0.40(128)
26	128	$2s2p^3(^3P)3p$	$4^2P_{1/2}$	$2s + 1(1)1\ 2p - 1(1)2\ 2p + 2(0)2\ 3p - 1(1)1$	$1/2^e$...	1.03583E+03	0.76(128)0.46(127)
26	129	$2s2p^3(^3P)3p$	$4^2P_{3/2}$	$2s + 1(1)1\ 2p - 1(1)0\ 2p + 2(0)0\ 3p + 1(3)3$	$3/2^e$...	1.03676E+03	-0.74(129)0.54(131)
26	130	$2s2p^3(^3P)3p$	$4^2P_{5/2}$	$2s + 1(1)1\ 2p - 1(1)2\ 2p + 2(0)2\ 3p + 1(3)5$	$5/2^e$...	1.03712E+03	0.81(130) - 0.41(134)
26	131	$2s2p^3(^3P)3p$	$2^2D_{3/2}$	$2s + 1(1)1\ 2p - 1(1)2\ 2p + 2(0)2\ 3p + 1(3)3$	$3/2^e$...	1.03793E+03	0.73(131)0.57(129)
26	132	$2s2p^3(^3P)3p$	$2^2P_{3/2}$	$2s + 1(1)1\ 2p + 3(3)4\ 3p + 1(3)3$	$3/2^e$...	1.04059E+03	0.75(132)0.52(117)
26	133	$2s2p^3(^3D)3d$	$4^2F_{3/2}$	$2s + 1(1)1\ 2p + 1(3)2\ 3d - 1(3)3$	$3/2^o$...	1.04070E+03	0.91(133)
26	134	$2s2p^3(^3P)3p$	$2^2D_{5/2}$	$2s + 1(1)1\ 2p + 3(3)4\ 3p + 1(3)5$	$5/2^e$...	1.04085E+03	-0.75(134) - 0.51(130)
26	135	$2s2p^3(^3D)3d$	$4^2F_{5/2}$	$2s + 1(1)1\ 2p - 1(1)0\ 2p + 2(4)4\ 3d - 1(3)5$	$5/2^o$...	1.04163E+03	0.83(135)
26	136	$2s2p^3(^3D)3d$	$4^2F_{7/2}$	$2s + 1(1)1\ 2p - 1(1)2\ 2p + 2(4)6\ 3d - 1(3)7$	$7/2^o$...	1.04285E+03	-0.70(136)0.59(139)
26	137	$2s2p^3(^3D)3d$	$4^2G_{5/2}$	$2s + 1(1)1\ 2p + 1(3)2\ 3d - 1(3)5$	$5/2^o$...	1.04430E+03	-0.88(137) - 0.42(135)
26	138	$2s2p^3(^3D)3d$	$4^2G_{9/2}$	$2s + 1(1)1\ 2p - 1(1)0\ 2p + 2(4)4\ 3d + 1(5)9$	$9/2^o$...	1.04458E+03	-0.89(138)
26	139	$2s2p^3(^3D)3d$	$4^2G_{7/2}$	$2s + 1(1)1\ 2p + 1(1)0\ 2p + 2(4)4\ 3d + 1(5)7$	$7/2^o$...	1.04472E+03	-0.73(139) - 0.64(136)
26	140	$2s2p^3(^3P)3p$	$2^2S_{1/2}$	$2s + 1(1)1\ 2p - 1(1)2\ 2p + 2(0)2\ 3p + 1(3)1$	$1/2^e$...	1.04598E+03	0.81(140)
26	141	$2s2p^3(^3D)3d$	$4^2F_{9/2}$	$2s + 1(1)1\ 2p - 1(1)2\ 2p + 2(4)6\ 3d + 1(5)9$	$9/2^o$...	1.04624E+03	0.97(141)
26	142	$2s2p^3(^3D)3d$	$4^2D_{1/2}$	$2s + 1(1)1\ 2p - 1(1)0\ 2p + 2(4)4\ 3d - 1(3)1$	$1/2^o$...	1.04659E+03	-0.90(142)
26	143	$2s2p^3(^1P)3s$	$2^2P_{3/2}$	$2s + 1(1)1\ 2p + 3(3)2\ 3s + 1(1)3$	$3/2^o$...	1.04667E+03	0.91(143)
26	144	$2s2p^3(^1P)3s$	$2^2P_{1/2}$	$2s + 1(1)1\ 2p + 3(3)2\ 3s + 1(1)1$	$1/2^o$...	1.04716E+03	0.87(144) - 0.44(119)
26	145	$2s2p^3(^3D)3d$	$4^2G_{11/2}$	$2s + 1(1)1\ 2p - 1(1)2\ 2p + 2(4)6\ 3d + 1(5)11$	$11/2^o$...	1.04724E+03	-1.00(145)
26	146	$2s2p^3(^3D)3d$	$4^2D_{3/2}$	$2s + 1(1)1\ 2p + 1(3)4\ 3d - 1(3)3$	$3/2^o$...	1.04725E+03	-0.87(146)
26	147	$2s2p^3(^3D)3d$	$4^2D_{5/2}$	$2s + 1(1)1\ 2p - 1(1)0\ 2p + 2(4)4\ 3d + 1(5)5$	$5/2^o$...	1.04863E+03	-0.78(147) - 0.43(154)
26	148	$2s2p^3(^3D)3d$	$2^2S_{1/2}$	$2s + 1(1)1\ 2p + 1(3)2\ 3d - 1(3)1$	$1/2^o$...	1.04872E+03	0.81(148)0.42(156)
26	149	$2s2p^3(^3D)3d$	$4^2D_{7/2}$	$2s + 1(1)1\ 2p - 1(1)2\ 2p + 2(4)6\ 3d - 1(3)7$	$7/2^o$...	1.04956E+03	0.69(149)0.64(150)
26	150	$2s2p^3(^3D)3d$	$2^2G_{7/2}$	$2s + 1(1)1\ 2p - 1(1)2\ 2p + 2(4)6\ 3d + 1(5)7$	$7/2^o$...	1.05077E+03	-0.71(150)0.65(149)
26	151	$2s2p^3(^3S)3p$	$4^2P_{3/2}$	$2s + 1(1)1\ 2p - 1(1)2\ 2p + 2(4)2\ 3p - 1(1)3$	$3/2^e$...	1.05102E+03	-0.77(151) - 0.46(178)
26	152	$2s2p^3(^3D)3d$	$2^2G_{9/2}$	$2s + 1(1)1\ 2p - 1(1)2\ 2p + 2(4)6\ 3d - 1(3)9$	$9/2^o$...	1.05129E+03	-0.93(152)
26	153	$2s2p^3(^3S)3p$	$4^2P_{1/2}$	$2s + 1(1)1\ 2p - 1(1)2\ 2p + 2(4)2\ 3p - 1(1)1$	$1/2^e$...	1.05137E+03	0.66(153)0.51(163) - 0.42(197)
26	154	$2s2p^3(^3D)3d$	$4^2P_{5/2}$	$2s + 1(1)1\ 2p - 1(1)2\ 2p + 2(4)6\ 3d - 1(3)5$	$5/2^o$...	1.05217E+03	0.78(154) - 0.55(147)
26	155	$2s2p^3(^3D)3d$	$4^2F_{9/2}$	$2s + 1(1)1\ 2p + 1(3)2\ 3d + 1(5)3$	$3/2^o$...	1.05275E+03	-0.68(155) - 0.48(160) - 0.42(177)
26	156	$2s2p^3(^3D)3d$	$4^2S_{3/2}$	$2s + 1(1)1\ 2p - 1(1)2\ 2p + 2(4)6\ 3d + 1(5)1$	$1/2^o$...	1.05299E+03	-0.82(156)0.50(148)
26	157	$2s2p^3(^3D)3d$	$2^2P_{3/2}$	$2s + 1(1)1\ 2p - 1(1)2\ 2p + 2(4)6\ 3d - 1(3)3$	$3/2^o$...	1.05341E+03	-0.65(155) - 0.60(157)0.41(146)
26	158	$2s2p^3(^3D)3d$	$2^2D_{5/2}$	$2s + 1(1)1\ 2p + 1(3)4\ 3d + 1(5)5$	$5/2^o$...	1.05347E+03	0.64(158) - 0.58(187)0.47(168)
26	159	$2s2p^3(^3S)3p$	$4^2P_{5/2}$	$2s + 1(1)1\ 2p - 1(1)2\ 2p + 2(4)2\ 3p + 1(3)5$	$5/2^e$...	1.05387E+03	-0.90(159)
26	160	$2s2p^3(^3D)3d$	$4^2S_{5/2}$	$2s + 1(1)1\ 2p - 1(1)2\ 2p + 2(4)6\ 3d + 1(5)3$	$3/2^o$...	1.05544E+03	-0.76(160) - 0.51(157)
26	161	$2s2p^3(^3D)3d$	$2^2P_{1/2}$	$2s + 1(1)1\ 2p - 1(1)2\ 2p + 2(4)6\ 3d + 1(5)1$	$1/2^o$...	1.05584E+03	-0.94(161)
26	162	$2s2p^3(^1D)3p$	$2^2P_{3/2}$	$2s + 1(1)1\ 2p - 1(1)2\ 2p + 2(4)2\ 3p + 1(3)3$	$3/2^e$...	1.05597E+03	-0.63(162)0.58(151) - 0.47(178)
26	163	$2s2p^3(^3S)3p$	$2^2P_{1/2}$	$2s + 1(1)1\ 2p - 1(1)2\ 2p + 2(4)2\ 3p + 1(3)1$	$1/2^e$...	1.05601E+03	-0.64(153)0.57(163)0.41(140)
26	164	$2s2p^3(^1D)3p$	$2^2F_{5/2}$	$2s + 1(1)1\ 2p - 1(1)2\ 2p + 2(4)4\ 3p - 1(1)5$	$5/2^e$...	1.05683E+03	-0.92(164)
26	165	$2s2p^3(^1D)3p$	$2^2F_{7/2}$	$2s + 1(1)1\ 2p - 1(1)2\ 2p + 2(4)4\ 3p + 1(3)7$	$7/2^e$...	1.05883E+03	0.96(165)
26	166	$2s2p^3(^3D)3d$	$2^2D_{3/2}$	$2s + 1(1)1\ 2p - 1(1)2\ 2p + 2(4)6\ 3d + 1(5)3$	$3/2^o$...	1.05943E+03	0.93(166)
26	167	$2s2p^3(^3D)3d$	$2^2F_{7/2}$	$2s + 1(1)1\ 2p - 1(1)2\ 2p + 2(4)6\ 3d + 1(5)7$	$7/2^o$...	1.06026E+03	0.91(167)
26	168	$2s2p^3(^3D)3d$	$2^2F_{5/2}$	$2s + 1(1)1\ 2p - 1(1)2\ 2p + 2(4)6\ 3d + 1(5)5$	$5/2^o$...	1.06066E+03	-0.78(168)0.57(158)
26	169	$2s2p^3(^1D)3p$	$2^2D_{3/2}$	$2s + 1(1)1\ 2p - 1(1)2\ 2p + 2(4)4\ 3p + 1(3)3$	$3/2^e$...	1.06201E+03	0.93(169)
26	170	$2s2p^3(^3P)3d$	$4^2F_{3/2}$	$2s + 1(1)1\ 2p - 1(1)0\ 2p + 2(0)0\ 3d - 1(3)3$	$3/2^o$...	1.06259E+03	-0.89(170)
26	171	$2s2p^3(^3P)3d$	$4^2F_{5/2}$	$2s + 1(1)1\ 2p - 1(1)0\ 2p + 2(0)0\ 3d + 1(5)5$	$5/2^o$...	1.06265E+03	-0.86(171)
26	172	$2s2p^3(^1D)3p$	$2^2D_{5/2}$	$2s + 1(1)1\ 2p - 1(1)2\ 2p + 2(4)4\ 3p + 1(3)5$	$5/2^e$...	1.06278E+03	-0.92(172)
26	173	$2s2p^3(^3P)3d$	$4^2F_{7/2}$	$2s + 1(1)1\ 2p - 1(1)2\ 2p + 2(0)2\ 3d + 1(5)7$	$7/2^o$...	1.06289E+03	0.83(173)0.41(182)
26	174	$2s2p^3(^3P)3d$	$4^2F_{9/2}$	$2s + 1(1)1\ 2p + 3(3)4\ 3d + 1(5)9$	$9/2^o$...	1.06431E+03	0.85(174)
26	175	$2s2p^3(^3P)3d$	$4^2P_{5/2}$	$2s + 1(1)1\ 2p - 1(1)2\ 2p + 2(0)2\ 3d + 1(5)5$	$5/2^o$...	1.06534E+03	-0.82(175) - 0.40(183)
26	176	$2s2p^3(^3P)3d$	$4^2P_{1/2}$	$2s + 1(1)1\ 2p - 1(1)2\ 2p + 2(0)2\ 3d - 1(3)1$	$1/2^o$...	1.06574E+03	-0.75(176) - 0.47(179)
26	177	$2s2p^3(^3P)3d$	$4^2P_{3/2}$	$2s + 1(1)1\ 2p - 1(1)2\ 2p + 2(0)2\ 3d + 1(5)3$	$3/2^o$...	1.06582E+03	0.69(177)0.55(184)
26	178	$2s2p^3(^3S)3p$	$2^2P_{3/2}$	$2s + 1(1)1\ 2p - 1(1)2\ 2p + 2(4)4\ 3p + 1(3)3$	$3/2^e$...	1.06682E+03	0.64(192) - 0.62(162)0.43(178)
26	179	$2s2p^3(^3P)3d$	$4^2D_{1/2}$	$2s + 1(1)1\ 2p + 3(3)4\ 3d - 1(3)1$	$1/2^o$...	1.06724E+03	-0.77(179)0.48(176)
26	180	$2s2p^3(^3P)3d$	$2^2D_{3/2}$	$2s + 1(1)1\ 2p + 3(3)4\ 3d + 1(5)3$	$3/2^o$...	1.06748E+03	0.75(180)0.46(177)

TABLE 1—Continued

Z	Key	Conf	LSJ	jj ^{a,b,c}	J ^π	Energy		Mixing coefficients	
						NIST ^d	MBPT ^e	LSJ ^f	
26	181	2s2p ³ (¹ D)3p	² F _{1/2}	2s + 1(1)1 2p - 1(1)2 2p + 2(4)4 3p + 1(3)1	1/2 ^e	...	1.06811E+03	-0.80(181) - 0.41(197)	
26	182	2s2p ³ (³ P)3d	⁴ D _{7/2}	2s + 1(1)1 2p + 3(3)4 3d + 1(5)7	7/2 ^o	...	1.06814E+03	-0.83(182)	
26	183	2s2p ³ (³ P)3d	⁴ D _{5/2}	2s + 1(1)1 2p + 3(3)4 3d - 1(3)5	5/2 ^o	...	1.06838E+03	-0.82(183)	
26	184	2s2p ³ (³ P)3d	⁴ D _{3/2}	2s + 1(1)1 2p + 3(3)4 3d - 1(3)3	3/2 ^o	...	1.06874E+03	0.70(184) 0.53(180)	
26	185	2s2p ³ (³ P)3d	² F _{5/2}	2s + 1(1)1 2p - 1(1)2 2p + 2(0)2 3d + 1(5)5	5/2 ^o	...	1.07111E+03	0.93(185)	
26	186	2s2p ³ (³ P)3d	² F _{7/2}	2s + 1(1)1 2p + 3(3)4 3d + 1(5)7	7/2 ^o	...	1.07325E+03	0.85(186)	
26	187	2s2p ³ (³ P)3d	² D _{5/2}	2s + 1(1)1 2p + 3(3)4 3d + 1(5)5	5/2 ^o	...	1.07513E+03	0.75(187) 0.49(158)	
26	188	2s2p ³ (¹ P)3p	² D _{5/2}	2s + 1(1)1 2p + 3(3)2 3p + 1(3)5	5/2 ^e	...	1.07592E+03	0.93(188)	
26	189	2s2p ³ (³ P)3d	² F _{1/2}	2s + 1(1)1 2p + 3(3)4 3d + 1(5)1	1/2 ^o	...	1.07675E+03	-0.87(189)	
26	190	2s2p ³ (¹ P)3p	² P _{3/2}	2s + 1(1)1 2p + 3(3)2 3p - 1(1)3	3/2 ^e	...	1.07696E+03	-0.86(190)	
26	191	2s2p ³ (¹ P)3p	² S _{1/2}	2s + 1(1)1 2p + 3(3)2 3p - 1(1)1	1/2 ^e	...	1.07716E+03	-0.69(191) 0.62(197)	
26	192	2s2p ³ (¹ P)3p	² D _{3/2}	2s + 1(1)1 2p + 3(3)2 3p + 1(3)3	3/2 ^e	...	1.07721E+03	-0.63(192) 0.55(178) - 0.44(190)	
26	193	2s2p ³ (³ P)3d	² P _{3/2}	2s + 1(1)1 2p - 1(1)2 2p + 2(0)2 3d + 1(5)3	3/2 ^o	...	1.08051E+03	-0.88(193)	
26	194	2s2p ³ (³ S)3d	⁴ D _{5/2}	2s + 1(1)1 2p - 1(1)2 2p + 2(4)2 3d - 1(3)5	5/2 ^o	...	1.08363E+03	-0.88(194)	
26	195	2s2p ³ (³ S)3d	⁴ D _{3/2}	2s + 1(1)1 2p - 1(1)2 2p + 2(4)2 3d - 1(3)3	3/2 ^o	...	1.08402E+03	0.73(195) - 0.43(219) 0.42(199)	
26	196	2s2p ³ (³ S)3d	⁴ D _{7/2}	2s + 1(1)1 2p - 1(1)2 2p + 2(4)2 3d + 1(5)7	7/2 ^o	...	1.08436E+03	-0.90(196)	
26	197	2s2p ³ (¹ P)3p	² F _{1/2}	2s + 1(1)1 2p + 3(3)2 3p + 1(3)1	1/2 ^e	...	1.08441E+03	0.56(163) 0.56(191) 0.55(197)	
26	198	2s2p ³ (³ S)3d	⁴ D _{1/2}	2s + 1(1)1 2p - 1(1)2 2p + 2(4)2 3d - 1(3)1	1/2 ^o	...	1.08510E+03	0.89(198)	
26	199	2s2p ³ (³ S)3d	² D _{3/2}	2s + 1(1)1 2p - 1(1)2 2p + 2(4)2 3d + 1(5)3	3/2 ^o	...	1.08712E+03	-0.67(199) 0.58(195)	
26	200	2s2p ³ (¹ D)3d	² D _{5/2}	2s + 1(1)1 2p - 1(1)2 2p + 2(4)4 3d + 1(5)5	5/2 ^o	...	1.08840E+03	-0.69(200) - 0.57(208)	
26	201	2s2p ³ (¹ D)3d	² G _{9/2}	2s + 1(1)1 2p - 1(1)2 2p + 2(4)4 3d + 1(5)9	9/2 ^o	...	1.08888E+03	0.97(201)	
26	202	2s2p ³ (¹ D)3d	² G _{7/2}	2s + 1(1)1 2p - 1(1)2 2p + 2(4)4 3d - 1(3)7	7/2 ^o	...	1.08933E+03	0.86(202)	
26	203	2s2p ³ (¹ D)3d	² F _{7/2}	2s + 1(1)1 2p - 1(1)2 2p + 2(4)4 3d + 1(5)7	7/2 ^o	...	1.09140E+03	-0.90(203)	
26	204	2s2p ³ (¹ D)3d	² F _{5/2}	2s + 1(1)1 2p - 1(1)2 2p + 2(4)4 3d - 1(3)5	5/2 ^o	...	1.09179E+03	-0.90(204)	
26	205	2s2p ³ (¹ D)3d	² P _{3/2}	2s + 1(1)1 2p - 1(1)2 2p + 2(4)4 3d - 1(3)3	3/2 ^o	...	1.09440E+03	-0.88(205)	
26	206	2s2p ³ (¹ D)3d	² F _{1/2}	2s + 1(1)1 2p - 1(1)2 2p + 2(4)4 3d - 1(3)1	1/2 ^o	...	1.09538E+03	0.75(206) - 0.62(210)	
26	207	2s2p ³ (¹ D)3d	² D _{3/2}	2s + 1(1)1 2p - 1(1)2 2p + 2(4)4 3d + 1(5)3	3/2 ^o	...	1.09699E+03	-0.75(207) - 0.48(205)	
26	208	2s2p ³ (³ S)3d	² D _{5/2}	2s + 1(1)1 2p - 1(1)2 2p + 2(4)4 3d + 1(5)5	5/2 ^o	...	1.09713E+03	0.62(200) - 0.55(208) - 0.52(217)	
26	209	2p ⁴ (³ P)3s	⁴ P _{5/2}	2p + 2(4)4 3s + 1(1)5	5/2 ^e	...	1.09773E+03	0.94(209)	
26	210	2s2p ³ (¹ D)3d	² S _{1/2}	2s + 1(1)1 2p - 1(1)2 2p + 2(4)4 3d + 1(5)1	1/2 ^o	...	1.09878E+03	0.75(210) 0.52(206)	
26	211	2p ⁴ (³ P)3s	² P _{3/2}	2p + 2(4)4 3s + 1(1)3	3/2 ^e	...	1.10202E+03	0.68(211) 0.64(218)	
26	212	2s2p ³ (¹ P)3d	² F _{7/2}	2s + 1(1)1 2p + 3(3)2 3d + 1(5)7	7/2 ^o	...	1.10646E+03	-0.92(212)	
26	213	2s2p ³ (¹ P)3d	² D _{5/2}	2s + 1(1)1 2p + 3(3)2 3d + 1(5)5	5/2 ^o	...	1.10688E+03	-0.71(213) - 0.55(217)	
26	214	2p ⁴ (³ P)3s	⁴ P _{1/2}	2p + 2(0)0 3s + 1(1)1	1/2 ^e	...	1.10873E+03	-0.95(214)	
26	215	2s2p ³ (¹ P)3d	² F _{3/2}	2s + 1(1)1 2p + 3(3)2 3d - 1(3)3	3/2 ^o	...	1.10889E+03	0.82(215) - 0.46(219)	
26	216	2s2p ³ (¹ P)3d	² F _{1/2}	2s + 1(1)1 2p + 3(3)2 3d - 1(3)1	1/2 ^o	...	1.10905E+03	0.92(216)	
26	217	2s2p ³ (¹ P)3d	² F _{5/2}	2s + 1(1)1 2p + 3(3)2 3d - 1(3)5	5/2 ^o	...	1.10953E+03	-0.65(213) 0.59(217)	
26	218	2p ⁴ (³ P)3s	⁴ P _{3/2}	2p - 1(1)1 2p + 3(3)2 3s + 1(1)3	3/2 ^e	...	1.11071E+03	-0.77(218) 0.59(211)	
26	219	2s2p ³ (¹ P)3d	² D _{3/2}	2s + 1(1)1 2p + 3(3)2 3d + 1(5)3	3/2 ^o	...	1.11418E+03	-0.71(219) - 0.57(199)	
26	220	2p ⁴ (³ P)3s	² P _{1/2}	2p - 1(1)1 2p + 3(3)2 3s + 1(1)1	1/2 ^e	...	1.11555E+03	0.96(220)	
26	221	2p ⁴ (¹ D)3s	² D _{5/2}	2p - 1(1)1 2p + 3(3)4 3s + 1(1)5	5/2 ^e	...	1.12037E+03	-0.94(221)	
26	222	2p ⁴ (¹ D)3s	² D _{3/2}	2p - 1(1)1 2p + 3(3)4 3s + 1(1)3	3/2 ^e	...	1.12101E+03	-0.91(222)	
26	223	2p ⁴ (³ P)3p	⁴ P _{3/2}	2p + 2(4)4 3p - 1(1)3	3/2 ^o	...	1.12142E+03	-0.82(223)	
26	224	2p ⁴ (³ P)3p	⁴ P _{5/2}	2p + 2(4)4 3p - 1(1)5	5/2 ^o	...	1.12193E+03	-0.82(224) 0.51(232)	
26	225	2p ⁴ (³ P)3p	² F _{1/2}	2p + 2(4)4 3p + 1(3)1	1/2 ^o	...	1.12570E+03	-0.65(228) - 0.47(225) 0.46(249)	
26	226	2p ⁴ (³ P)3p	⁴ D _{7/2}	2p + 2(4)4 3p + 1(3)7	7/2 ^o	...	1.12605E+03	0.93(226)	
26	227	2p ⁴ (³ P)3p	² D _{5/2}	2p + 2(4)4 3p + 1(3)5	5/2 ^o	...	1.12621E+03	-0.77(227) - 0.42(224)	
26	228	2p ⁴ (³ P)3p	⁴ P _{1/2}	2p - 1(1)1 2p + 3(3)2 3p - 1(1)1	1/2 ^o	...	1.13295E+03	0.73(228) - 0.41(230)	
26	229	2p ⁴ (³ P)3p	⁴ D _{3/2}	2p + 2(4)4 3p + 1(3)3	3/2 ^o	...	1.13307E+03	-0.72(229) - 0.47(235) 0.41(233)	
26	230	2p ⁴ (³ P)3p	⁴ D _{1/2}	2p + 2(0)0 3p - 1(1)1	1/2 ^o	...	1.13410E+03	-0.82(230)	
26	231	2p ⁴ (³ P)3p	² P _{3/2}	2p - 1(1)1 2p + 3(3)2 3p - 1(1)3	3/2 ^o	...	1.13550E+03	-0.63(231) - 0.62(229)	
26	232	2p ⁴ (³ P)3p	⁴ D _{5/2}	2p - 1(1)1 2p + 3(3)2 3p + 1(3)5	5/2 ^o	...	1.13740E+03	-0.76(232) 0.50(227)	
26	233	2p ⁴ (³ P)3p	⁴ S _{3/2}	2p + 2(0)0 3p + 1(3)3	3/2 ^o	...	1.13846E+03	0.67(233) 0.57(223)	
26	234	2p ⁴ (³ P)3p	² S _{1/2}	2p - 1(1)1 2p + 3(3)2 3p + 1(3)1	1/2 ^o	...	1.14019E+03	0.77(234) 0.44(225)	
26	235	2p ⁴ (³ P)3p	² D _{3/2}	2p - 1(1)1 2p + 3(3)2 3p + 1(3)3	3/2 ^o	...	1.14081E+03	0.83(235) 0.49(233)	
26	236	2p ⁴ (¹ D)3p	² F _{5/2}	2p - 1(1)1 2p + 3(3)4 3p - 1(1)5	5/2 ^o	...	1.14377E+03	0.90(236)	
26	237	2p ⁴ (¹ D)3p	² F _{7/2}	2p - 1(1)1 2p + 3(3)4 3p + 1(3)7	7/2 ^o	...	1.14674E+03	-0.93(237)	
26	238	2p ⁴ (¹ S)3s	² S _{1/2}	3s + 1(1)1	1/2 ^e	...	1.14848E+03	-0.91(238)	
26	239	2p ⁴ (¹ D)3p	² D _{3/2}	2p - 1(1)1 2p + 3(3)4 3p + 1(3)3	3/2 ^o	...	1.14914E+03	-0.91(239)	
26	240	2p ⁴ (¹ D)3p	² D _{5/2}	2p - 1(1)1 2p + 3(3)4 3p + 1(3)5	5/2 ^o	...	1.15077E+03	-0.92(240)	

TABLE 1—Continued

Z	Key	Conf	LSJ	$jj^{a,b,c}$	J^π	Energy		Mixing coefficients
						NIST ^d	MBPT ^e	LSJ ^f
26	241	$2p^4(3P)3d$	$4D_{7/2}$	$2p + 2(4)4\ 3d + 1(5)7$	$7/2^e$...	1.15207E+03	0.87(241) - 0.42(255)
26	242	$2p^4(3P)3d$	$4D_{5/2}$	$2p + 2(4)4\ 3d - 1(3)5$	$5/2^e$...	1.15211E+03	0.88(242)
26	243	$2p^4(3P)3d$	$4D_{3/2}$	$2p + 2(4)4\ 3d - 1(3)3$	$3/2^e$...	1.15292E+03	-0.84(243) 0.42(250)
26	244	$2p^4(3P)3d$	$4D_{1/2}$	$2p + 2(4)4\ 3d - 1(3)1$	$1/2^e$...	1.15417E+03	-0.71(244) 0.42(252) 0.41(248)
26	245	$2p^4(3P)3d$	$4F_{9/2}$	$2p + 2(4)4\ 3d + 1(5)9$	$9/2^e$...	1.15484E+03	0.93(245)
26	246	$2p^4(3P)3d$	$2F_{7/2}$	$2p + 2(4)4\ 3d - 1(3)7$	$7/2^e$...	1.15627E+03	-0.76(246) - 0.51(255)
26	247	$2p^4(1D)3p$	$2F_{3/2}$	$2p - 1(1)1\ 2p + 3(3)4\ 3p - 1(1)3$	$3/2^o$...	1.15671E+03	-0.71(247) - 0.65(231)
26	248	$2p^4(3P)3d$	$4F_{1/2}$	$2p + 2(4)4\ 3d + 1(5)1$	$1/2^e$...	1.15952E+03	-0.83(248) 0.44(252)
26	249	$2p^4(1D)3p$	$2F_{1/2}$	$2p - 1(1)1\ 2p + 3(3)4\ 3p + 1(3)1$	$1/2^o$...	1.16135E+03	0.75(249) 0.56(225)
26	250	$2p^4(3P)3d$	$4F_{3/2}$	$2p + 2(4)4\ 3d + 1(5)3$	$3/2^e$...	1.16172E+03	0.74(250) 0.53(256)
26	251	$2p^4(3P)3d$	$2F_{5/2}$	$2p + 2(4)4\ 3d + 1(5)5$	$5/2^e$...	1.16223E+03	0.60(254) 0.53(251) - 0.42(259) - 0.42(257)
26	252	$2p^4(3P)3d$	$2F_{1/2}$	$2p - 1(1)1\ 2p + 3(3)2\ 3d - 1(3)1$	$1/2^e$...	1.16436E+03	0.69(244) 0.53(252) - 0.41(270)
26	253	$2p^4(3P)3d$	$4F_{3/2}$	$2p + 2(0)0\ 3d - 1(3)3$	$3/2^e$...	1.16547E+03	0.91(253)
26	254	$2p^4(3P)3d$	$4F_{5/2}$	$2p + 2(0)0\ 3d + 1(5)5$	$5/2^e$...	1.16603E+03	-0.73(254) - 0.51(257)
26	255	$2p^4(3P)3d$	$4F_{7/2}$	$2p - 1(1)1\ 2p + 3(3)2\ 3d + 1(5)7$	$7/2^e$...	1.16611E+03	0.72(255) - 0.51(246) 0.58(241)
26	256	$2p^4(3P)3d$	$2D_{3/2}$	$2p - 1(1)1\ 2p + 3(3)2\ 3d - 1(3)3$	$3/2^e$...	1.16705E+03	0.59(243) 0.49(250) - 0.48(256) 0.43(269)
26	257	$2p^4(3P)3d$	$4F_{5/2}$	$2p - 1(1)1\ 2p + 3(3)2\ 3d + 1(5)5$	$5/2^e$...	1.16929E+03	-0.70(257) - 0.62(251)
26	258	$2p^4(3P)3d$	$2F_{3/2}$	$2p - 1(1)1\ 2p + 3(3)2\ 3d + 1(5)3$	$3/2^e$...	1.17106E+03	-0.72(258) 0.52(268)
26	259	$2p^4(3P)3d$	$2D_{5/2}$	$2p - 1(1)1\ 2p + 3(3)2\ 3d - 1(3)5$	$5/2^e$...	1.17228E+03	0.65(259) 0.54(251) - 0.42(267)
26	260	$2p^4(1D)3d$	$2G_{7/2}$	$2p - 1(1)1\ 2p + 3(3)4\ 3d - 1(3)7$	$7/2^e$...	1.17424E+03	-0.91(260)
26	261	$2p^4(1D)3d$	$2G_{9/2}$	$2p - 1(1)1\ 2p + 3(3)4\ 3d + 1(5)9$	$9/2^e$...	1.17470E+03	-0.93(261)
26	262	$2p^4(1S)3p$	$2F_{1/2}$	$3p - 1(1)1$	$1/2^o$...	1.17681E+03	-0.86(262) 0.42(225)
26	263	$2p^4(1S)3p$	$2F_{3/2}$	$3p + 1(3)3$	$3/2^o$...	1.17691E+03	0.94(263)
26	264	$2p^4(1D)3d$	$2F_{5/2}$	$2p - 1(1)1\ 2p + 3(3)4\ 3d + 1(5)5$	$5/2^e$...	1.17878E+03	-0.82(264) - 0.54(267)
26	265	$2p^4(1D)3d$	$2S_{1/2}$	$2p - 1(1)1\ 2p + 3(3)4\ 3d - 1(3)1$	$1/2^e$...	1.18009E+03	0.92(265)
26	266	$2p^4(1D)3d$	$2F_{7/2}$	$2p - 1(1)1\ 2p + 3(3)4\ 3d + 1(5)7$	$7/2^e$...	1.18015E+03	0.95(266)
26	267	$2p^4(1D)3d$	$2D_{5/2}$	$2p - 1(1)1\ 2p + 3(3)4\ 3d - 1(3)5$	$5/2^e$...	1.18382E+03	-0.70(267) - 0.56(259) 0.40(264)
26	268	$2p^4(1D)3d$	$2F_{3/2}$	$2p - 1(1)1\ 2p + 3(3)4\ 3d - 1(3)3$	$3/2^e$...	1.18397E+03	-0.80(268) - 0.53(258)
26	269	$2p^4(1D)3d$	$2D_{3/2}$	$2p - 1(1)1\ 2p + 3(3)4\ 3d + 1(5)3$	$3/2^e$...	1.18731E+03	0.79(269) 0.58(256)
26	270	$2p^4(1D)3d$	$2F_{1/2}$	$2p - 1(1)1\ 2p + 3(3)4\ 3d + 1(5)1$	$1/2^e$...	1.18862E+03	0.77(270) 0.59(252)
26	271	$2s^2 2p^2(3P)4s$	$4F_{1/2}$	$4s + 1(1)1$	$1/2^e$...	1.20056E+03	0.82(271) - 0.48(275)
26	272	$2p^4(1S)3d$	$2D_{5/2}$	$3d + 1(5)5$	$5/2^e$...	1.20623E+03	-0.95(272)
26	273	$2p^4(1S)3d$	$2D_{3/2}$	$3d - 1(3)3$	$3/2^e$...	1.20825E+03	-0.90(273)
26	274	$2s^2 2p^2(3P)4s$	$4F_{3/2}$	$2p - 1(1)1\ 2p + 1(3)2\ 4s + 1(1)3$	$3/2^e$...	1.20938E+03	0.94(274)
26	275	$2s^2 2p^2(3P)4s$	$2F_{1/2}$	$2p - 1(1)1\ 2p + 1(3)2\ 4s + 1(1)1$	$1/2^e$...	1.21039E+03	0.86(275) 0.51(271)
26	276	$2s^2 2p^2(3P)4p$	$4D_{1/2}$	$4p - 1(1)1$	$1/2^o$...	1.21098E+03	0.77(276)
26	277	$2s^2 2p^2(3P)4p$	$4F_{3/2}$	$4p + 1(3)3$	$3/2^o$...	1.21351E+03	0.64(281) 0.56(277) - 0.44(284)
26	278	$2s^2 2p^2(3P)4s$	$4F_{5/2}$	$2p - 1(1)1\ 2p + 1(3)4\ 4s + 1(1)5$	$5/2^e$...	1.21463E+03	0.88(278) - 0.47(293)
26	279	$2s^2 2p^2(3P)4s$	$2F_{3/2}$	$2p - 1(1)1\ 2p + 1(3)4\ 4s + 1(1)3$	$3/2^e$...	1.21583E+03	-0.82(279) 0.51(294)
26	280	$2s^2 2p^2(3P)4p$	$2S_{1/2}$	$2p - 1(1)1\ 2p + 1(3)2\ 4p - 1(1)1$	$1/2^o$...	1.21955E+03	-0.61(280) 0.58(276) - 0.54(283)
26	281	$2s^2 2p^2(3P)4p$	$4D_{3/2}$	$2p - 1(1)1\ 2p + 1(3)2\ 4p - 1(1)3$	$3/2^o$...	1.22105E+03	-0.78(281)
26	282	$2s^2 2p^2(3P)4p$	$4D_{5/2}$	$2p - 1(1)1\ 2p + 1(3)2\ 4p + 1(3)5$	$5/2^o$...	1.22167E+03	0.82(282) 0.50(286)
26	283	$2s^2 2p^2(3P)4p$	$4F_{1/2}$	$2p - 1(1)1\ 2p + 1(3)2\ 4p + 1(3)1$	$1/2^o$...	1.22266E+03	-0.74(283) 0.48(292) 0.43(280)
26	284	$2s^2 2p^2(3P)4p$	$2D_{3/2}$	$2p - 1(1)1\ 2p + 1(3)2\ 4p + 1(3)3$	$3/2^o$...	1.22338E+03	-0.76(284) - 0.49(277)
26	285	$2s^2 2p^2(3P)4d$	$4F_{3/2}$	$4d - 1(3)3$	$3/2^e$...	1.22408E+03	-0.76(285) - 0.41(301)
26	286	$2s^2 2p^2(3P)4p$	$4F_{5/2}$	$2p - 1(1)1\ 2p + 1(3)4\ 4p - 1(1)5$	$5/2^o$...	1.22548E+03	-0.60(286) 0.51(282) 0.47(291) 0.40(320)
26	287	$2s^2 2p^2(3P)4d$	$4F_{5/2}$	$4d + 1(5)5$	$5/2^e$	1.22500E+03	1.22550E+03	-0.58(300) - 0.56(305) 0.42(302) - 0.42(287)
26	288	$2s^2 2p^2(3P)4p$	$4D_{7/2}$	$2p - 1(1)1\ 2p + 1(3)4\ 4p + 1(3)7$	$7/2^o$...	1.22673E+03	-0.89(288) 0.46(321)
26	289	$2s^2 2p^2(3P)4p$	$4S_{3/2}$	$2p - 1(1)1\ 2p + 1(3)4\ 4p - 1(1)3$	$3/2^o$...	1.22763E+03	0.72(289) - 0.53(277) - 0.40(334)
26	290	$2s^2 2p^2(3P)4p$	$2F_{3/2}$	$2p - 1(1)1\ 2p + 1(3)4\ 4p + 1(3)3$	$3/2^o$...	1.22845E+03	-0.80(290) 0.48(319)
26	291	$2s^2 2p^2(3P)4p$	$2D_{5/2}$	$2p - 1(1)1\ 2p + 1(3)4\ 4p + 1(3)5$	$5/2^o$...	1.22950E+03	0.70(291) 0.53(286) - 0.41(318)
26	292	$2s^2 2p^2(3P)4p$	$2F_{1/2}$	$2p - 1(1)1\ 2p + 1(3)4\ 4p + 1(3)1$	$1/2^o$...	1.22980E+03	-0.77(292) 0.48(280)
26	293	$2s^2 2p^2(1D)4s$	$2D_{5/2}$	$2p + 2(4)4\ 4s + 1(1)5$	$5/2^e$...	1.23061E+03	-0.88(293) - 0.47(278)
26	294	$2s^2 2p^2(1D)4s$	$2D_{3/2}$	$2p + 2(4)4\ 4s + 1(1)3$	$3/2^e$...	1.23102E+03	-0.86(294) - 0.47(279)
26	295	$2s^2 2p^2(3P)4f$	$4G_{5/2}$	$4f - 1(5)5$	$5/2^o$...	1.23166E+03	0.70(295) 0.45(308) 0.42(329)
26	296	$2s^2 2p^2(3P)4f$	$4G_{7/2}$	$4f + 1(7)7$	$7/2^o$...	1.23186E+03	-0.52(311) 0.52(309) 0.50(327) 0.46(296)
26	297	$2s^2 2p^2(3P)4d$	$2F_{3/2}$	$2p - 1(1)1\ 2p + 1(3)2\ 4d - 1(3)3$	$3/2^e$...	1.23307E+03	-0.63(285) 0.60(297) 0.40(301)
26	298	$2s^2 2p^2(3P)4d$	$4F_{7/2}$	$2p - 1(1)1\ 2p + 1(3)2\ 4d + 1(5)7$	$7/2^e$...	1.23335E+03	0.77(298) 0.58(303)
26	299	$2s^2 2p^2(3P)4d$	$4D_{1/2}$	$2p - 1(1)1\ 2p + 1(3)2\ 4d - 1(3)1$	$1/2^e$...	1.23345E+03	-0.89(299)
26	300	$2s^2 2p^2(3P)4d$	$4F_{5/2}$	$2p - 1(1)1\ 2p + 1(3)2\ 4d - 1(3)5$	$5/2^e$	1.23265E+03	1.23382E+03	-0.79(300) 0.50(287)

TABLE 1—Continued

Z	Key	Conf	LSJ	jj ^{a,b,c}	J ^π	Energy		Mixing coefficients
						NIST ^d	MBPT ^e	LSJ ^f
26	301	2s ² 2p ² (³ P)4d	4D _{3/2}	2p−1(1)1 2p+1(3)2 4d+1(5)3	3/2 ^e	...	1.23531E+03	0.63(301)−0.51(297)−0.43(316)
26	302	2s ² 2p ² (³ P)4d	2F _{5/2}	2p−1(1)1 2p+1(3)2 4d+1(5)5	5/2 ^e	1.23538E+03	1.23546E+03	−0.82(302)−0.45(287)
26	303	2s ² 2p ² (³ P)4d	4D _{7/2}	2p−1(1)1 2p+1(3)4 4d−1(3)7	7/2 ^e	...	1.23809E+03	−0.60(303)0.58(298)0.42(335)
26	304	2s ² 2p ² (³ P)4d	4F _{9/2}	2p−1(1)1 2p+1(3)4 4d+1(5)9	9/2 ^e	...	1.23827E+03	0.89(304)−0.46(336)
26	305	2s ² 2p ² (³ P)4d	4D _{5/2}	2p−1(1)1 2p+1(3)4 4d−1(3)5	5/2 ^e	1.23885E+03	1.23940E+03	−0.72(305)0.51(287)
26	306	2s ² 2p ² (³ P)4d	4F _{3/2}	2p−1(1)1 2p+1(3)4 4d−1(3)3	3/2 ^e	1.24096E+03	1.24002E+03	−0.77(306)0.45(301)
26	307	2s ² 2p ² (³ P)4d	4F _{1/2}	2p−1(1)1 2p+1(3)4 4d−1(3)1	1/2 ^e	1.24096E+03	1.24033E+03	−0.85(307)0.41(342)
26	308	2s ² 2p ² (³ P)4f	2D _{5/2}	2p−1(1)1 2p+1(3)2 4f−1(5)5	5/2 ^o	...	1.24050E+03	0.68(295)−0.60(308)
26	309	2s ² 2p ² (³ P)4f	4F _{7/2}	2p−1(1)1 2p+1(3)2 4f+1(7)7	7/2 ^o	...	1.24066E+03	0.67(309)−0.63(296)
26	310	2s ² 2p ² (³ P)4d	2F _{1/2}	2p−1(1)1 2p+1(3)4 4d+1(5)1	1/2 ^e	...	1.24085E+03	−0.82(310)
26	311	2s ² 2p ² (³ P)4f	2G _{7/2}	2p−1(1)1 2p+1(3)2 4f−1(5)7	7/2 ^o	...	1.24094E+03	−0.71(311)−0.47(296)−0.42(332)
26	312	2s ² 2p ² (³ P)4f	4G _{9/2}	2p−1(1)1 2p+1(3)2 4f+1(7)9	9/2 ^o	...	1.24095E+03	−0.72(312)−0.56(330)0.41(323)
26	313	2s ² 2p ² (³ P)4f	4F _{3/2}	2p−1(1)1 2p+1(3)2 4f−1(5)3	3/2 ^o	...	1.24114E+03	−0.77(313)−0.45(328)−0.45(331)
26	314	2s ² 2p ² (³ P)4f	4D _{5/2}	2p−1(1)1 2p+1(3)2 4f+1(7)5	5/2 ^o	...	1.24140E+03	0.57(333)−0.54(314)−0.50(329)
26	315	2s ² 2p ² (³ P)4d	2D _{5/2}	2p−1(1)1 2p+1(3)4 4d+1(5)5	5/2 ^e	1.24220E+03	1.24152E+03	0.80(315)−0.46(341)
26	316	2s ² 2p ² (³ P)4d	2D _{3/2}	2p−1(1)1 2p+1(3)4 4d+1(5)3	3/2 ^e	1.24517E+03	1.24159E+03	0.79(316)
26	317	2s ² 2p ² (³ P)4d	2F _{7/2}	2p−1(1)1 2p+1(3)4 4d+1(5)7	7/2 ^e	1.24220E+03	1.24180E+03	0.76(317)−0.44(339)0.43(303)
26	318	2s ² 2p ² (¹ D)4p	2F _{5/2}	2p+2(4)4 4p+1(3)5	5/2 ^o	...	1.24233E+03	0.73(318)0.48(320)0.41(291)
26	319	2s ² 2p ² (¹ D)4p	2D _{3/2}	2p+2(4)4 4p−1(1)3	3/2 ^o	...	1.24264E+03	0.71(319)−0.59(334)
26	320	2s ² 2p ² (¹ D)4p	2D _{5/2}	2p+2(4)4 4p−1(1)5	5/2 ^o	...	1.24298E+03	0.79(320)−0.44(318)
26	321	2s ² 2p ² (¹ D)4p	2F _{7/2}	2p+2(4)4 4p+1(3)7	7/2 ^o	...	1.24299E+03	0.89(321)0.46(288)
26	322	2s ² 2p ² (¹ D)4p	2F _{1/2}	2p+2(4)4 4p+1(3)1	1/2 ^o	...	1.24370E+03	0.93(322)
26	323	2s ² 2p ² (³ P)4f	2G _{9/2}	2p−1(1)1 2p+1(3)4 4f−1(5)9	9/2 ^o	...	1.24603E+03	0.65(323)0.56(312)−0.45(350)
26	324	2s ² 2p ² (³ P)4f	4G _{11/2}	2p−1(1)1 2p+1(3)4 4f+1(7)11	11/2 ^o	...	1.24607E+03	0.88(324)−0.47(351)
26	325	2s ² 2p ² (¹ S)4s	2S _{1/2}	2p+2(0)0 4s+1(1)1	1/2 ^e	...	1.24621E+03	−0.94(325)
26	326	2s ² 2p ² (³ P)4f	4D _{1/2}	2p−1(1)1 2p+1(3)4 4f−1(5)1	1/2 ^o	...	1.24630E+03	−0.90(326)0.44(354)
26	327	2s ² 2p ² (³ P)4f	4F _{7/2}	2p−1(1)1 2p+1(3)4 4f−1(5)7	7/2 ^o	...	1.24633E+03	0.67(327)−0.48(346)−0.40(296)
26	328	2s ² 2p ² (³ P)4f	4D _{3/2}	2p−1(1)1 2p+1(3)4 4f−1(5)3	3/2 ^o	...	1.24635E+03	0.80(328)
26	329	2s ² 2p ² (³ P)4f	4F _{5/2}	2p−1(1)1 2p+1(3)4 4f−1(5)5	5/2 ^o	...	1.24640E+03	0.67(329)−0.54(314)0.41(348)
26	330	2s ² 2p ² (³ P)4f	4F _{9/2}	2p−1(1)1 2p+1(3)4 4f+1(7)9	9/2 ^o	...	1.24651E+03	0.68(330)0.49(323)−0.49(347)
26	331	2s ² 2p ² (³ P)4f	2D _{3/2}	2p−1(1)1 2p+1(3)4 4f+1(7)3	3/2 ^o	...	1.24654E+03	−0.77(331)0.41(313)
26	332	2s ² 2p ² (³ P)4f	2F _{7/2}	2p−1(1)1 2p+1(3)4 4f+1(7)7	7/2 ^o	...	1.24662E+03	−0.69(332)0.48(349)
26	333	2s ² 2p ² (³ P)4f	2F _{5/2}	2p−1(1)1 2p+1(3)4 4f+1(7)5	5/2 ^o	...	1.24666E+03	−0.69(333)0.49(308)−0.40(353)
26	334	2s ² 2p ² (¹ D)4p	2F _{3/2}	2p+2(4)4 4p+1(3)3	3/2 ^o	...	1.24677E+03	−0.64(334)−0.49(319)−0.44(290)
26	335	2s ² 2p ² (¹ D)4d	2F _{7/2}	2p+2(4)4 4d+1(5)7	7/2 ^e	...	1.25394E+03	−0.75(335)−0.48(339)
26	336	2s ² 2p ² (¹ D)4d	2G _{9/2}	2p+2(4)4 4d+1(5)9	9/2 ^e	...	1.25480E+03	−0.89(336)−0.45(304)
26	337	2s ² 2p ² (¹ D)4d	2D _{5/2}	2p+2(4)4 4d−1(3)5	5/2 ^e	1.25745E+03	1.25537E+03	−0.71(337)0.57(341)
26	338	2s ² 2p ² (¹ D)4d	2D _{3/2}	2p+2(4)4 4d−1(3)3	3/2 ^e	1.25600E+03	1.25546E+03	0.89(338)
26	339	2s ² 2p ² (¹ D)4d	2G _{7/2}	2p+2(4)4 4d−1(3)7	7/2 ^e	1.25745E+03	1.25577E+03	−0.71(339)0.49(335)−0.41(317)
26	340	2s ² 2p ² (¹ D)4d	2F _{1/2}	2p+2(4)4 4d+1(5)1	1/2 ^e	...	1.25585E+03	−0.92(340)
26	341	2s ² 2p ² (¹ D)4d	2F _{5/2}	2p+2(4)4 4d+1(5)5	5/2 ^e	1.25832E+03	1.25743E+03	0.62(341)0.55(337)0.48(315)
26	342	2s ² 2p ² (¹ D)4d	2S _{1/2}	2p+2(4)4 4d−1(3)1	1/2 ^e	...	1.25770E+03	0.89(342)
26	343	2s ² 2p ² (¹ D)4d	2F _{3/2}	2p+2(4)4 4d+1(5)3	3/2 ^e	1.25832E+03	1.25787E+03	−0.86(343)
26	344	2s ² 2p ² (¹ S)4p	2F _{1/2}	2p+2(0)0 4p−1(1)1	1/2 ^o	...	1.25812E+03	0.95(344)
26	345	2s ² 2p ² (¹ S)4p	2F _{3/2}	2p+2(0)0 4p+1(3)3	3/2 ^o	...	1.25903E+03	−0.95(345)
26	346	2s ² 2p ² (¹ D)4f	2G _{7/2}	2p+2(4)4 4f−1(5)7	7/2 ^o	...	1.26157E+03	−0.84(346)
26	347	2s ² 2p ² (¹ D)4f	2G _{9/2}	2p+2(4)4 4f+1(7)9	9/2 ^o	...	1.26158E+03	−0.86(347)−0.41(330)
26	348	2s ² 2p ² (¹ D)4f	2F _{5/2}	2p+2(4)4 4f−1(5)5	5/2 ^o	...	1.26174E+03	0.89(348)
26	349	2s ² 2p ² (¹ D)4f	2F _{7/2}	2p+2(4)4 4f+1(7)7	7/2 ^o	...	1.26192E+03	−0.85(349)
26	350	2s ² 2p ² (¹ D)4f	2H _{9/2}	2p+2(4)4 4f−1(5)9	9/2 ^o	...	1.26211E+03	0.88(350)0.41(323)
26	351	2s ² 2p ² (¹ D)4f	2H _{11/2}	2p+2(4)4 4f+1(7)11	11/2 ^o	...	1.26221E+03	0.88(351)0.47(324)
26	352	2s ² 2p ² (¹ D)4f	2D _{3/2}	2p+2(4)4 4f−1(5)3	3/2 ^o	...	1.26242E+03	−0.88(352)
26	353	2s ² 2p ² (¹ D)4f	2D _{5/2}	2p+2(4)4 4f+1(7)5	5/2 ^o	...	1.26265E+03	0.89(353)
26	354	2s ² 2p ² (¹ D)4f	2F _{1/2}	2p+2(4)4 4f−1(5)1	1/2 ^o	...	1.26315E+03	0.90(354)0.44(326)
26	355	2s ² 2p ² (¹ D)4f	2F _{3/2}	2p+2(4)4 4f+1(7)3	3/2 ^o	...	1.26328E+03	−0.90(355)
26	356	2s ² 2p ² (¹ S)4d	2D _{5/2}	2p+2(0)0 4d+1(5)5	5/2 ^e	1.27567E+03	1.27100E+03	−0.96(356)
26	357	2s ² 2p ² (¹ S)4d	2D _{3/2}	2p+2(0)0 4d−1(3)3	3/2 ^e	1.27319E+03	1.27126E+03	−0.95(357)
26	358	2s ² 2p ² (¹ S)4f	2F _{5/2}	2p+2(0)0 4f−1(5)5	5/2 ^o	...	1.27750E+03	−0.96(358)
26	359	2s ² 2p ² (¹ S)4f	2F _{7/2}	2p+2(0)0 4f+1(7)7	7/2 ^o	...	1.27763E+03	−0.96(359)

^aThe number at the end or inside of the bracket is 2J.^bs⁺ = s_{1/2}, p[−] = p_{1/2}, p⁺ = p_{3/2}, d[−] = d_{3/2}, d⁺ = d_{5/2}, f[−] = f_{5/2}, and f⁺ = f_{7/2}.^cThe number after ± is the occupation number of the corresponding sub-shell. For example, the jj configuration of level 7 is 2s_{1/2}2p_{1/2}2p_{3/2}³.^dThe observed energies from the NIST ASD (Kramida et al. 2014).^eThe present MBPT results.^fThe mixing coefficient of the LSJ basis of the state indicated by the key in parenthesis.

Note: Only the 359 levels in N-like Fe are shown here. Table 1 is available online in its entirety in the home page of *ApJS*. A portion is shown here for guidance regarding its form and content.

TABLE 2

Wavelengths(λ , in Å), line strengths(S , in atomic units), absorption oscillator strengths (f , dimensionless) and transition rates(A , in s^{-1}) for the transitions in N-like ions with $Z = 18 - 30$.

Z	$j - i$	Type	λ	S	f	A
26	2 - 1	M1	7.2170E+02	8.729E-01	1.223E-06	1.566E+04
26	2 - 1	E2	7.2170E+02	5.198E-04	5.804E-11	7.433E-01
26	3 - 1	M1	5.6788E+02	5.106E-02	9.091E-08	1.254E+03
26	3 - 1	E2	5.6788E+02	1.066E-03	2.443E-10	3.369E+00
26	3 - 2	M1	2.6644E+03	1.780E+00	6.752E-07	4.230E+02
26	3 - 2	E2	2.6644E+03	1.909E-03	4.237E-12	2.654E-03
26	4 - 1	M1	3.8407E+02	1.316E-01	3.464E-07	3.133E+04
26	4 - 1	E2	3.8407E+02	1.016E-04	7.528E-11	6.808E+00
26	4 - 2	M1	8.2097E+02	2.373E-01	2.922E-07	5.783E+03
26	4 - 2	E2	8.2097E+02	3.518E-03	2.669E-10	5.283E+00
26	4 - 3	E2	1.1866E+03	3.125E-03	5.234E-11	7.439E-01
26	5 - 1	M1	3.0918E+02	1.273E-01	4.164E-07	2.905E+04
26	5 - 1	E2	3.0918E+02	3.867E-06	5.492E-12	3.832E-01
26	5 - 2	M1	5.4092E+02	1.020E+00	1.906E-06	4.344E+04
26	5 - 2	E2	5.4092E+02	1.235E-03	3.275E-10	7.466E+00
26	5 - 3	M1	6.7870E+02	5.600E-01	5.561E-07	1.208E+04
26	5 - 3	E2	6.7870E+02	7.691E-03	6.884E-10	1.495E+01
26	5 - 4	M1	1.5857E+03	9.556E-01	1.219E-06	1.616E+03
26	5 - 4	E2	1.5857E+03	1.005E-03	2.115E-11	2.806E-02
26	6 - 1	E1	1.3287E+02	8.191E-02	4.681E-02	1.179E+10
26	6 - 1	M2	1.3287E+02	1.586E+00	3.778E-10	9.517E+01
26	6 - 2	E1	1.6285E+02	6.935E-03	3.234E-03	5.423E+08
26	6 - 2	M2	1.6285E+02	4.569E-01	5.912E-11	9.914E+00
26	6 - 3	E1	1.7345E+02	3.624E-03	1.058E-03	2.345E+08
26	6 - 3	M2	1.7345E+02	3.208E-01	2.291E-11	5.079E+00
26	6 - 4	M2	2.0314E+02	1.613E-01	2.150E-11	1.158E+00
26	6 - 5	E1	2.3299E+02	8.312E-04	2.709E-04	2.219E+07
26	6 - 5	M2	2.3299E+02	2.804E-01	1.239E-11	1.015E+00
26	7 - 1	E1	1.2186E+02	5.958E-02	3.713E-02	1.668E+10
26	7 - 1	M2	1.2186E+02	1.259E-01	3.888E-11	1.746E+01
26	7 - 2	E1	1.4662E+02	4.934E-04	2.556E-04	7.930E+07
26	7 - 2	M2	1.4662E+02	8.682E-01	1.539E-10	4.776E+01
26	7 - 3	E1	1.5516E+02	3.537E-04	1.154E-04	4.797E+07
26	7 - 3	M2	1.5516E+02	3.142E-01	3.133E-11	1.302E+01
26	7 - 4	E1	1.7850E+02	3.719E-05	3.165E-05	3.313E+06
26	7 - 4	M2	1.7850E+02	4.655E-01	9.148E-11	9.576E+00
26	7 - 5	E1	2.0114E+02	2.477E-03	9.350E-04	1.541E+08
26	7 - 5	M2	2.0114E+02	1.879E-03	1.290E-13	2.127E-02
26	7 - 6	M1	1.4715E+03	3.521E+00	1.613E-06	7.452E+03
26	7 - 6	E2	1.4715E+03	2.981E-03	2.618E-11	1.210E-01

TABLE 2—Continued

Z	$j - i$	Type	λ	S	f	A
26	8 - 1	E1	1.1870E+02	3.080E-02	1.970E-02	1.865E+10
26	8 - 1	M2	1.1870E+02	9.276E-02	3.099E-11	2.934E+01
26	8 - 2	E1	1.4207E+02	7.929E-04	4.238E-04	2.801E+08
26	8 - 2	M2	1.4207E+02	2.760E-01	5.378E-11	3.555E+01
26	8 - 3	M2	1.5007E+02	6.761E-02	7.453E-12	6.622E+00
26	8 - 4	E1	1.7180E+02	1.070E-03	9.455E-04	2.137E+08
26	8 - 5	E1	1.9267E+02	5.282E-05	2.082E-05	7.481E+06
26	8 - 5	M2	1.9267E+02	2.527E-01	1.974E-11	7.094E+00
26	8 - 6	E2	1.1135E+03	2.452E-03	4.970E-11	8.022E-01
26	8 - 7	M1	4.5763E+03	3.091E+00	6.829E-07	4.350E+02
26	8 - 7	E2	4.5763E+03	2.980E-04	1.305E-13	8.315E-05
26	9 - 1	E1	9.5944E+01	2.710E-03	2.145E-03	1.554E+09
26	9 - 1	M2	9.5944E+01	1.329E-01	8.407E-11	6.092E+01
26	9 - 2	E1	1.1066E+02	1.023E-01	7.022E-02	3.825E+10
26	9 - 2	M2	1.1066E+02	7.046E-02	2.906E-11	1.583E+01
26	9 - 3	E1	1.1545E+02	9.015E-05	3.953E-05	2.968E+07
26	9 - 3	M2	1.1545E+02	6.343E-01	1.536E-10	1.153E+02
26	9 - 4	E1	1.2789E+02	1.094E-02	1.300E-02	2.650E+09
26	9 - 4	M2	1.2789E+02	8.441E-02	4.510E-11	9.196E+00
26	9 - 5	E1	1.3911E+02	2.620E-03	1.430E-03	4.929E+08
26	9 - 5	M2	1.3911E+02	2.916E-02	6.052E-12	2.086E+00
26	9 - 6	M1	3.4526E+02	5.357E-04	1.046E-09	8.777E+01
26	9 - 6	E2	3.4526E+02	2.185E-04	1.486E-10	1.247E+01
26	9 - 7	M1	4.5111E+02	1.660E-01	3.720E-07	1.219E+04
26	9 - 7	E2	4.5111E+02	1.326E-06	6.062E-13	1.987E-02
26	9 - 8	M1	5.0044E+02	4.812E-02	1.944E-07	2.589E+03
26	9 - 8	E2	5.0044E+02	1.509E-04	1.011E-10	1.346E+00
26	10 - 1	E1	9.4510E+01	3.994E-05	3.209E-05	1.598E+07
26	10 - 1	M2	9.4510E+01	1.781E-02	1.179E-11	5.870E+00
26	10 - 2	E1	1.0875E+02	5.550E-05	3.876E-05	1.457E+07
26	10 - 2	M2	1.0875E+02	8.255E-01	3.587E-10	1.349E+02
26	10 - 3	E1	1.1338E+02	1.257E-01	5.611E-02	2.912E+10
26	10 - 3	M2	1.1338E+02	1.552E+00	3.967E-10	2.058E+02
26	10 - 4	M2	1.2536E+02	7.344E-01	4.166E-10	5.895E+01
26	10 - 5	E1	1.3612E+02	4.019E-02	2.242E-02	5.381E+09
26	10 - 5	M2	1.3612E+02	1.922E-02	4.259E-12	1.022E+00
26	10 - 6	M1	3.2738E+02	2.362E-01	4.862E-07	3.026E+04
26	10 - 6	E2	3.2738E+02	5.495E-04	4.382E-10	2.727E+01
26	10 - 7	M1	4.2106E+02	2.492E-02	5.984E-08	1.501E+03
26	10 - 7	E2	4.2106E+02	2.290E-04	1.288E-10	3.230E+00

TABLE 2—*Continued*

Z	$j - i$	Type	λ	S	f	A
26	10 - 8	E2	4.6373E+02	9.146E-05	7.700E-11	7.961E-01
26	10 - 9	M1	6.3211E+03	2.284E+00	3.653E-07	4.066E+01
26	10 - 9	E2	6.3211E+03	1.964E-03	3.265E-13	3.633E-05
26	11 - 1	E1	8.3677E+01	9.587E-04	8.701E-04	1.658E+09
26	11 - 1	M2	8.3677E+01	2.016E-01	1.923E-10	3.664E+02
26	11 - 2	E1	9.4651E+01	3.466E-02	2.781E-02	4.141E+10
26	11 - 2	M2	9.4651E+01	6.441E-03	4.244E-12	6.320E+00
26	11 - 3	M2	9.8137E+01	5.754E-02	2.268E-11	4.712E+01
26	11 - 4	E1	1.0699E+02	4.123E-02	5.853E-02	3.411E+10
26	11 - 5	E1	1.1473E+02	3.138E-03	2.077E-03	2.105E+09
26	11 - 5	M2	1.1473E+02	2.480E-01	9.179E-11	9.303E+01
26	11 - 6	E2	2.2602E+02	9.446E-06	2.289E-11	8.967E+00
26	11 - 7	M1	2.6704E+02	1.512E-01	5.725E-07	1.071E+05
26	11 - 7	E2	2.6704E+02	2.530E-05	5.578E-11	1.043E+01
26	11 - 8	M1	2.8359E+02	2.118E-02	1.510E-07	1.252E+04
26	11 - 9	M1	6.5444E+02	7.051E-03	1.089E-08	3.393E+02
26	11 - 9	E2	6.5444E+02	3.435E-03	5.144E-10	1.602E+01
26	11 - 10	E2	7.3002E+02	4.756E-03	3.421E-10	1.285E+01
26	12 - 1	E1	8.0493E+01	4.195E-03	3.957E-03	4.074E+09
26	12 - 1	M2	8.0493E+01	4.967E-01	5.322E-10	5.479E+02
26	12 - 2	E1	9.0597E+01	1.984E-02	1.663E-02	1.352E+10
26	12 - 2	M2	9.0597E+01	9.584E-02	7.202E-11	5.853E+01
26	12 - 3	E1	9.3787E+01	1.508E-01	8.141E-02	9.260E+10
26	12 - 3	M2	9.3787E+01	2.176E-01	9.825E-11	1.118E+02
26	12 - 4	E1	1.0184E+02	1.738E-02	2.593E-02	8.338E+09
26	12 - 4	M2	1.0184E+02	4.189E-02	4.433E-11	1.426E+01
26	12 - 5	E1	1.0882E+02	2.289E-02	1.597E-02	8.995E+09
26	12 - 5	M2	1.0882E+02	5.286E-02	2.292E-11	1.291E+01
26	12 - 6	M1	2.0420E+02	2.546E-02	8.404E-08	2.017E+04
26	12 - 6	E2	2.0420E+02	3.048E-06	1.002E-11	2.404E+00
26	12 - 7	M1	2.3711E+02	8.340E-04	3.556E-09	4.219E+02
26	12 - 7	E2	2.3711E+02	6.680E-05	2.103E-10	2.496E+01
26	12 - 8	M1	2.5006E+02	7.027E-03	5.682E-08	3.030E+03
26	12 - 8	E2	2.5006E+02	2.066E-05	1.109E-10	5.917E+00
26	12 - 9	M1	4.9981E+02	2.248E-01	4.547E-07	1.214E+04
26	12 - 9	E2	4.9981E+02	8.670E-04	2.915E-10	7.782E+00
26	12 - 10	M1	5.4273E+02	1.128E-01	1.401E-07	4.759E+03
26	12 - 10	E2	5.4273E+02	7.284E-05	1.275E-11	4.331E-01
26	12 - 11	M1	2.1154E+03	2.869E-01	2.742E-07	2.044E+02
26	12 - 11	E2	2.1154E+03	1.834E-04	1.627E-12	1.212E-03

TABLE 2—Continued

Z	$j - i$	Type	λ	S	f	A
26	13 - 1	E1	7.4627E+01	4.883E-05	4.969E-05	1.190E+08
26	13 - 1	M2	7.4627E+01	1.819E-01	2.446E-10	5.860E+02
26	13 - 2	E1	8.3233E+01	1.497E-02	1.366E-02	2.630E+10
26	13 - 2	M2	8.3233E+01	7.836E-02	7.594E-11	1.462E+02
26	13 - 3	M2	8.5917E+01	8.036E-02	4.720E-11	1.280E+02
26	13 - 4	E1	9.2624E+01	2.873E-03	4.711E-03	3.663E+09
26	13 - 5	E1	9.8370E+01	8.249E-02	6.368E-02	8.779E+10
26	13 - 5	M2	9.8370E+01	5.010E-01	2.941E-10	4.054E+02
26	13 - 6	E2	1.7025E+02	7.128E-07	4.042E-12	2.790E+00
26	13 - 7	M1	1.9253E+02	1.713E-02	8.993E-08	3.237E+04
26	13 - 7	E2	1.9253E+02	3.238E-06	1.905E-11	6.855E+00
26	13 - 8	M1	2.0098E+02	1.057E-02	1.063E-07	1.755E+04
26	13 - 9	M1	3.3587E+02	6.243E-02	1.879E-07	2.222E+04
26	13 - 9	E2	3.3587E+02	4.754E-04	5.267E-10	6.229E+01
26	13 - 10	E2	3.5472E+02	1.369E-03	8.586E-10	1.366E+02
26	13 - 11	M1	6.8998E+02	5.152E-01	1.510E-06	2.115E+04
26	13 - 12	M1	1.0240E+03	9.664E-01	9.541E-07	1.214E+04
26	13 - 12	E2	1.0240E+03	2.761E-03	1.079E-10	1.373E+00
26	14 - 1	M1	5.1189E+01	1.023E-04	2.020E-09	5.142E+03
26	14 - 1	E2	5.1189E+01	1.560E-05	4.883E-09	1.243E+04
26	14 - 2	M1	5.5097E+01	1.866E-04	3.424E-09	7.523E+03
26	14 - 2	E2	5.5097E+01	1.632E-04	4.096E-08	9.001E+04
26	14 - 3	M1	5.6260E+01	8.306E-05	9.950E-10	3.145E+03
26	14 - 3	E2	5.6260E+01	2.862E-04	4.498E-08	1.422E+05
26	14 - 4	M1	5.9061E+01	8.144E-05	2.788E-09	2.666E+03
26	14 - 4	E2	5.9061E+01	6.797E-05	2.770E-08	2.648E+04
26	14 - 5	M1	6.1346E+01	1.471E-05	2.424E-10	4.296E+02
26	14 - 5	E2	6.1346E+01	2.373E-06	4.315E-10	7.648E+02
26	14 - 6	E1	8.3270E+01	3.158E-03	1.920E-03	2.770E+09
26	14 - 6	M2	8.3270E+01	1.550E+00	1.000E-09	1.443E+03
26	14 - 7	E1	8.8265E+01	2.046E-03	1.761E-03	1.507E+09
26	14 - 7	M2	8.8265E+01	7.668E-02	6.232E-11	5.335E+01
26	14 - 8	E1	9.0001E+01	6.885E-04	1.162E-03	4.784E+08
26	14 - 8	M2	9.0001E+01	2.121E-01	3.252E-10	1.339E+02
26	14 - 9	E1	1.0974E+02	4.008E-02	2.773E-02	1.536E+10
26	14 - 9	M2	1.0974E+02	1.823E-01	7.708E-11	4.269E+01
26	14 - 10	E1	1.1168E+02	1.053E-01	4.773E-02	3.829E+10
26	14 - 10	M2	1.1168E+02	3.159E-01	8.449E-11	6.778E+01
26	14 - 11	E1	1.3184E+02	3.709E-02	4.273E-02	8.198E+09
26	14 - 11	M2	1.3184E+02	4.290E-01	2.092E-10	4.014E+01

TABLE 2—*Continued*

Z	$j - i$	Type	λ	S	f	A
26	14 - 12	E1	1.4061E+02	1.465E-01	7.913E-02	2.670E+10
26	14 - 12	M2	1.4061E+02	1.403E-01	2.821E-11	9.519E+00
26	14 - 13	E1	1.6299E+02	1.178E-02	1.098E-02	1.378E+09
26	14 - 13	M2	1.6299E+02	1.230E-02	3.176E-12	3.987E-01
26	15 - 1	M1	4.8512E+01	1.080E-05	2.252E-10	1.276E+03
26	15 - 1	E2	4.8512E+01	6.872E-07	2.527E-10	1.432E+03
26	15 - 2	M1	5.2008E+01	1.277E-07	2.481E-12	1.224E+01
26	15 - 2	E2	5.2008E+01	3.422E-05	1.021E-08	5.036E+04
26	15 - 3	E2	5.3043E+01	7.596E-05	1.424E-08	1.013E+05
26	15 - 4	M1	5.5525E+01	1.117E-08	4.068E-13	8.801E-01
26	15 - 5	M1	5.7540E+01	1.536E-04	2.699E-09	1.088E+04
26	15 - 5	E2	5.7540E+01	1.519E-04	3.348E-08	1.349E+05
26	15 - 6	M2	7.6411E+01	2.033E-01	1.697E-10	5.817E+02
26	15 - 7	E1	8.0596E+01	1.378E-04	1.299E-04	2.667E+08
26	15 - 7	M2	8.0596E+01	5.794E-01	6.185E-10	1.270E+03
26	15 - 8	E1	8.2041E+01	4.628E-04	8.567E-04	8.490E+08
26	15 - 9	E1	9.8128E+01	3.794E-02	2.936E-02	4.068E+10
26	15 - 9	M2	9.8128E+01	1.089E-01	6.439E-11	8.920E+01
26	15 - 10	M2	9.9676E+01	8.885E-01	3.342E-10	6.732E+02
26	15 - 11	E1	1.1544E+02	3.698E-03	4.865E-03	2.435E+09
26	15 - 12	E1	1.2210E+02	5.737E-02	3.568E-02	3.193E+10
26	15 - 12	M2	1.2210E+02	4.963E-02	1.523E-11	1.363E+01
26	15 - 13	E1	1.3863E+02	7.299E-02	7.996E-02	2.775E+10
26	15 - 14	M1	9.2763E+02	1.321E+00	1.440E-06	2.232E+04
26	15 - 14	E2	9.2763E+02	2.538E-03	1.335E-10	2.069E+00

Note: Only transitions among the $n = 2$ levels in Fe XX are shown here. Table 2 is available online in its entirety in the home page of *ApJS*. A portion is shown here for guidance regarding its form and content.

TABLE 3
Level energies (in eV) for the $n = 3, 4$ levels in Fe XX.

Level	Energy (eV)				
	NIST ^a	CHIANTI ^b	MBPT ^c	MCDHF/RCI ^d	AS ^e
$2s^2 2p^2 ({}^3P) 3s {}^4P_{1/2}$...	887.355	887.256	887.403	889.851
$2s^2 2p^2 ({}^3P) 3s {}^4P_{3/2}$...	895.581	895.508	895.656	897.924
$2s^2 2p^2 ({}^3P) 3s {}^2P_{1/2}$	899.163	899.367	901.900
$2s^2 2p^2 ({}^3P) 3s {}^4P_{5/2}$...	899.702	900.731	900.888	903.450
$2s^2 2p^2 ({}^3P) 3s {}^2P_{3/2}$	904.521	904.731	907.556
$2s^2 2p^2 ({}^3P) 3p {}^4D_{1/2}$	912.215	912.364	914.791
$2s^2 2p^2 ({}^1D) 3s {}^2D_{5/2}$	917.442	917.635	920.142
$2s^2 2p^2 ({}^3P) 3p {}^4D_{3/2}$...	916.602	917.687	917.834	920.134
$2s^2 2p^2 ({}^1D) 3s {}^2D_{3/2}$	918.679	918.887	921.394
$2s^2 2p^2 ({}^3P) 3p {}^2S_{1/2}$	920.003	920.158	922.438
$2s^2 2p^2 ({}^3P) 3p {}^4P_{3/2}$...	923.659	923.572	923.737	926.195
$2s^2 2p^2 ({}^3P) 3p {}^4D_{5/2}$...	924.884	924.893	925.038	927.226
$2s^2 2p^2 ({}^3P) 3p {}^4P_{1/2}$	926.421	926.581	928.810
$2s^2 2p^2 ({}^3P) 3p {}^4P_{5/2}$	927.206	927.372	929.974
$2s^2 2p^2 ({}^3P) 3p {}^2D_{3/2}$	928.803	928.983	931.354
$2s^2 2p^2 ({}^3P) 3p {}^4D_{7/2}$...	930.341	930.078	930.233	932.688
$2s^2 2p^2 ({}^3P) 3p {}^4S_{3/2}$...	933.122	933.058	933.234	935.582
$2s^2 2p^2 ({}^1S) 3s {}^2S_{1/2}$	933.892	934.065	935.557
$2s^2 2p^2 ({}^3P) 3p {}^2P_{3/2}$	935.816	936.045	938.679
$2s^2 2p^2 ({}^3P) 3p {}^2D_{5/2}$	936.508	936.707	939.294
$2s^2 2p^2 ({}^3P) 3p {}^2P_{1/2}$	939.099	939.320	941.691
$2s^2 2p^2 ({}^1D) 3p {}^2F_{5/2}$	945.675	945.858	948.449
$2s^2 2p^2 ({}^3P) 3d {}^4F_{3/2}$...	947.095	946.845	947.053	949.554
$2s 2p^3 ({}^5S) 3s {}^6S_{5/2}$	947.222	947.223	947.807
$2s^2 2p^2 ({}^1D) 3p {}^2F_{7/2}$	947.512	947.704	950.125
$2s^2 2p^2 ({}^1D) 3p {}^2D_{3/2}$	948.346	948.590	951.169
$2s^2 2p^2 ({}^3P) 3d {}^4D_{5/2}$...	949.925	949.663	949.876	952.528
$2s^2 2p^2 ({}^1D) 3p {}^2D_{5/2}$	950.483	950.752	953.573
$2s^2 2p^2 ({}^1D) 3p {}^2P_{1/2}$	951.568	951.810	954.445
$2s^2 2p^2 ({}^3P) 3d {}^2P_{3/2}$...	956.225	955.961	956.185	958.636
$2s^2 2p^2 ({}^3P) 3d {}^4F_{7/2}$...	956.364	956.098	956.314	958.844
$2s^2 2p^2 ({}^3P) 3d {}^4F_{5/2}$...	957.333	957.029	957.261	959.879
$2s^2 2p^2 ({}^3P) 3d {}^4D_{1/2}$	957.031	957.246	959.493
$2s^2 2p^2 ({}^1D) 3p {}^2P_{3/2}$...	959.600	958.815	959.069	961.314
$2s^2 2p^2 ({}^3P) 3d {}^4D_{3/2}$	960.139	960.367	962.993
$2s^2 2p^2 ({}^3P) 3d {}^4D_{7/2}$	960.413	960.644	963.407
$2s^2 2p^2 ({}^3P) 3d {}^2F_{5/2}$...	960.711	960.594	960.842	963.608
$2s^2 2p^2 ({}^3P) 3d {}^4F_{9/2}$	960.748	960.978	963.815
$2s 2p^3 ({}^5S) 3s {}^4S_{3/2}$...	962.581	961.962	962.170	963.986

TABLE 3—Continued

Level	Energy (eV)				
	NIST ^a	CHIANTI ^b	MBPT ^c	MCDHF/RCI ^d	AS ^e
$2s^2 2p^2 ({}^1S) 3p {}^2P_{1/2}$	964.255	964.474	966.222
$2s^2 2p^2 ({}^3P) 3d {}^4P_{5/2}$	967.32	965.205	964.894	965.127	967.940
$2s^2 2p^2 ({}^1S) 3p {}^2P_{3/2}$	966.050	966.263	967.950
$2s^2 2p^2 ({}^3P) 3d {}^4P_{3/2}$	967.32	966.588	966.340	966.573	969.375
$2s^2 2p^2 ({}^3P) 3d {}^2P_{1/2}$...	966.801	966.610	966.856	969.639
$2s^2 2p^2 ({}^3P) 3d {}^4P_{1/2}$...	967.719	967.502	967.741	970.474
$2s^2 2p^2 ({}^3P) 3d {}^2F_{7/2}$	969.6	968.928	968.982	969.263	972.189
$2s^2 2p^2 ({}^3P) 3d {}^2D_{3/2}$	974.39	...	971.784	972.089	975.183
$2s^2 2p^2 ({}^3P) 3d {}^2D_{5/2}$	972.41	972.230	971.812	972.133	975.394
$2s 2p^3 ({}^5S) 3p {}^6P_{3/2}$	974.484	974.453	975.024
$2s 2p^3 ({}^5S) 3p {}^6P_{5/2}$...	973.408	975.301	975.275	976.016
$2s^2 2p^2 ({}^1D) 3d {}^2G_{7/2}$	976.874	977.113	979.996
$2s 2p^3 ({}^5S) 3p {}^6P_{7/2}$	977.608	977.603	978.090
$2s^2 2p^2 ({}^1D) 3d {}^2G_{9/2}$	978.936	979.216	982.038
$2s^2 2p^2 ({}^1D) 3d {}^2D_{3/2}$	981.83	...	980.739	981.006	983.687
$2s^2 2p^2 ({}^1D) 3d {}^2D_{5/2}$	981.09	...	981.172	981.448	984.323
$2s^2 2p^2 ({}^1D) 3d {}^2P_{1/2}$	983.193	983.450	986.182
$2s^2 2p^2 ({}^1D) 3d {}^2F_{7/2}$	983.81	...	983.605	983.933	987.124
$2s 2p^3 ({}^3D) 3s {}^4D_{3/2}$	985.101	985.226	987.295
$2s 2p^3 ({}^5S) 3p {}^4P_{3/2}$...	985.488	985.218	985.294	986.373
$2s 2p^3 ({}^5S) 3p {}^4P_{5/2}$...	985.488	985.272	985.357	986.458
$2s 2p^3 ({}^3D) 3s {}^4D_{1/2}$	985.295	985.426	987.492
$2s 2p^3 ({}^3D) 3s {}^4D_{5/2}$	985.360	985.481	987.617
$2s 2p^3 ({}^5S) 3p {}^4P_{1/2}$...	986.664	986.208	986.290	987.327
$2s^2 2p^2 ({}^1D) 3d {}^2S_{1/2}$	987.258	987.553	990.464
$2s^2 2p^2 ({}^1D) 3d {}^2F_{5/2}$	989.77	...	987.413	987.728	990.671
$2s^2 2p^2 ({}^1D) 3d {}^2P_{3/2}$	987.78	...	987.692	987.956	990.609
$2s 2p^3 ({}^3D) 3s {}^4D_{7/2}$	988.095	988.222	990.744
$2s 2p^3 ({}^3D) 3s {}^2D_{3/2}$	993.651	993.870	996.273
$2s 2p^3 ({}^3D) 3s {}^2D_{5/2}$	995.696	995.903	998.604
$2s^2 2p^2 ({}^1S) 3d {}^2D_{5/2}$	997.70	...	997.849	998.085	1000.112
$2s^2 2p^2 ({}^1S) 3d {}^2D_{3/2}$	999.148	999.399	1001.402
$2s 2p^3 ({}^3P) 3s {}^4P_{1/2}$	1002.53	1002.64	1004.31
$2s 2p^3 ({}^3P) 3s {}^4P_{3/2}$	1003.87	1003.99	1005.86
$2s 2p^3 ({}^5S) 3d {}^6D_{1/2}$	1006.16	1006.18	1006.59
$2s 2p^3 ({}^5S) 3d {}^6D_{3/2}$	1006.19	1006.21	1006.70
$2s 2p^3 ({}^5S) 3d {}^6D_{5/2}$	1006.20	1006.25	1006.86
$2s 2p^3 ({}^3P) 3s {}^4P_{5/2}$	1006.30	1006.41	1008.45
$2s 2p^3 ({}^5S) 3d {}^6D_{7/2}$	1006.33	1006.35	1007.10

TABLE 3—Continued

Level	Energy (eV)				
	NIST ^a	CHIANTI ^b	MBPT ^c	MCDHF/RCI ^d	AS ^e
$2s2p^3(^5S)3d\ ^6D_{9/2}$	1006.60	1006.62	1007.50
$2s2p^3(^3D)3p\ ^4D_{1/2}$	1009.69	1009.78	1011.64
$2s2p^3(^3D)3p\ ^4D_{3/2}$	1009.97	1010.06	1011.98
$2s2p^3(^3P)3s\ ^2P_{1/2}$	1010.75	1010.96	1013.03
$2s2p^3(^3D)3p\ ^4F_{5/2}$	1011.62	1011.71	1013.82
$2s2p^3(^3D)3p\ ^4F_{3/2}$	1011.82	1011.94	1014.03
$2s2p^3(^3P)3s\ ^2P_{3/2}$	1012.43	1012.64	1014.97
$2s2p^3(^3D)3p\ ^4F_{7/2}$	1014.11	1014.21	1016.53
$2s2p^3(^3D)3p\ ^4D_{5/2}$	1014.75	1014.84	1016.84
$2s2p^3(^3D)3p\ ^2P_{3/2}$	1015.99	1016.10	1018.12
$2s2p^3(^3D)3p\ ^4D_{7/2}$	1016.25	1016.35	1018.46
$2s2p^3(^3D)3p\ ^2P_{1/2}$	1017.15	1017.28	1019.36
$2s2p^3(^3D)3p\ ^2F_{5/2}$	1017.63	1017.77	1019.90
$2s2p^3(^3D)3p\ ^4F_{9/2}$	1018.02	1018.13	1020.57
$2s2p^3(^3D)3p\ ^2F_{7/2}$	1019.07	1019.20	1021.71
$2s2p^3(^5S)3d\ ^4D_{5/2}$...	1019.03	1019.28	1019.43	1020.93
$2s2p^3(^5S)3d\ ^4D_{3/2}$...	1019.82	1019.63	1019.77	1021.21
$2s2p^3(^5S)3d\ ^4D_{7/2}$...	1018.24	1020.08	1020.23	1021.76
$2s2p^3(^5S)3d\ ^4D_{1/2}$	1020.20	1020.34	1021.72
$2s2p^3(^3D)3p\ ^4P_{3/2}$	1022.43	1022.57	1024.67
$2s2p^3(^3D)3p\ ^4P_{1/2}$	1023.14	1023.31	1025.48
$2s2p^3(^3D)3p\ ^4P_{5/2}$	1024.68	1024.88	1027.44
$2s2p^3(^3S)3s\ ^4S_{3/2}$	1024.87	1025.03	1027.88
$2s2p^3(^3D)3p\ ^2D_{3/2}$	1025.45	1025.64	1028.17
$2s2p^3(^3D)3p\ ^2D_{5/2}$	1028.19	1028.38	1031.02
$2s2p^3(^3S)3s\ ^2S_{1/2}$	1028.92	1029.11	1032.08
$2s2p^3(^3P)3p\ ^4D_{1/2}$	1029.35	1029.45	1031.22
$2s2p^3(^1D)3s\ ^2D_{5/2}$	1030.04	1030.22	1033.53
$2s2p^3(^3P)3p\ ^4D_{3/2}$	1030.91	1031.01	1032.90
$2s2p^3(^1D)3s\ ^2D_{3/2}$	1030.93	1031.12	1034.31
$2s2p^3(^3P)3p\ ^4D_{5/2}$	1032.42	1032.52	1034.46
$2s2p^3(^3P)3p\ ^4S_{3/2}$	1033.61	1033.72	1035.45
$2s2p^3(^3P)3p\ ^4D_{7/2}$	1034.92	1035.02	1036.92
$2s2p^3(^3P)3p\ ^2P_{1/2}$	1035.02	1035.14	1037.05
$2s2p^3(^3P)3p\ ^4P_{1/2}$	1035.83	1035.99	1038.05
$2s2p^3(^3P)3p\ ^4P_{3/2}$	1036.76	1036.91	1038.91
$2s2p^3(^3P)3p\ ^4P_{5/2}$	1037.12	1037.27	1039.45
$2s2p^3(^3P)3p\ ^2D_{3/2}$	1037.93	1038.08	1040.01
$2s2p^3(^3P)3p\ ^2P_{3/2}$	1040.59	1040.75	1042.86

TABLE 3—Continued

Level	Energy (eV)				
	NIST ^a	CHIANTI ^b	MBPT ^c	MCDHF/RCI ^d	AS ^e
$2s2p^3(^3D)3d^4F_{3/2}$	1040.70	1040.84	1042.75
$2s2p^3(^3P)3p^2D_{5/2}$	1040.85	1041.01	1043.16
$2s2p^3(^3D)3d^4F_{5/2}$	1041.63	1041.77	1043.79
$2s2p^3(^3D)3d^4F_{7/2}$	1042.85	1043.00	1045.21
$2s2p^3(^3D)3d^4G_{5/2}$	1044.30	1044.48	1046.48
$2s2p^3(^3D)3d^4G_{9/2}$	1044.58	1044.75	1047.10
$2s2p^3(^3D)3d^4G_{7/2}$	1044.72	1044.89	1047.07
$2s2p^3(^3P)3p^2S_{1/2}$	1045.98	1046.21	1048.59
$2s2p^3(^3D)3d^4F_{9/2}$	1046.24	1046.38	1048.87
$2s2p^3(^3D)3d^4D_{1/2}$	1046.59	1046.74	1048.76
$2s2p^3(^1P)3s^2P_{3/2}$	1046.67	1046.88	1049.77
$2s2p^3(^1P)3s^2P_{1/2}$	1047.16	1047.37	1050.15
$2s2p^3(^3D)3d^4G_{11/2}$	1047.24	1047.41	1050.12
$2s2p^3(^3D)3d^4D_{3/2}$	1047.25	1047.40	1049.42
$2s2p^3(^3D)3d^4D_{5/2}$...	1048.85	1048.63	1048.78	1050.94
$2s2p^3(^3D)3d^2S_{1/2}$	1048.72	1048.89	1051.09
$2s2p^3(^3D)3d^4D_{7/2}$...	1049.56	1049.56	1049.75	1052.37
$2s2p^3(^3D)3d^2G_{7/2}$	1050.77	1050.97	1053.62
$2s2p^3(^3S)3p^4P_{3/2}$	1051.02	1051.17	1054.08
$2s2p^3(^3D)3d^2G_{9/2}$	1051.29	1051.52	1054.31
$2s2p^3(^3S)3p^4P_{1/2}$	1051.37	1051.53	1058.97
$2s2p^3(^3D)3d^4P_{5/2}$	1052.17	1052.32	1054.76
$2s2p^3(^3D)3d^4P_{3/2}$	1052.75	1052.94	1055.28
$2s2p^3(^3D)3d^4P_{1/2}$	1052.99	1053.16	1055.54
$2s2p^3(^3D)3d^2P_{3/2}$	1053.41	1053.59	1068.07
$2s2p^3(^3D)3d^2D_{5/2}$	1053.47	1053.67	1056.06
$2s2p^3(^3S)3p^4P_{5/2}$...	1056.17	1053.87	1054.01	1056.80
$2s2p^3(^3D)3d^4S_{3/2}$	1055.44	1055.65	1058.46
$2s2p^3(^3D)3d^2P_{1/2}$	1055.84	1056.07	1058.85
$2s2p^3(^1D)3p^2P_{3/2}$	1055.97	1056.11	1079.98
$2s2p^3(^3S)3p^2P_{1/2}$	1056.01	1056.18	1054.35
$2s2p^3(^1D)3p^2F_{5/2}$	1056.83	1056.99	1060.23
$2s2p^3(^1D)3p^2F_{7/2}$	1058.83	1058.99	1062.22
$2s2p^3(^3D)3d^2D_{3/2}$	1059.43	1059.65	1062.26
$2s2p^3(^3D)3d^2F_{7/2}$	1060.26	1060.51	1063.44
$2s2p^3(^3D)3d^2F_{5/2}$	1060.66	1060.91	1063.87
$2s2p^3(^1D)3p^2D_{3/2}$	1062.01	1062.25	1065.76
$2s2p^3(^3P)3d^4F_{3/2}$	1062.59	1062.75	1064.45
$2s2p^3(^3P)3d^4F_{5/2}$	1062.65	1062.81	1064.65

TABLE 3—Continued

Level	Energy (eV)				
	NIST ^a	CHIANTI ^b	MBPT ^c	MCDHF/RCI ^d	AS ^e
$2s2p^3(^1D)3p^2D_{5/2}$	1062.78	1063.01	1066.54
$2s2p^3(^3P)3d^4F_{7/2}$	1062.89	1063.05	1065.13
$2s2p^3(^3P)3d^4F_{9/2}$	1064.31	1064.47	1066.68
$2s2p^3(^3P)3d^4P_{5/2}$	1065.34	1065.50	1067.47
$2s2p^3(^3P)3d^4P_{1/2}$	1065.74	1065.89	1067.71
$2s2p^3(^3P)3d^4P_{3/2}$	1065.82	1065.99	...
$2s2p^3(^3S)3p^2P_{3/2}$	1066.82	1067.06	1059.06
$2s2p^3(^3P)3d^4D_{1/2}$	1067.24	1067.42	1069.61
$2s2p^3(^3P)3d^2D_{3/2}$	1067.48	1067.66	1071.35
$2s2p^3(^1D)3p^2P_{1/2}$	1068.11	1068.33	1071.59
$2s2p^3(^3P)3d^4D_{7/2}$	1068.14	1068.32	1070.69
$2s2p^3(^3P)3d^4D_{5/2}$	1068.38	1068.57	1070.87
$2s2p^3(^3P)3d^4D_{3/2}$	1068.74	1068.94	1069.90
$2s2p^3(^3P)3d^2F_{5/2}$	1071.11	1071.34	1073.68
$2s2p^3(^3P)3d^2F_{7/2}$	1073.25	1073.50	1076.20
$2s2p^3(^3P)3d^2D_{5/2}$	1075.13	1075.38	1078.14
$2s2p^3(^1P)3p^2D_{5/2}$	1075.92	1076.12	1078.99
$2s2p^3(^3P)3d^2P_{1/2}$	1076.75	1076.98	1079.64
$2s2p^3(^1P)3p^2P_{3/2}$	1076.96	1077.17	1080.70
$2s2p^3(^1P)3p^2S_{1/2}$	1077.16	1077.42	1080.59
$2s2p^3(^1P)3p^2D_{3/2}$	1077.21	1077.44	1070.44
$2s2p^3(^3P)3d^2P_{3/2}$	1080.51	1080.78	1083.60
$2s2p^3(^3S)3d^4D_{5/2}$...	1085.76	1083.63	1083.84	1086.97
$2s2p^3(^3S)3d^4D_{3/2}$...	1085.76	1084.02	1084.23	1087.24
$2s2p^3(^3S)3d^4D_{7/2}$	1084.36	1084.56	1087.81
$2s2p^3(^1P)3p^2P_{1/2}$	1084.41	1084.70	1088.06
$2s2p^3(^3S)3d^4D_{1/2}$	1085.10	1085.31	1088.29
$2s2p^3(^3S)3d^2D_{3/2}$	1087.12	1087.34	1090.57
$2s2p^3(^1D)3d^2D_{5/2}$	1088.40	1088.62	1101.54
$2s2p^3(^1D)3d^2G_{9/2}$	1088.88	1089.12	1092.78
$2s2p^3(^1D)3d^2G_{7/2}$	1089.33	1089.57	1092.95
$2s2p^3(^1D)3d^2F_{7/2}$	1091.40	1091.68	1095.47
$2s2p^3(^1D)3d^2F_{5/2}$	1091.79	1092.06	1095.73
$2s2p^3(^1D)3d^2P_{3/2}$	1094.40	1094.65	1098.28
$2s2p^3(^1D)3d^2P_{1/2}$	1095.38	1095.60	1099.07
$2s2p^3(^1D)3d^2D_{3/2}$	1096.99	1097.28	1101.12
$2s2p^3(^3S)3d^2D_{5/2}$	1097.13	1097.46	1092.06
$2p^4(^3P)3s^4P_{5/2}$	1097.73	1097.86	...
$2s2p^3(^1D)3d^2S_{1/2}$	1098.78	1099.00	1102.40

TABLE 3—Continued

Level	Energy (eV)				
	NIST ^a	CHIANTI ^b	MBPT ^c	MCDHF/RCI ^d	AS ^e
$2p^4(^3P)3s^2P_{3/2}$	1102.02	1102.21	...
$2s2p^3(^1P)3d^2F_{7/2}$	1106.46	1106.73	1110.01
$2s2p^3(^1P)3d^2D_{5/2}$	1106.88	1107.14	1110.40
$2p^4(^3P)3s^4P_{1/2}$	1108.73	1108.71	...
$2s2p^3(^1P)3d^2P_{3/2}$	1108.89	1109.16	1112.47
$2s2p^3(^1P)3d^2P_{1/2}$	1109.05	1109.34	1112.70
$2s2p^3(^1P)3d^2F_{5/2}$	1109.53	1109.83	1113.38
$2p^4(^3P)3s^4P_{3/2}$	1110.71	1110.88	...
$2s2p^3(^1P)3d^2D_{3/2}$	1114.18	1114.50	1118.31
$2p^4(^3P)3s^2P_{1/2}$	1115.55	1115.75	...
$2p^4(^1D)3s^2D_{5/2}$	1120.37	1120.58	...
$2p^4(^1D)3s^2D_{3/2}$	1121.01	1121.23	...
$2p^4(^3P)3p^4P_{3/2}$	1121.42	1121.53	...
$2p^4(^3P)3p^4P_{5/2}$	1121.93	1122.04	...
$2p^4(^3P)3p^2P_{1/2}$	1125.70	1125.81	...
$2p^4(^3P)3p^4D_{7/2}$	1126.05	1126.19	...
$2p^4(^3P)3p^2D_{5/2}$	1126.21	1126.37	...
$2p^4(^3P)3p^4P_{1/2}$	1132.95	1133.07	...
$2p^4(^3P)3p^4D_{3/2}$	1133.07	1133.23	...
$2p^4(^3P)3p^4D_{1/2}$	1134.10	1134.07	...
$2p^4(^3P)3p^2P_{3/2}$	1135.50	1135.65	...
$2p^4(^3P)3p^4D_{5/2}$	1137.40	1137.53	...
$2p^4(^3P)3p^4S_{3/2}$	1138.46	1138.49	...
$2p^4(^3P)3p^2S_{1/2}$	1140.19	1140.36	...
$2p^4(^3P)3p^2D_{3/2}$	1140.81	1140.96	...
$2p^4(^1D)3p^2F_{5/2}$	1143.77	1143.97	...
$2p^4(^1D)3p^2F_{7/2}$	1146.74	1146.94	...
$2p^4(^1S)3s^2S_{1/2}$	1148.48	1148.90	...
$2p^4(^1D)3p^2D_{3/2}$	1149.14	1149.38	...
$2p^4(^1D)3p^2D_{5/2}$	1150.77	1151.02	...
$2p^4(^3P)3d^4D_{7/2}$	1152.07	1152.20	...
$2p^4(^3P)3d^4D_{5/2}$	1152.11	1152.23	...
$2p^4(^3P)3d^4D_{3/2}$	1152.92	1153.05	...
$2p^4(^3P)3d^4D_{1/2}$	1154.17	1154.30	...
$2p^4(^3P)3d^4F_{9/2}$	1154.84	1155.03	...
$2p^4(^3P)3d^2F_{7/2}$	1156.27	1156.50	...
$2p^4(^1D)3p^2P_{3/2}$	1156.71	1157.16	...
$2p^4(^3P)3d^4P_{1/2}$	1159.52	1159.68	...
$2p^4(^1D)3p^2P_{1/2}$	1161.35	1161.78	...

TABLE 3—Continued

Level	Energy (eV)				
	NIST ^a	CHIANTI ^b	MBPT ^c	MCDHF/RCI ^d	AS ^e
$2p^4(^3P)3d^4P_{3/2}$	1161.72	1161.90	...
$2p^4(^3P)3d^2F_{5/2}$	1162.23	1162.45	...
$2p^4(^3P)3d^2P_{1/2}$	1164.36	1164.50	...
$2p^4(^3P)3d^4F_{3/2}$	1165.47	1165.50	...
$2p^4(^3P)3d^4F_{5/2}$	1166.03	1166.08	...
$2p^4(^3P)3d^4F_{7/2}$	1166.11	1166.30	...
$2p^4(^3P)3d^2D_{3/2}$	1167.05	1167.21	...
$2p^4(^3P)3d^4P_{5/2}$	1169.29	1169.48	...
$2p^4(^3P)3d^2P_{3/2}$	1171.06	1171.24	...
$2p^4(^3P)3d^2D_{5/2}$	1172.28	1172.45	...
$2p^4(^1D)3d^2G_{7/2}$	1174.24	1174.52	...
$2p^4(^1D)3d^2G_{9/2}$	1174.70	1174.98	...
$2p^4(^1S)3p^2P_{1/2}$	1176.81	1177.29	...
$2p^4(^1S)3p^2P_{3/2}$	1176.91	1177.35	...
$2p^4(^1D)3d^2F_{5/2}$	1178.78	1179.06	...
$2p^4(^1D)3d^2S_{1/2}$	1180.09	1180.28	...
$2p^4(^1D)3d^2F_{7/2}$	1180.15	1180.45	...
$2p^4(^1D)3d^2D_{5/2}$	1183.82	1184.16	...
$2p^4(^1D)3d^2P_{3/2}$	1183.97	1184.31	...
$2p^4(^1D)3d^2D_{3/2}$	1187.31	1187.66	...
$2p^4(^1D)3d^2P_{1/2}$	1188.62	1188.98	...
$2s^22p^2(^3P)4s^4P_{1/2}$	1200.56	1200.97	1203.85
$2p^4(^1S)3d^2D_{5/2}$	1206.23	1206.70	...
$2p^4(^1S)3d^2D_{3/2}$	1208.25	1208.72	...
$2s^22p^2(^3P)4s^4P_{3/2}$	1209.38	1209.78	1212.48
$2s^22p^2(^3P)4s^2P_{1/2}$	1210.39	1210.80	1213.48
$2s^22p^2(^3P)4p^4D_{1/2}$	1210.98	1211.41	1214.30
$2s^22p^2(^3P)4p^4P_{3/2}$	1213.51	1213.90	1216.63
$2s^22p^2(^3P)4s^4P_{5/2}$	1214.63	1215.06	1218.04
$2s^22p^2(^3P)4s^2P_{3/2}$	1215.83	1216.26	1219.23
$2s^22p^2(^3P)4p^2S_{1/2}$	1219.55	1220.02	1222.74
$2s^22p^2(^3P)4p^4D_{3/2}$	1221.05	1221.45	1224.15
$2s^22p^2(^3P)4p^4D_{5/2}$	1221.67	1222.05	1224.60
$2s^22p^2(^3P)4p^4P_{1/2}$	1222.66	1223.07	1225.67
$2s^22p^2(^3P)4p^2D_{3/2}$	1223.38	1223.77	1226.35
$2s^22p^2(^3P)4d^4F_{3/2}$	1224.08	1224.47	1227.31
$2s^22p^2(^3P)4p^4P_{5/2}$	1225.48	1225.88	1228.89
$2s^22p^2(^3P)4d^4P_{5/2}$	1225.0	...	1225.50	1225.90	1228.77
$2s^22p^2(^3P)4p^4D_{7/2}$	1226.73	1227.15	1229.97

TABLE 3—Continued

Level	Energy (eV)				
	NIST ^a	CHIANTI ^b	MBPT ^c	MCDHF/RCI ^d	AS ^e
$2s^2 2p^2 ({}^3P) 4p \ 4S_{3/2}$	1227.63	1228.01	1230.81
$2s^2 2p^2 ({}^3P) 4p \ 2P_{3/2}$	1228.45	1228.87	1231.74
$2s^2 2p^2 ({}^3P) 4p \ 2D_{5/2}$	1229.50	1229.89	1232.72
$2s^2 2p^2 ({}^3P) 4p \ 2P_{1/2}$	1229.80	1230.31	1233.06
$2s^2 2p^2 ({}^1D) 4s \ 2D_{5/2}$	1230.61	1231.11	1233.86
$2s^2 2p^2 ({}^1D) 4s \ 2D_{3/2}$	1231.02	1231.52	1234.24
$2s^2 2p^2 ({}^3P) 4f \ 4G_{5/2}$	1231.66	1232.04	1243.56
$2s^2 2p^2 ({}^3P) 4f \ 2G_{7/2}$	1231.86	1232.24	1244.09
$2s^2 2p^2 ({}^3P) 4d \ 2P_{3/2}$	1233.07	1233.48	1236.13
$2s^2 2p^2 ({}^3P) 4d \ 4F_{7/2}$	1233.35	1233.72	1236.43
$2s^2 2p^2 ({}^3P) 4d \ 4D_{1/2}$	1233.45	1233.80	1236.41
$2s^2 2p^2 ({}^3P) 4d \ 4F_{5/2}$	1232.65	...	1233.82	1234.22	1236.93
$2s^2 2p^2 ({}^3P) 4d \ 4D_{3/2}$	1235.31	1235.70	1238.41
$2s^2 2p^2 ({}^3P) 4d \ 2F_{5/2}$	1235.38	...	1235.46	1235.87	1238.64
$2s^2 2p^2 ({}^3P) 4d \ 4D_{7/2}$	1238.09	1238.48	1241.45
$2s^2 2p^2 ({}^3P) 4d \ 4F_{9/2}$	1238.27	1238.68	1241.66
$2s^2 2p^2 ({}^3P) 4d \ 4D_{5/2}$	1238.85	1240.09	1239.40	1239.79	1242.70
$2s^2 2p^2 ({}^3P) 4d \ 4P_{3/2}$	1240.96	1240.09	1240.02	1240.43	1243.30
$2s^2 2p^2 ({}^3P) 4d \ 4P_{1/2}$	1240.96	1240.09	1240.33	1240.77	1243.64
$2s^2 2p^2 ({}^3P) 4f \ 2D_{5/2}$	1240.50	1240.88	1234.94
$2s^2 2p^2 ({}^3P) 4f \ 4D_{7/2}$	1240.66	1241.04	1243.76
$2s^2 2p^2 ({}^3P) 4d \ 2P_{1/2}$	1240.85	1241.33	1244.13
$2s^2 2p^2 ({}^3P) 4f \ 2G_{7/2}$	1240.94	1241.33	1244.09
$2s^2 2p^2 ({}^3P) 4f \ 4G_{9/2}$	1240.95	1241.33	1244.07
$2s^2 2p^2 ({}^3P) 4f \ 4F_{3/2}$	1241.14	1241.50	1244.17
$2s^2 2p^2 ({}^3P) 4f \ 4D_{5/2}$	1241.40	1241.77	1244.51
$2s^2 2p^2 ({}^3P) 4d \ 2D_{5/2}$	1242.20	...	1241.52	1241.93	1244.98
$2s^2 2p^2 ({}^3P) 4d \ 2D_{3/2}$	1245.17	...	1241.59	1242.03	1245.00
$2s^2 2p^2 ({}^3P) 4d \ 2F_{7/2}$	1242.20	...	1241.80	1242.20	1245.23
$2s^2 2p^2 ({}^1D) 4p \ 2F_{5/2}$	1242.33	1242.80	1245.45
$2s^2 2p^2 ({}^1D) 4p \ 2D_{3/2}$	1242.64	1243.10	1245.79
$2s^2 2p^2 ({}^1D) 4p \ 2D_{5/2}$	1242.98	1243.45	1246.15
$2s^2 2p^2 ({}^1D) 4p \ 2F_{7/2}$	1242.99	1243.43	1246.04
$2s^2 2p^2 ({}^1D) 4p \ 2P_{1/2}$	1243.70	1244.15	1246.81
$2s^2 2p^2 ({}^3P) 4f \ 2G_{9/2}$	1246.03	1246.44	1249.44
$2s^2 2p^2 ({}^3P) 4f \ 4G_{11/2}$	1246.07	1246.48	1249.49
$2s^2 2p^2 ({}^1S) 4s \ 2S_{1/2}$	1246.21	1247.18	1248.85
$2s^2 2p^2 ({}^3P) 4f \ 4D_{1/2}$	1246.30	1246.68	1249.57
$2s^2 2p^2 ({}^3P) 4f \ 4F_{7/2}$	1246.33	1246.71	1249.70

TABLE 3—Continued

Level	Energy (eV)				
	NIST ^a	CHIANTI ^b	MBPT ^c	MCDHF/RCI ^d	AS ^e
$2s^22p^2(^3P)4f\ ^4D_{3/2}$	1246.35	1246.73	1249.64
$2s^22p^2(^3P)4f\ ^4F_{5/2}$	1246.40	1246.78	1249.73
$2s^22p^2(^3P)4f\ ^4F_{9/2}$	1246.51	1246.91	1249.95
$2s^22p^2(^3P)4f\ ^2D_{3/2}$	1246.54	1246.94	1249.98
$2s^22p^2(^3P)4f\ ^2F_{7/2}$	1246.62	1247.01	1250.05
$2s^22p^2(^3P)4f\ ^2F_{5/2}$	1246.66	1247.05	1250.06
$2s^22p^2(^1D)4p\ ^2P_{3/2}$	1246.77	1247.23	1249.73
$2s^22p^2(^1D)4d\ ^2F_{7/2}$	1253.94	1254.41	1257.18
$2s^22p^2(^1D)4d\ ^2G_{9/2}$	1254.80	1255.23	1257.98
$2s^22p^2(^1D)4d\ ^2D_{5/2}$	1257.45	...	1255.37	1255.85	1258.58
$2s^22p^2(^1D)4d\ ^2D_{3/2}$	1256.0	...	1255.46	1255.92	1258.60
$2s^22p^2(^1D)4d\ ^2G_{7/2}$	1257.45	...	1255.77	1256.21	1258.96
$2s^22p^2(^1D)4d\ ^2P_{1/2}$	1255.85	1256.27	1258.99
$2s^22p^2(^1D)4d\ ^2F_{5/2}$	1258.32	...	1257.43	1257.93	1260.66
$2s^22p^2(^1D)4d\ ^2S_{1/2}$	1257.70	1258.12	1260.81
$2s^22p^2(^1D)4d\ ^2P_{3/2}$	1258.32	...	1257.87	1258.33	1260.97
$2s^22p^2(^1S)4p\ ^2P_{1/2}$	1258.12	1259.02	1260.66
$2s^22p^2(^1S)4p\ ^2P_{3/2}$	1259.03	1259.94	1261.46
$2s^22p^2(^1D)4f\ ^2G_{7/2}$	1261.57	1262.02	1264.74
$2s^22p^2(^1D)4f\ ^2G_{9/2}$	1261.58	1262.03	1264.75
$2s^22p^2(^1D)4f\ ^2F_{5/2}$	1261.74	1262.18	1264.87
$2s^22p^2(^1D)4f\ ^2F_{7/2}$	1261.92	1262.37	1265.09
$2s^22p^2(^1D)4f\ ^2H_{9/2}$	1262.11	1262.56	1265.34
$2s^22p^2(^1D)4f\ ^2H_{11/2}$	1262.21	1262.66	1265.45
$2s^22p^2(^1D)4f\ ^2D_{3/2}$	1262.42	1262.83	1265.52
$2s^22p^2(^1D)4f\ ^2D_{5/2}$	1262.65	1263.07	1265.81
$2s^22p^2(^1D)4f\ ^2P_{1/2}$	1263.15	1263.54	1266.26
$2s^22p^2(^1D)4f\ ^2P_{3/2}$	1263.28	1263.68	1266.43
$2s^22p^2(^1S)4d\ ^2D_{5/2}$	1275.67	...	1271.00	1271.88	1273.55
$2s^22p^2(^1S)4d\ ^2D_{3/2}$	1273.19	...	1271.26	1272.15	1273.81
$2s^22p^2(^1S)4f\ ^2F_{5/2}$	1277.50	1278.34	1279.97
$2s^22p^2(^1S)4f\ ^2F_{7/2}$	1277.63	1278.47	1280.12

^aThe observed energies from the NIST ASD (Kramida et al. 2014).

^bThe observed energies from the Chianti database (Landi et al. 2013; Dere et al. 1997).

^cThe present MBPT energies.

^dThe present MCDHF/RCI energies.

^eThe energies calculated by Witthoef et al. (2007) using the AS code.

TABLE 4

Comparisons of the levels with differences larger than 0.2% between our MBPT energies and the experimental values of the NIST ASD.

Z	Key ^a	State	Energy (eV)		Difference (%)
			NIST ^b	MBPT ^c	
18	33	$2s^22p^2(^3P)3p\ ^4S_{3/2}$	379.27	376.264	0.79
18	41	$2s^22p^2(^1D)3p\ ^2D_{5/2}$	387.43	385.478	0.50
18	42	$2s^22p^2(^1D)3p\ ^2P_{1/2}$	388.54	387.446	0.28
18	43	$2s^22p^2(^1D)3p\ ^2P_{3/2}$	389.62	388.648	0.25
18	63	$2s^22p^2(^3P)3d\ ^2D_{5/2}$	400.07	399.251	0.20
18	67	$2s^22p^2(^1D)3d\ ^2G_{7/2}$	404.004	401.334	0.66
19	63	$2s^22p^2(^3P)3d\ ^2D_{5/2}$	458.5	457.275	0.27
19	70	$2s^22p^2(^1D)3d\ ^2D_{5/2}$	463.2	461.403	0.39
20	63	$2s^22p^2(^3P)3d\ ^2D_{5/2}$	520.66	519.134	0.29
20	70	$2s^22p^2(^1D)3d\ ^2D_{5/2}$	525.94	523.578	0.45
21	63	$2s^22p^2(^3P)3d\ ^2D_{5/2}$	586.85	584.843	0.34
21	83	$2s^22p^2(^1S)3d\ ^2D_{5/2}$	605.0	601.518	0.58
21	86	$2s^22p^2(^1S)3d\ ^2D_{3/2}$	606.03	602.287	0.62
22	47	$2s^22p^2(^3P)3d\ ^2P_{3/2}$	643.986	642.590	0.22
22	62	$2s^22p^2(^3P)3d\ ^2D_{3/2}$	655.50	654.134	0.21
22	63	$2s^22p^2(^3P)3d\ ^2D_{5/2}$	656.286	654.415	0.29
23	63	$2s^22p^2(^3P)3d\ ^2D_{5/2}$	731.13	727.870	0.45
23	70	$2s^22p^2(^1D)3d\ ^2D_{5/2}$	738.70	733.890	0.65
26	56	$2s^22p^2(^3P)3d\ ^4P_{5/2}$	967.32	964.894	0.25
26	62	$2s^22p^2(^3P)3d\ ^2D_{3/2}$	974.39	971.784	0.27
26	80	$2s^22p^2(^1D)3d\ ^2F_{5/2}$	989.77	987.413	0.24
26	316	$2s^22p^2(^3P)4d\ ^2D_{3/2}$	1245.17	1241.59	0.29
26	356	$2s^22p^2(^1S)4d\ ^2D_{5/2}$	1275.67	1271.00	0.37

^aThe index number of the level given in Table 1.

^bThe NIST recommended energies (Kramida et al. 2014).

^cThe present MBPT energies.

TABLE 5

Comparisons of the line strengths with differences large than 10% between our MBPT results and the NIST values for transitions among the $n = 2$ levels. The MCDHF/RCI2 results are also listed for comparison.

Z	Transition	Line Strengths			Difference (%)	
		MBPT	MCDHF/RCI2	NIST	MBPT&MCDHF/RCI2	MBPT&NIST
21	$2s2p^4 \ ^4P_{5/2} - 2s^22p^3 \ ^4S_{3/2}$	1.429E-01	1.441E-01	1.600E-01	0.1	12
21	$2s2p^4 \ ^4P_{5/2} - 2s^22p^3 \ ^2D_{3/2}$	1.527E-03	1.529E-03	1.900E-03	0.1	24
21	$2s2p^4 \ ^4P_{5/2} - 2s^22p^3 \ ^2P_{3/2}$	7.145E-04	7.211E-04	9.500E-04	0.9	33
21	$2s2p^4 \ ^4P_{3/2} - 2s^22p^3 \ ^4S_{3/2}$	9.674E-02	9.757E-02	1.120E-01	0.9	16
21	$2s2p^4 \ ^4P_{3/2} - 2s^22p^3 \ ^2P_{3/2}$	1.326E-03	1.333E-03	1.700E-03	0.5	28
21	$2s2p^4 \ ^4P_{1/2} - 2s^22p^3 \ ^4S_{3/2}$	4.921E-02	4.963E-02	5.670E-02	0.9	15
21	$2s2p^4 \ ^4P_{1/2} - 2s^22p^3 \ ^2P_{1/2}$	3.323E-04	3.326E-04	3.800E-04	0.1	14
21	$2s2p^4 \ ^2D_{3/2} - 2s^22p^3 \ ^4S_{3/2}$	2.972E-04	2.979E-04	3.600E-04	0.3	21
21	$2s2p^4 \ ^2D_{3/2} - 2s^22p^3 \ ^2D_{3/2}$	1.540E-01	1.553E-01	1.800E-01	0.9	17
21	$2s2p^4 \ ^2D_{3/2} - 2s^22p^3 \ ^2D_{5/2}$	4.680E-03	4.734E-03	5.600E-03	1.2	20
21	$2s2p^4 \ ^2D_{3/2} - 2s^22p^3 \ ^2P_{1/2}$	2.206E-02	2.224E-02	2.550E-02	0.8	16
21	$2s2p^4 \ ^2D_{3/2} - 2s^22p^3 \ ^2P_{3/2}$	1.842E-03	1.872E-03	3.500E-03	1.6	90
21	$2s2p^4 \ ^2D_{5/2} - 2s^22p^3 \ ^2D_{5/2}$	2.055E-01	2.072E-01	2.350E-01	0.9	14
21	$2s2p^4 \ ^2D_{5/2} - 2s^22p^3 \ ^2P_{3/2}$	6.145E-02	6.195E-02	7.130E-02	0.8	16
21	$2s2p^4 \ ^2S_{1/2} - 2s^22p^3 \ ^4S_{3/2}$	3.061E-04	3.076E-04	4.000E-04	0.5	31
21	$2s2p^4 \ ^2S_{1/2} - 2s^22p^3 \ ^2P_{3/2}$	2.342E-02	2.364E-02	3.120E-02	0.9	33
21	$2s2p^4 \ ^2P_{3/2} - 2s^22p^3 \ ^4S_{3/2}$	1.752E-03	1.753E-03	2.000E-03	0.1	14
21	$2s2p^4 \ ^2P_{3/2} - 2s^22p^3 \ ^2D_{3/2}$	4.465E-02	4.502E-02	5.170E-02	0.8	16
21	$2s2p^4 \ ^2P_{3/2} - 2s^22p^3 \ ^2D_{5/2}$	2.395E-01	2.416E-01	2.710E-01	0.9	13
21	$2s2p^4 \ ^2P_{3/2} - 2s^22p^3 \ ^2P_{1/2}$	2.169E-02	2.182E-02	2.420E-02	0.6	12
21	$2s2p^4 \ ^2P_{1/2} - 2s^22p^3 \ ^4S_{3/2}$	1.139E-04	1.147E-04	1.400E-04	0.7	23
21	$2s2p^4 \ ^2P_{1/2} - 2s^22p^3 \ ^2D_{3/2}$	5.269E-02	5.320E-02	5.850E-02	1.0	11
21	$2s2p^4 \ ^2P_{1/2} - 2s^22p^3 \ ^2P_{1/2}$	1.040E-02	1.046E-02	1.300E-02	0.6	25
21	$2s2p^4 \ ^2P_{1/2} - 2s^22p^3 \ ^2P_{3/2}$	1.059E-01	1.068E-01	1.210E-01	0.8	14
21	$2p^5 \ ^2P_{3/2} - 2s2p^4 \ ^4P_{5/2}$	1.485E-03	1.484E-03	1.700E-03	0.1	15
21	$2p^5 \ ^2P_{3/2} - 2s2p^4 \ ^4P_{1/2}$	1.904E-04	1.903E-04	2.200E-04	-0.1	16
21	$2p^5 \ ^2P_{3/2} - 2s2p^4 \ ^2D_{3/2}$	3.907E-02	3.936E-02	4.600E-02	0.7	18
21	$2p^5 \ ^2P_{3/2} - 2s2p^4 \ ^2D_{5/2}$	1.735E-01	1.748E-01	2.030E-01	0.8	17
21	$2p^5 \ ^2P_{3/2} - 2s2p^4 \ ^2P_{3/2}$	2.631E-01	2.657E-01	3.210E-01	1.0	22
21	$2p^5 \ ^2P_{3/2} - 2s2p^4 \ ^2P_{1/2}$	2.962E-02	2.993E-02	3.960E-02	1.0	34
21	$2p^5 \ ^2P_{1/2} - 2s2p^4 \ ^4P_{1/2}$	2.428E-04	2.428E-04	2.900E-04	0.1	19
21	$2p^5 \ ^2P_{1/2} - 2s2p^4 \ ^2D_{3/2}$	8.001E-02	8.068E-02	9.480E-02	0.8	19
21	$2p^5 \ ^2P_{1/2} - 2s2p^4 \ ^2P_{3/2}$	7.380E-02	7.447E-02	8.950E-02	0.9	21
21	$2p^5 \ ^2P_{1/2} - 2s2p^4 \ ^2P_{1/2}$	1.228E-01	1.239E-01	1.490E-01	0.9	21
22	$2s2p^4 \ ^4P_{5/2} - 2s^22p^3 \ ^2D_{3/2}$	2.172E-03	2.173E-03	2.700E-03	0.1	24
22	$2s2p^4 \ ^4P_{5/2} - 2s^22p^3 \ ^2P_{3/2}$	7.666E-04	7.724E-04	9.900E-04	0.8	29
22	$2s2p^4 \ ^4P_{3/2} - 2s^22p^3 \ ^4S_{3/2}$	8.708E-02	8.776E-02	9.920E-02	0.8	14
22	$2s2p^4 \ ^4P_{3/2} - 2s^22p^3 \ ^2P_{3/2}$	1.558E-03	1.565E-03	1.900E-03	0.4	22
22	$2s2p^4 \ ^4P_{1/2} - 2s^22p^3 \ ^4S_{3/2}$	4.447E-02	4.480E-02	5.120E-02	0.7	15

TABLE 5—Continued

Z	Transition	Line Strengths			Difference (%)	
		MBPT	MCDHF/RCI2	NIST	MBPT&MCDHF/RCI2	MBPT&NIST
22	$2s2p^4 \ ^4P_{1/2} - 2s^22p^3 \ ^2D_{3/2}$	2.585E-04	2.590E-04	3.100E-04	0.2	20
22	$2s2p^4 \ ^4P_{1/2} - 2s^22p^3 \ ^2P_{1/2}$	4.272E-04	4.271E-04	4.900E-04	0.1	15
22	$2s2p^4 \ ^2D_{3/2} - 2s^22p^3 \ ^4S_{3/2}$	4.996E-04	5.002E-04	6.200E-04	0.1	24
22	$2s2p^4 \ ^2D_{3/2} - 2s^22p^3 \ ^2D_{3/2}$	1.407E-01	1.418E-01	1.600E-01	0.8	14
22	$2s2p^4 \ ^2D_{3/2} - 2s^22p^3 \ ^2D_{5/2}$	3.131E-03	3.166E-03	3.800E-03	1.1	21
22	$2s2p^4 \ ^2D_{3/2} - 2s^22p^3 \ ^2P_{1/2}$	1.926E-02	1.940E-02	2.210E-02	0.7	15
22	$2s2p^4 \ ^2D_{3/2} - 2s^22p^3 \ ^2P_{3/2}$	2.343E-03	2.375E-03	4.000E-03	1.4	71
22	$2s2p^4 \ ^2D_{5/2} - 2s^22p^3 \ ^2D_{5/2}$	1.849E-01	1.863E-01	2.100E-01	0.8	14
22	$2s2p^4 \ ^2D_{5/2} - 2s^22p^3 \ ^2P_{3/2}$	5.615E-02	5.655E-02	6.430E-02	0.7	15
22	$2s2p^4 \ ^2S_{1/2} - 2s^22p^3 \ ^4S_{3/2}$	3.846E-04	3.863E-04	4.900E-04	0.4	27
22	$2s2p^4 \ ^2S_{1/2} - 2s^22p^3 \ ^2P_{1/2}$	5.655E-02	5.696E-02	6.300E-02	0.7	11
22	$2s2p^4 \ ^2S_{1/2} - 2s^22p^3 \ ^2P_{3/2}$	1.637E-02	1.652E-02	2.200E-02	0.9	34
22	$2s2p^4 \ ^2P_{3/2} - 2s^22p^3 \ ^4S_{3/2}$	2.175E-03	2.175E-03	2.500E-03	0.1	15
22	$2s2p^4 \ ^2P_{3/2} - 2s^22p^3 \ ^2D_{3/2}$	3.948E-02	3.980E-02	4.490E-02	0.8	14
22	$2s2p^4 \ ^2P_{3/2} - 2s^22p^3 \ ^2D_{5/2}$	2.166E-01	2.183E-01	2.410E-01	0.8	11
22	$2s2p^4 \ ^2P_{3/2} - 2s^22p^3 \ ^2P_{1/2}$	2.048E-02	2.060E-02	2.300E-02	0.6	12
22	$2s2p^4 \ ^2P_{1/2} - 2s^22p^3 \ ^4S_{3/2}$	1.113E-04	1.121E-04	1.400E-04	0.7	26
22	$2s2p^4 \ ^2P_{1/2} - 2s^22p^3 \ ^2D_{3/2}$	4.050E-02	4.085E-02	4.480E-02	0.9	11
22	$2s2p^4 \ ^2P_{1/2} - 2s^22p^3 \ ^2P_{1/2}$	7.992E-03	8.034E-03	9.900E-03	0.5	24
22	$2s2p^4 \ ^2P_{1/2} - 2s^22p^3 \ ^2P_{3/2}$	1.025E-01	1.032E-01	1.200E-01	0.7	17
22	$2p^5 \ ^2P_{3/2} - 2s2p^4 \ ^4P_{5/2}$	1.776E-03	1.775E-03	2.000E-03	-0.1	13
22	$2p^5 \ ^2P_{3/2} - 2s2p^4 \ ^4P_{1/2}$	2.499E-04	2.494E-04	2.900E-04	-0.2	16
22	$2p^5 \ ^2P_{3/2} - 2s2p^4 \ ^2D_{3/2}$	3.882E-02	3.907E-02	4.600E-02	0.6	19
22	$2p^5 \ ^2P_{3/2} - 2s2p^4 \ ^2D_{5/2}$	1.558E-01	1.569E-01	1.800E-01	0.7	16
22	$2p^5 \ ^2P_{3/2} - 2s2p^4 \ ^2S_{1/2}$	4.620E-02	4.654E-02	5.100E-02	0.7	10
22	$2p^5 \ ^2P_{3/2} - 2s2p^4 \ ^2P_{3/2}$	2.336E-01	2.356E-01	2.820E-01	0.9	21
22	$2p^5 \ ^2P_{3/2} - 2s2p^4 \ ^2P_{1/2}$	2.442E-02	2.466E-02	3.240E-02	1.0	33
22	$2p^5 \ ^2P_{1/2} - 2s2p^4 \ ^4P_{1/2}$	2.870E-04	2.874E-04	3.300E-04	0.1	15
22	$2p^5 \ ^2P_{1/2} - 2s2p^4 \ ^2D_{3/2}$	6.925E-02	6.978E-02	8.090E-02	0.8	17
22	$2p^5 \ ^2P_{1/2} - 2s2p^4 \ ^2P_{3/2}$	6.936E-02	6.990E-02	8.300E-02	0.8	20
22	$2p^5 \ ^2P_{1/2} - 2s2p^4 \ ^2P_{1/2}$	1.101E-01	1.110E-01	1.320E-01	0.9	20
23	$2s2p^4 \ ^4P_{5/2} - 2s^22p^3 \ ^4S_{3/2}$	1.145E-01	1.153E-01	1.300E-01	0.7	14
23	$2s2p^4 \ ^4P_{5/2} - 2s^22p^3 \ ^2D_{3/2}$	3.015E-03	3.016E-03	3.600E-03	0.1	19
23	$2s2p^4 \ ^4P_{5/2} - 2s^22p^3 \ ^2P_{3/2}$	8.041E-04	8.101E-04	1.000E-03	0.7	24
23	$2s2p^4 \ ^4P_{3/2} - 2s^22p^3 \ ^4S_{3/2}$	7.874E-02	7.928E-02	8.950E-02	0.7	14
23	$2s2p^4 \ ^4P_{3/2} - 2s^22p^3 \ ^2D_{3/2}$	1.249E-04	1.263E-04	2.700E-04	1.1	116
23	$2s2p^4 \ ^4P_{3/2} - 2s^22p^3 \ ^2P_{3/2}$	1.794E-03	1.801E-03	2.200E-03	0.4	23
23	$2s2p^4 \ ^4P_{1/2} - 2s^22p^3 \ ^4S_{3/2}$	4.036E-02	4.063E-02	4.580E-02	0.7	14
23	$2s2p^4 \ ^4P_{1/2} - 2s^22p^3 \ ^2D_{3/2}$	3.535E-04	3.538E-04	4.200E-04	0.1	19

TABLE 5—Continued

Z	Transition	Line Strengths			Difference (%)	
		MBPT	MCDHF/RCI2	NIST	MBPT&MCDHF/RCI2	MBPT&NIST
23	$2s2p^4\ ^4P_{1/2} - 2s^22p^3\ ^2P_{1/2}$	5.441E-04	5.438E-04	6.200E-04	-0.1	14
23	$2s2p^4\ ^2D_{3/2} - 2s^22p^3\ ^4S_{3/2}$	8.098E-04	8.094E-04	1.000E-03	-0.1	24
23	$2s2p^4\ ^2D_{3/2} - 2s^22p^3\ ^2D_{3/2}$	1.292E-01	1.301E-01	1.500E-01	0.7	16
23	$2s2p^4\ ^2D_{3/2} - 2s^22p^3\ ^2D_{5/2}$	1.921E-03	1.942E-03	2.300E-03	1.1	20
23	$2s2p^4\ ^2D_{3/2} - 2s^22p^3\ ^2P_{1/2}$	1.679E-02	1.691E-02	1.920E-02	0.7	14
23	$2s2p^4\ ^2D_{3/2} - 2s^22p^3\ ^2P_{3/2}$	2.676E-03	2.709E-03	4.200E-03	1.2	57
23	$2s2p^4\ ^2D_{5/2} - 2s^22p^3\ ^2D_{5/2}$	1.670E-01	1.681E-01	1.900E-01	0.7	14
23	$2s2p^4\ ^2D_{5/2} - 2s^22p^3\ ^2P_{3/2}$	5.142E-02	5.175E-02	5.900E-02	0.7	15
23	$2s2p^4\ ^2S_{1/2} - 2s^22p^3\ ^4S_{3/2}$	4.861E-04	4.875E-04	6.200E-04	0.3	28
23	$2s2p^4\ ^2S_{1/2} - 2s^22p^3\ ^2P_{1/2}$	5.225E-02	5.258E-02	5.800E-02	0.6	11
23	$2s2p^4\ ^2S_{1/2} - 2s^22p^3\ ^2P_{3/2}$	1.123E-02	1.133E-02	1.500E-02	0.9	34
23	$2s2p^4\ ^2P_{3/2} - 2s^22p^3\ ^4S_{3/2}$	2.652E-03	2.653E-03	3.000E-03	0.1	13
23	$2s2p^4\ ^2P_{3/2} - 2s^22p^3\ ^2D_{3/2}$	3.432E-02	3.458E-02	3.860E-02	0.8	13
23	$2s2p^4\ ^2P_{3/2} - 2s^22p^3\ ^2D_{5/2}$	1.969E-01	1.982E-01	2.200E-01	0.7	12
23	$2s2p^4\ ^2P_{3/2} - 2s^22p^3\ ^2P_{1/2}$	1.949E-02	1.958E-02	2.200E-02	0.5	13
23	$2s2p^4\ ^2P_{1/2} - 2s^22p^3\ ^4S_{3/2}$	1.018E-04	1.028E-04	1.200E-04	1.0	18
23	$2s2p^4\ ^2P_{1/2} - 2s^22p^3\ ^2D_{3/2}$	3.122E-02	3.146E-02	3.460E-02	0.8	11
23	$2s2p^4\ ^2P_{1/2} - 2s^22p^3\ ^2P_{1/2}$	6.159E-03	6.188E-03	7.500E-03	0.5	22
23	$2s2p^4\ ^2P_{1/2} - 2s^22p^3\ ^2P_{3/2}$	9.809E-02	9.874E-02	1.100E-01	0.7	12
23	$2p^5\ ^2P_{3/2} - 2s2p^4\ ^4P_{3/2}$	9.900E-04	9.890E-04	1.100E-03	-0.1	11
23	$2p^5\ ^2P_{3/2} - 2s2p^4\ ^4P_{1/2}$	3.253E-04	3.246E-04	3.600E-04	-0.2	11
23	$2p^5\ ^2P_{3/2} - 2s2p^4\ ^2D_{3/2}$	3.887E-02	3.909E-02	4.550E-02	0.6	17
23	$2p^5\ ^2P_{3/2} - 2s2p^4\ ^2D_{5/2}$	1.406E-01	1.415E-01	1.600E-01	0.6	14
23	$2p^5\ ^2P_{3/2} - 2s2p^4\ ^2P_{3/2}$	2.077E-01	2.093E-01	2.470E-01	0.8	19
23	$2p^5\ ^2P_{3/2} - 2s2p^4\ ^2P_{1/2}$	2.022E-02	2.040E-02	2.670E-02	0.9	32
23	$2p^5\ ^2P_{1/2} - 2s2p^4\ ^4P_{1/2}$	3.332E-04	3.335E-04	3.900E-04	0.1	17
23	$2p^5\ ^2P_{1/2} - 2s2p^4\ ^2D_{3/2}$	5.986E-02	6.025E-02	6.940E-02	0.7	16
23	$2p^5\ ^2P_{1/2} - 2s2p^4\ ^2P_{3/2}$	6.563E-02	6.609E-02	7.780E-02	0.7	19
23	$2p^5\ ^2P_{1/2} - 2s2p^4\ ^2P_{1/2}$	9.902E-02	9.976E-02	1.180E-01	0.8	19
24	$2s2p^4\ ^4P_{5/2} - 2s^22p^3\ ^4S_{3/2}$	1.026E-01	1.033E-01	1.200E-01	0.7	17
24	$2s2p^4\ ^4P_{5/2} - 2s^22p^3\ ^2D_{3/2}$	4.083E-03	4.086E-03	4.900E-03	0.1	20
24	$2s2p^4\ ^4P_{5/2} - 2s^22p^3\ ^2P_{3/2}$	8.274E-04	8.334E-04	1.000E-03	0.7	21
24	$2s2p^4\ ^4P_{3/2} - 2s^22p^3\ ^4S_{3/2}$	7.146E-02	7.191E-02	8.070E-02	0.6	13
24	$2s2p^4\ ^4P_{3/2} - 2s^22p^3\ ^2D_{3/2}$	2.206E-04	2.223E-04	4.100E-04	0.8	86
24	$2s2p^4\ ^4P_{3/2} - 2s^22p^3\ ^2P_{3/2}$	2.030E-03	2.037E-03	2.400E-03	0.4	18
24	$2s2p^4\ ^4P_{1/2} - 2s^22p^3\ ^4S_{3/2}$	3.677E-02	3.699E-02	4.180E-02	0.6	14
24	$2s2p^4\ ^4P_{1/2} - 2s^22p^3\ ^2D_{3/2}$	4.739E-04	4.740E-04	5.800E-04	0.1	22
24	$2s2p^4\ ^4P_{1/2} - 2s^22p^3\ ^2P_{1/2}$	6.869E-04	6.873E-04	7.600E-04	0.1	11
24	$2s2p^4\ ^2D_{3/2} - 2s^22p^3\ ^4S_{3/2}$	1.262E-03	1.262E-03	1.600E-03	0.1	27

TABLE 5—Continued

Z	Transition	Line Strengths			Difference (%)	
		MBPT	MCDHF/RCI2	NIST	MBPT&MCDHF/RCI2	MBPT&NIST
24	$2s2p^4 \ ^2D_{3/2} - 2s^22p^3 \ ^2D_{5/2}$	1.025E-03	1.037E-03	1.200E-03	1.1	17
24	$2s2p^4 \ ^2D_{3/2} - 2s^22p^3 \ ^2P_{1/2}$	1.461E-02	1.470E-02	1.660E-02	0.6	14
24	$2s2p^4 \ ^2D_{3/2} - 2s^22p^3 \ ^2P_{3/2}$	2.827E-03	2.859E-03	4.200E-03	1.1	49
24	$2s2p^4 \ ^2D_{5/2} - 2s^22p^3 \ ^2D_{5/2}$	1.514E-01	1.524E-01	1.700E-01	0.7	12
24	$2s2p^4 \ ^2D_{5/2} - 2s^22p^3 \ ^2P_{3/2}$	4.722E-02	4.750E-02	5.300E-02	0.6	12
24	$2s2p^4 \ ^2S_{1/2} - 2s^22p^3 \ ^4S_{3/2}$	6.147E-04	6.161E-04	7.600E-04	0.2	24
24	$2s2p^4 \ ^2S_{1/2} - 2s^22p^3 \ ^2P_{1/2}$	4.827E-02	4.857E-02	5.400E-02	0.6	12
24	$2s2p^4 \ ^2S_{1/2} - 2s^22p^3 \ ^2P_{3/2}$	7.549E-03	7.609E-03	1.000E-02	0.8	33
24	$2s2p^4 \ ^2P_{3/2} - 2s^22p^3 \ ^4S_{3/2}$	3.168E-03	3.169E-03	3.500E-03	0.1	11
24	$2s2p^4 \ ^2P_{3/2} - 2s^22p^3 \ ^2D_{3/2}$	2.926E-02	2.948E-02	3.260E-02	0.8	11
24	$2s2p^4 \ ^2P_{3/2} - 2s^22p^3 \ ^2D_{5/2}$	1.796E-01	1.808E-01	2.000E-01	0.7	11
24	$2s2p^4 \ ^2P_{1/2} - 2s^22p^3 \ ^2D_{3/2}$	2.421E-02	2.439E-02	2.670E-02	0.7	10
24	$2s2p^4 \ ^2P_{1/2} - 2s^22p^3 \ ^2P_{1/2}$	4.765E-03	4.780E-03	5.700E-03	0.3	20
24	$2p^5 \ ^2P_{3/2} - 2s2p^4 \ ^4P_{5/2}$	2.433E-03	2.432E-03	2.700E-03	-0.1	11
24	$2p^5 \ ^2P_{3/2} - 2s2p^4 \ ^4P_{1/2}$	4.204E-04	4.198E-04	4.800E-04	-0.2	14
24	$2p^5 \ ^2P_{3/2} - 2s2p^4 \ ^2D_{3/2}$	3.915E-02	3.936E-02	4.510E-02	0.5	15
24	$2p^5 \ ^2P_{3/2} - 2s2p^4 \ ^2D_{5/2}$	1.273E-01	1.280E-01	1.500E-01	0.6	18
24	$2p^5 \ ^2P_{3/2} - 2s2p^4 \ ^2S_{1/2}$	4.156E-02	4.182E-02	4.600E-02	0.6	11
24	$2p^5 \ ^2P_{3/2} - 2s2p^4 \ ^2P_{3/2}$	1.849E-01	1.862E-01	2.180E-01	0.7	18
24	$2p^5 \ ^2P_{3/2} - 2s2p^4 \ ^2P_{1/2}$	1.682E-02	1.695E-02	2.210E-02	0.8	31
24	$2p^5 \ ^2P_{1/2} - 2s2p^4 \ ^4P_{1/2}$	3.796E-04	3.796E-04	4.300E-04	0.1	13
24	$2p^5 \ ^2P_{1/2} - 2s2p^4 \ ^2D_{3/2}$	5.160E-02	5.194E-02	5.920E-02	0.7	15
24	$2p^5 \ ^2P_{1/2} - 2s2p^4 \ ^2P_{3/2}$	6.246E-02	6.286E-02	7.330E-02	0.6	17
24	$2p^5 \ ^2P_{1/2} - 2s2p^4 \ ^2P_{1/2}$	8.925E-02	8.986E-02	1.050E-01	0.7	18
25	$2s2p^4 \ ^2S_{1/2} - 2s^22p^3 \ ^4S_{3/2}$	7.729E-04	7.741E-04	9.700E-04	0.2	26
25	$2s2p^4 \ ^2P_{3/2} - 2s^22p^3 \ ^4S_{3/2}$	3.695E-03	3.698E-03	4.200E-03	0.1	14
25	$2s2p^4 \ ^2P_{3/2} - 2s^22p^3 \ ^2D_{3/2}$	2.440E-02	2.457E-02	2.690E-02	0.7	10
25	$2s2p^4 \ ^2P_{1/2} - 2s^22p^3 \ ^2D_{3/2}$	1.894E-02	1.907E-02	2.090E-02	0.7	10
25	$2s2p^4 \ ^2P_{1/2} - 2s^22p^3 \ ^2P_{1/2}$	3.693E-03	3.705E-03	4.500E-03	0.3	22
25	$2p^5 \ ^2P_{3/2} - 2s2p^4 \ ^4P_{5/2}$	2.789E-03	2.787E-03	3.100E-03	-0.1	11
25	$2p^5 \ ^2P_{3/2} - 2s2p^4 \ ^4P_{1/2}$	5.401E-04	5.391E-04	6.200E-04	-0.2	15
25	$2p^5 \ ^2P_{1/2} - 2s2p^4 \ ^4P_{1/2}$	4.233E-04	4.237E-04	4.800E-04	0.1	13
26	$2s2p^4 \ ^4P_{5/2} - 2s^22p^3 \ ^2D_{3/2}$	6.935E-03	6.936E-03	8.200E-03	0.1	18
26	$2s2p^4 \ ^4P_{5/2} - 2s^22p^3 \ ^2D_{5/2}$	3.624E-03	3.626E-03	4.200E-03	0.1	16
26	$2s2p^4 \ ^4P_{5/2} - 2s^22p^3 \ ^2P_{3/2}$	8.312E-04	8.365E-04	1.000E-03	0.6	20
26	$2s2p^4 \ ^4P_{3/2} - 2s^22p^3 \ ^4S_{3/2}$	5.958E-02	5.988E-02	6.640E-02	0.5	11
26	$2s2p^4 \ ^4P_{3/2} - 2s^22p^3 \ ^2D_{3/2}$	4.934E-04	4.957E-04	8.100E-04	0.5	64
26	$2s2p^4 \ ^4P_{3/2} - 2s^22p^3 \ ^2P_{3/2}$	2.477E-03	2.484E-03	2.900E-03	0.3	17
26	$2s2p^4 \ ^4P_{1/2} - 2s^22p^3 \ ^4S_{3/2}$	3.080E-02	3.095E-02	3.450E-02	0.5	12

TABLE 5—Continued

Z	Transition	Line Strengths			Difference (%)	
		MBPT	MCDHF/RCI2	NIST	MBPT&MCDHF/RCI2	MBPT&NIST
26	$2s2p^4 \ ^4P_{1/2} - 2s^22p^3 \ ^2D_{3/2}$	7.929E-04	7.925E-04	9.600E-04	-0.1	21
26	$2s2p^4 \ ^4P_{1/2} - 2s^22p^3 \ ^2P_{1/2}$	1.070E-03	1.069E-03	1.300E-03	-0.1	22
26	$2s2p^4 \ ^2D_{3/2} - 2s^22p^3 \ ^4S_{3/2}$	2.710E-03	2.707E-03	3.300E-03	-0.1	22
26	$2s2p^4 \ ^2D_{3/2} - 2s^22p^3 \ ^2D_{5/2}$	9.015E-05	9.214E-05	1.300E-04	2.2	44
26	$2s2p^4 \ ^2D_{3/2} - 2s^22p^3 \ ^2P_{1/2}$	1.094E-02	1.100E-02	1.230E-02	0.6	12
26	$2s2p^4 \ ^2D_{3/2} - 2s^22p^3 \ ^2P_{3/2}$	2.620E-03	2.649E-03	3.700E-03	1.1	41
26	$2s2p^4 \ ^2D_{5/2} - 2s^22p^3 \ ^2D_{3/2}$	5.550E-05	5.503E-05	1.000E-04	-0.9	80
26	$2s2p^4 \ ^2D_{5/2} - 2s^22p^3 \ ^2D_{5/2}$	1.257E-01	1.264E-01	1.400E-01	0.5	11
26	$2s2p^4 \ ^2D_{5/2} - 2s^22p^3 \ ^2P_{3/2}$	4.019E-02	4.039E-02	4.500E-02	0.5	12
26	$2s2p^4 \ ^2S_{1/2} - 2s^22p^3 \ ^4S_{3/2}$	9.587E-04	9.602E-04	1.100E-03	0.2	15
26	$2s2p^4 \ ^2S_{1/2} - 2s^22p^3 \ ^2P_{3/2}$	3.138E-03	3.163E-03	4.500E-03	0.8	43
26	$2s2p^4 \ ^2P_{3/2} - 2s^22p^3 \ ^4S_{3/2}$	4.195E-03	4.197E-03	4.700E-03	0.1	12
26	$2s2p^4 \ ^2P_{1/2} - 2s^22p^3 \ ^2D_{3/2}$	1.497E-02	1.506E-02	1.660E-02	0.6	11
26	$2s2p^4 \ ^2P_{1/2} - 2s^22p^3 \ ^2P_{1/2}$	2.873E-03	2.882E-03	3.500E-03	0.3	22
26	$2p^5 \ ^2P_{3/2} - 2s2p^4 \ ^4P_{1/2}$	6.885E-04	6.870E-04	7.800E-04	-0.2	13
26	$2p^5 \ ^2P_{3/2} - 2s2p^4 \ ^2D_{3/2}$	4.008E-02	4.025E-02	4.580E-02	0.4	14
26	$2p^5 \ ^2P_{3/2} - 2s2p^4 \ ^2D_{5/2}$	1.053E-01	1.058E-01	1.200E-01	0.5	14
26	$2p^5 \ ^2P_{3/2} - 2s2p^4 \ ^2S_{1/2}$	3.709E-02	3.728E-02	4.100E-02	0.5	11
26	$2p^5 \ ^2P_{3/2} - 2s2p^4 \ ^2P_{3/2}$	1.465E-01	1.474E-01	1.700E-01	0.6	16
26	$2p^5 \ ^2P_{3/2} - 2s2p^4 \ ^2P_{1/2}$	1.178E-02	1.186E-02	1.520E-02	0.7	29
26	$2p^5 \ ^2P_{1/2} - 2s2p^4 \ ^4P_{1/2}$	4.628E-04	4.631E-04	5.200E-04	0.1	12
26	$2p^5 \ ^2P_{1/2} - 2s2p^4 \ ^2D_{3/2}$	3.794E-02	3.813E-02	4.300E-02	0.5	13
26	$2p^5 \ ^2P_{1/2} - 2s2p^4 \ ^2P_{3/2}$	5.737E-02	5.766E-02	6.600E-02	0.5	15
26	$2p^5 \ ^2P_{1/2} - 2s2p^4 \ ^2P_{1/2}$	7.299E-02	7.341E-02	8.400E-02	0.6	15
27	$2s2p^4 \ ^4P_{5/2} - 2s^22p^3 \ ^4S_{3/2}$	7.280E-02	7.325E-02	8.070E-02	0.6	11
27	$2s2p^4 \ ^4P_{5/2} - 2s^22p^3 \ ^2D_{3/2}$	8.660E-03	8.661E-03	1.000E-02	0.1	16
27	$2s2p^4 \ ^4P_{5/2} - 2s^22p^3 \ ^2D_{5/2}$	4.067E-03	4.068E-03	4.500E-03	0.1	11
27	$2s2p^4 \ ^4P_{5/2} - 2s^22p^3 \ ^2P_{3/2}$	8.149E-04	8.198E-04	9.700E-04	0.6	19
27	$2s2p^4 \ ^4P_{3/2} - 2s^22p^3 \ ^4S_{3/2}$	5.476E-02	5.503E-02	6.040E-02	0.5	10
27	$2s2p^4 \ ^4P_{3/2} - 2s^22p^3 \ ^2D_{3/2}$	6.422E-04	6.452E-04	1.000E-03	0.5	56
27	$2s2p^4 \ ^4P_{3/2} - 2s^22p^3 \ ^2P_{3/2}$	2.679E-03	2.687E-03	3.200E-03	0.3	19
27	$2s2p^4 \ ^4P_{1/2} - 2s^22p^3 \ ^4S_{3/2}$	2.828E-02	2.842E-02	3.160E-02	0.5	12
27	$2s2p^4 \ ^4P_{1/2} - 2s^22p^3 \ ^2D_{3/2}$	9.795E-04	9.792E-04	1.200E-03	0.1	23
27	$2s2p^4 \ ^4P_{1/2} - 2s^22p^3 \ ^2P_{1/2}$	1.317E-03	1.316E-03	1.500E-03	-0.1	14
27	$2s2p^4 \ ^2D_{3/2} - 2s^22p^3 \ ^4S_{3/2}$	3.705E-03	3.702E-03	4.400E-03	-0.1	19
27	$2s2p^4 \ ^2D_{3/2} - 2s^22p^3 \ ^2P_{1/2}$	9.408E-03	9.457E-03	1.060E-02	0.5	13
27	$2s2p^4 \ ^2D_{3/2} - 2s^22p^3 \ ^2P_{3/2}$	2.333E-03	2.359E-03	3.200E-03	1.1	37
27	$2s2p^4 \ ^2D_{5/2} - 2s^22p^3 \ ^2D_{3/2}$	1.335E-04	1.329E-04	2.000E-04	-0.4	50
27	$2s2p^4 \ ^2D_{5/2} - 2s^22p^3 \ ^2D_{5/2}$	1.149E-01	1.156E-01	1.300E-01	0.6	13

TABLE 5—Continued

Z	Transition	Line Strengths			Difference (%)	
		MBPT	MCDHF/RCI2	NIST	MBPT&MCDHF/RCI2	MBPT&NIST
27	$2s2p^4 \ ^2D_{5/2} - 2s^22p^3 \ ^2P_{3/2}$	3.725E-02	3.742E-02	4.100E-02	0.5	10
27	$2s2p^4 \ ^2S_{1/2} - 2s^22p^3 \ ^4S_{3/2}$	1.163E-03	1.164E-03	1.400E-03	0.1	20
27	$2s2p^4 \ ^2S_{1/2} - 2s^22p^3 \ ^2P_{3/2}$	1.903E-03	1.920E-03	2.900E-03	0.9	52
27	$2s2p^4 \ ^2P_{3/2} - 2s^22p^3 \ ^4S_{3/2}$	4.615E-03	4.618E-03	5.200E-03	0.1	13
27	$2s2p^4 \ ^2P_{1/2} - 2s^22p^3 \ ^2D_{3/2}$	1.195E-02	1.202E-02	1.320E-02	0.6	11
27	$2s2p^4 \ ^2P_{1/2} - 2s^22p^3 \ ^2P_{1/2}$	2.241E-03	2.247E-03	2.700E-03	0.3	21
27	$2s2p^4 \ ^2P_{1/2} - 2s^22p^3 \ ^2P_{3/2}$	7.721E-02	7.758E-02	8.700E-02	0.5	13
27	$2p^5 \ ^2P_{3/2} - 2s2p^4 \ ^4P_{5/2}$	3.531E-03	3.530E-03	3.900E-03	0.1	11
27	$2p^5 \ ^2P_{3/2} - 2s2p^4 \ ^4P_{1/2}$	8.703E-04	8.684E-04	9.600E-04	-0.2	10
27	$2p^5 \ ^2P_{3/2} - 2s2p^4 \ ^2D_{3/2}$	4.054E-02	4.071E-02	4.610E-02	0.4	14
27	$2p^5 \ ^2P_{3/2} - 2s2p^4 \ ^2D_{5/2}$	9.614E-02	9.655E-02	1.100E-01	0.4	14
27	$2p^5 \ ^2P_{3/2} - 2s2p^4 \ ^2P_{3/2}$	1.303E-01	1.311E-01	1.500E-01	0.6	15
27	$2p^5 \ ^2P_{3/2} - 2s2p^4 \ ^2P_{1/2}$	9.916E-03	9.973E-03	1.280E-02	0.6	29
27	$2p^5 \ ^2P_{1/2} - 2s2p^4 \ ^4P_{1/2}$	4.945E-04	4.954E-04	5.500E-04	0.2	11
27	$2p^5 \ ^2P_{1/2} - 2s2p^4 \ ^2D_{3/2}$	3.230E-02	3.246E-02	3.640E-02	0.5	13
27	$2p^5 \ ^2P_{1/2} - 2s2p^4 \ ^2P_{3/2}$	5.525E-02	5.550E-02	6.350E-02	0.5	15
27	$2p^5 \ ^2P_{1/2} - 2s2p^4 \ ^2P_{1/2}$	6.621E-02	6.657E-02	7.800E-02	0.5	18
28	$2s2p^4 \ ^4P_{5/2} - 2s^22p^3 \ ^4S_{3/2}$	6.443E-02	6.486E-02	7.090E-02	0.7	10
28	$2s2p^4 \ ^4P_{5/2} - 2s^22p^3 \ ^2D_{3/2}$	1.048E-02	1.050E-02	1.200E-02	0.2	15
28	$2s2p^4 \ ^4P_{5/2} - 2s^22p^3 \ ^2D_{5/2}$	4.510E-03	4.515E-03	5.000E-03	0.1	11
28	$2s2p^4 \ ^4P_{5/2} - 2s^22p^3 \ ^2P_{3/2}$	7.887E-04	7.944E-04	9.600E-04	0.7	22
28	$2s2p^4 \ ^4P_{3/2} - 2s^22p^3 \ ^2D_{3/2}$	7.643E-04	7.699E-04	1.200E-03	0.7	57
28	$2s2p^4 \ ^4P_{3/2} - 2s^22p^3 \ ^2P_{3/2}$	2.860E-03	2.872E-03	3.500E-03	0.4	22
28	$2s2p^4 \ ^4P_{1/2} - 2s^22p^3 \ ^4S_{3/2}$	2.603E-02	2.617E-02	2.900E-02	0.5	11
28	$2s2p^4 \ ^4P_{1/2} - 2s^22p^3 \ ^2D_{3/2}$	1.166E-03	1.167E-03	1.400E-03	0.1	20
28	$2s2p^4 \ ^4P_{1/2} - 2s^22p^3 \ ^2P_{1/2}$	1.605E-03	1.605E-03	1.800E-03	0.1	12
28	$2s2p^4 \ ^2D_{3/2} - 2s^22p^3 \ ^4S_{3/2}$	4.812E-03	4.812E-03	5.700E-03	0.1	19
28	$2s2p^4 \ ^2D_{3/2} - 2s^22p^3 \ ^2D_{3/2}$	8.805E-02	8.850E-02	9.700E-02	0.5	10
28	$2s2p^4 \ ^2D_{3/2} - 2s^22p^3 \ ^2P_{1/2}$	8.045E-03	8.093E-03	8.980E-03	0.6	12
28	$2s2p^4 \ ^2D_{3/2} - 2s^22p^3 \ ^2P_{3/2}$	1.976E-03	2.000E-03	2.700E-03	1.2	37
28	$2s2p^4 \ ^2D_{5/2} - 2s^22p^3 \ ^2D_{3/2}$	2.255E-04	2.254E-04	3.100E-04	-0.1	38
28	$2s2p^4 \ ^2D_{5/2} - 2s^22p^3 \ ^2D_{5/2}$	1.054E-01	1.060E-01	1.200E-01	0.6	14
28	$2s2p^4 \ ^2S_{1/2} - 2s^22p^3 \ ^4S_{3/2}$	1.369E-03	1.371E-03	1.600E-03	0.1	17
28	$2s2p^4 \ ^2S_{1/2} - 2s^22p^3 \ ^2P_{3/2}$	1.079E-03	1.091E-03	1.600E-03	1.2	48
28	$2s2p^4 \ ^2P_{3/2} - 2s^22p^3 \ ^4S_{3/2}$	4.906E-03	4.910E-03	5.500E-03	0.1	12
28	$2s2p^4 \ ^2P_{1/2} - 2s^22p^3 \ ^2D_{3/2}$	9.645E-03	9.696E-03	1.070E-02	0.5	11
28	$2s2p^4 \ ^2P_{1/2} - 2s^22p^3 \ ^2P_{1/2}$	1.752E-03	1.757E-03	2.100E-03	0.3	20
28	$2s2p^4 \ ^2P_{1/2} - 2s^22p^3 \ ^2P_{3/2}$	7.210E-02	7.244E-02	8.100E-02	0.5	12
28	$2p^5 \ ^2P_{3/2} - 2s2p^4 \ ^4P_{1/2}$	1.089E-03	1.087E-03	1.200E-03	-0.2	10

TABLE 5—*Continued*

<i>Z</i>	Transition	Line Strengths			Difference (%)	
		MBPT	MCDHF/RCI2	NIST	MBPT&MCDHF/RCI2	MBPT&NIST
28	$2p^5 \ ^2P_{3/2} - 2s2p^4 \ ^2D_{3/2}$	4.087E-02	4.105E-02	4.640E-02	0.4	14
28	$2p^5 \ ^2P_{3/2} - 2s2p^4 \ ^2D_{5/2}$	8.799E-02	8.841E-02	9.920E-02	0.5	13
28	$2p^5 \ ^2P_{3/2} - 2s2p^4 \ ^2S_{1/2}$	3.286E-02	3.304E-02	3.620E-02	0.5	10
28	$2p^5 \ ^2P_{3/2} - 2s2p^4 \ ^2P_{3/2}$	1.158E-01	1.165E-01	1.300E-01	0.6	12
28	$2p^5 \ ^2P_{3/2} - 2s2p^4 \ ^2P_{1/2}$	8.376E-03	8.429E-03	1.070E-02	0.6	28
28	$2p^5 \ ^2P_{1/2} - 2s2p^4 \ ^4P_{1/2}$	5.168E-04	5.177E-04	5.700E-04	0.2	10
28	$2p^5 \ ^2P_{1/2} - 2s2p^4 \ ^2D_{3/2}$	2.734E-02	2.749E-02	3.100E-02	0.6	13
28	$2p^5 \ ^2P_{1/2} - 2s2p^4 \ ^2P_{3/2}$	5.330E-02	5.357E-02	6.000E-02	0.5	13
28	$2p^5 \ ^2P_{1/2} - 2s2p^4 \ ^2P_{1/2}$	6.016E-02	6.050E-02	7.000E-02	0.6	16

TABLE 6

Comparisons of the MCDHF/RCI line strengths and the NIST values relative to the present MBPT results for transitions involving the $n = 3, 4$ levels.

Z	Transition	Line Strengths			Difference (%)	
		MBPT	MCDHF/RCI	NIST	MBPT&MCDHF/RCI	MBPT&NIST
26	$2s^2 2p^2 ({}^3P) 3d {}^4P_{3/2} - 2s^2 2p^3 {}^4S_{3/2}$	8.230E-02	8.25E-02	8.70E-02	0.2	6
26	$2s^2 2p^2 ({}^3P) 3d {}^4P_{3/2} - 2s^2 2p^3 {}^2D_{5/2}$	3.902E-03	3.92E-03	3.60E-03	0.6	-8
26	$2s^2 2p^2 ({}^3P) 3d {}^2D_{3/2} - 2s^2 2p^3 {}^4S_{3/2}$	9.373E-04	9.62E-04	8.50E-04	2.6	-9
26	$2s^2 2p^2 ({}^3P) 3d {}^2D_{3/2} - 2s^2 2p^3 {}^2D_{5/2}$	4.479E-03	4.51E-03	4.80E-03	0.7	7
26	$2s^2 2p^2 ({}^3P) 3d {}^2D_{3/2} - 2s^2 2p^3 {}^2P_{1/2}$	4.412E-02	4.43E-02	4.00E-02	0.4	-9
26	$2s^2 2p^2 ({}^3P) 3d {}^2D_{3/2} - 2s^2 2p^3 {}^2P_{3/2}$	5.593E-03	5.58E-03	5.50E-03	-0.2	-2
26	$2s^2 2p^2 ({}^3P) 3d {}^2D_{5/2} - 2s^2 2p^3 {}^4S_{3/2}$	7.721E-03	7.89E-03	6.80E-03	2.2	-12
26	$2s^2 2p^2 ({}^3P) 3d {}^2D_{5/2} - 2s^2 2p^3 {}^2D_{3/2}$	1.082E-01	1.09E-01	1.00E-01	0.6	-8
26	$2s^2 2p^2 ({}^3P) 3d {}^2D_{5/2} - 2s^2 2p^3 {}^2D_{5/2}$	3.125E-02	3.15E-02	3.40E-02	0.7	9
26	$2s^2 2p^2 ({}^3P) 3d {}^2D_{5/2} - 2s^2 2p^3 {}^2P_{3/2}$	1.611E-03	1.61E-03	1.10E-03	-0.2	-32
26	$2s^2 2p^2 ({}^1D) 3d {}^2D_{3/2} - 2s^2 2p^3 {}^4S_{3/2}$	8.106E-04	8.29E-04	5.20E-04	2.2	-36
26	$2s^2 2p^2 ({}^1D) 3d {}^2D_{3/2} - 2s^2 2p^3 {}^2D_{3/2}$	4.761E-02	4.77E-02	4.60E-02	0.3	-3
26	$2s^2 2p^2 ({}^1D) 3d {}^2D_{3/2} - 2s^2 2p^3 {}^2D_{5/2}$	1.188E-02	1.19E-02	1.10E-02	0.3	-7
26	$2s^2 2p^2 ({}^1D) 3d {}^2D_{3/2} - 2s^2 2p^3 {}^2P_{1/2}$	1.155E-02	1.16E-02	1.30E-02	0.3	13
26	$2s^2 2p^2 ({}^1D) 3d {}^2D_{3/2} - 2s^2 2p^3 {}^2P_{3/2}$	1.868E-03	1.86E-03	1.90E-03	-0.5	2
26	$2s^2 2p^2 ({}^1D) 3d {}^2D_{5/2} - 2s^2 2p^3 {}^4S_{3/2}$	8.639E-04	8.45E-04	7.20E-03	-2.2	733
26	$2s^2 2p^2 ({}^1D) 3d {}^2D_{5/2} - 2s^2 2p^3 {}^2D_{3/2}$	5.639E-02	5.69E-02	6.90E-02	0.9	22
26	$2s^2 2p^2 ({}^1D) 3d {}^2D_{5/2} - 2s^2 2p^3 {}^2D_{5/2}$	6.775E-02	6.78E-02	6.10E-02	0.1	-10
26	$2s^2 2p^2 ({}^1D) 3d {}^2D_{5/2} - 2s^2 2p^3 {}^2P_{3/2}$	6.201E-03	6.33E-03	1.08E-03	2.0	-83
26	$2s^2 2p^2 ({}^1D) 3d {}^2P_{3/2} - 2s^2 2p^3 {}^4S_{3/2}$	5.602E-04	5.70E-04	4.70E-04	1.8	-16
26	$2s^2 2p^2 ({}^1D) 3d {}^2P_{3/2} - 2s^2 2p^3 {}^2D_{3/2}$	1.188E-03	1.19E-03	1.40E-03	-0.1	18
26	$2s^2 2p^2 ({}^1D) 3d {}^2P_{3/2} - 2s^2 2p^3 {}^2D_{5/2}$	6.278E-03	6.34E-03	6.70E-03	1.0	7
26	$2s^2 2p^2 ({}^1D) 3d {}^2P_{3/2} - 2s^2 2p^3 {}^2P_{1/2}$	6.113E-03	6.16E-03	7.30E-03	0.8	19
26	$2s^2 2p^2 ({}^1D) 3d {}^2P_{3/2} - 2s^2 2p^3 {}^2P_{3/2}$	6.458E-02	6.49E-02	6.20E-02	0.6	-4
26	$2s^2 2p^2 ({}^1S) 3d {}^2D_{5/2} - 2s^2 2p^3 {}^2D_{5/2}$	4.953E-03	5.11E-03	6.10E-03	3.1	23
26	$2s^2 2p^2 ({}^1S) 3d {}^2D_{5/2} - 2s^2 2p^3 {}^2P_{3/2}$	7.838E-02	7.93E-02	9.00E-02	1.2	15

TABLE 7

Comparisons of the MCDHF/RCI2 line strengths and the NIST values relative to the present MBPT results for the M1 and E2 transitions among the $n = 2$ levels.

Z	Transition	Type	Line strengths			Difference (%)	
			MBPT	MCDHF/RCI2	NIST	MBPT&MCDHF/RCI2	MBPT&NIST
19	$2s^2 2p^3 \ ^2D_{3/2} - 2s^2 2p^3 \ ^4S_{3/2}$	M1	3.312E-02	3.303E-02	3.190E-02	-0.3	-4
19	$2s^2 2p^3 \ ^2P_{1/2} - 2s^2 2p^3 \ ^4S_{3/2}$	M1	1.642E-02	1.641E-02	1.600E-02	-0.1	-3
19	$2s^2 2p^3 \ ^2P_{3/2} - 2s^2 2p^3 \ ^4S_{3/2}$	M1	5.796E-02	5.816E-02	5.680E-02	0.3	-2
21	$2s^2 2p^3 \ ^2D_{3/2} - 2s^2 2p^3 \ ^4S_{3/2}$	M1	1.048E-01	1.045E-01	1.186E-01	-0.3	13
21	$2s^2 2p^3 \ ^2D_{5/2} - 2s^2 2p^3 \ ^2D_{3/2}$	M1	2.055E+00	2.064E+00	2.020E+00	0.5	-2
21	$2s^2 2p^3 \ ^2D_{5/2} - 2s^2 2p^3 \ ^2D_{3/2}$	E2	3.768E-03	...	4.500E-03	...	19
21	$2s^2 2p^3 \ ^2P_{1/2} - 2s^2 2p^3 \ ^4S_{3/2}$	M1	3.253E-02	3.250E-02	3.522E-02	-0.1	8
21	$2s^2 2p^3 \ ^2P_{1/2} - 2s^2 2p^3 \ ^2D_{3/2}$	M1	1.722E-01	1.731E-01	1.857E-01	0.5	8
21	$2s^2 2p^3 \ ^2P_{1/2} - 2s^2 2p^3 \ ^2D_{3/2}$	E2	1.102E-02	1.109E-02	1.100E-02	0.6	0
21	$2s^2 2p^3 \ ^2P_{1/2} - 2s^2 2p^3 \ ^2D_{5/2}$	E2	8.440E-03	...	8.700E-03	...	3
21	$2s^2 2p^3 \ ^2P_{3/2} - 2s^2 2p^3 \ ^4S_{3/2}$	M1	8.954E-02	8.978E-02	9.390E-02	0.3	5
21	$2s^2 2p^3 \ ^2P_{3/2} - 2s^2 2p^3 \ ^2D_{3/2}$	M1	5.492E-01	5.509E-01	6.049E-01	0.3	10
21	$2s^2 2p^3 \ ^2P_{3/2} - 2s^2 2p^3 \ ^2D_{3/2}$	E2	6.318E-03	6.353E-03	6.000E-03	0.6	-5
21	$2s^2 2p^3 \ ^2P_{3/2} - 2s^2 2p^3 \ ^2D_{5/2}$	M1	3.280E-01	3.299E-01	3.680E-01	0.6	12
21	$2s^2 2p^3 \ ^2P_{3/2} - 2s^2 2p^3 \ ^2D_{5/2}$	E2	2.459E-02	2.478E-02	2.400E-02	0.8	-2
21	$2s^2 2p^3 \ ^2P_{3/2} - 2s^2 2p^3 \ ^2P_{1/2}$	M1	1.119E+00	1.125E+00	1.100E+00	0.5	-2
21	$2s^2 2p^3 \ ^2P_{3/2} - 2s^2 2p^3 \ ^2P_{1/2}$	E2	1.519E-03	...	1.800E-03	...	19
21	$2p^5 \ ^2P_{1/2} - 2p^5 \ ^2P_{3/2}$	M1	1.319E+00	1.330E+00	1.386E+00	0.9	5
21	$2p^5 \ ^2P_{1/2} - 2p^5 \ ^2P_{3/2}$	E2	6.929E-03	...	7.900E-03	...	14
22	$2s^2 2p^3 \ ^2D_{3/2} - 2s^2 2p^3 \ ^4S_{3/2}$	M1	1.741E-01	1.735E-01	1.900E-01	-0.3	9
22	$2s^2 2p^3 \ ^2D_{5/2} - 2s^2 2p^3 \ ^2D_{3/2}$	M1	1.997E+00	2.007E+00	1.970E+00	0.5	-1
22	$2s^2 2p^3 \ ^2D_{5/2} - 2s^2 2p^3 \ ^2D_{3/2}$	E2	3.453E-03	...	3.900E-03	...	13
22	$2s^2 2p^3 \ ^2P_{1/2} - 2s^2 2p^3 \ ^4S_{3/2}$	M1	4.456E-02	4.451E-02	4.700E-02	-0.1	5
22	$2s^2 2p^3 \ ^2P_{1/2} - 2s^2 2p^3 \ ^2D_{3/2}$	M1	1.967E-01	1.976E-01	2.200E-01	0.5	12
22	$2s^2 2p^3 \ ^2P_{1/2} - 2s^2 2p^3 \ ^2D_{3/2}$	E2	8.595E-03	8.648E-03	8.400E-03	0.6	-2
22	$2s^2 2p^3 \ ^2P_{1/2} - 2s^2 2p^3 \ ^2D_{5/2}$	E2	6.777E-03	...	6.900E-03	...	2
22	$2s^2 2p^3 \ ^2P_{3/2} - 2s^2 2p^3 \ ^4S_{3/2}$	M1	1.046E-01	1.049E-01	1.100E-01	0.3	5
22	$2s^2 2p^3 \ ^2P_{3/2} - 2s^2 2p^3 \ ^2D_{3/2}$	M1	6.426E-01	6.441E-01	7.000E-01	0.2	9
22	$2s^2 2p^3 \ ^2P_{3/2} - 2s^2 2p^3 \ ^2D_{3/2}$	E2	4.418E-03	4.438E-03	4.300E-03	0.5	-3
22	$2s^2 2p^3 \ ^2P_{3/2} - 2s^2 2p^3 \ ^2D_{5/2}$	M1	3.833E-01	3.852E-01	4.300E-01	0.5	12
22	$2s^2 2p^3 \ ^2P_{3/2} - 2s^2 2p^3 \ ^2D_{5/2}$	E2	1.907E-02	1.919E-02	2.000E-02	0.6	5
22	$2s^2 2p^3 \ ^2P_{3/2} - 2s^2 2p^3 \ ^2P_{1/2}$	M1	1.083E+00	1.088E+00	1.100E+00	0.4	2
22	$2s^2 2p^3 \ ^2P_{3/2} - 2s^2 2p^3 \ ^2P_{1/2}$	E2	1.447E-03	...	1.700E-03	...	18
22	$2s^1 2p^4 \ ^4P_{3/2} - 2s^1 2p^4 \ ^4P_{5/2}$	M1	3.558E+00	3.572E+00	3.600E+00	0.4	1
22	$2s^1 2p^4 \ ^4P_{1/2} - 2s^1 2p^4 \ ^4P_{5/2}$	E2	5.176E-03	...	5.500E-03	...	6
22	$2s^1 2p^4 \ ^4P_{1/2} - 2s^1 2p^4 \ ^4P_{3/2}$	M1	3.246E+00	3.259E+00	3.260E+00	0.4	0
22	$2s^1 2p^4 \ ^2D_{3/2} - 2s^1 2p^4 \ ^4P_{3/2}$	M1	4.358E-02	4.318E-02	3.700E-02	-0.9	-15
22	$2s^1 2p^4 \ ^2D_{3/2} - 2s^1 2p^4 \ ^4P_{1/2}$	M1	1.188E-02	1.178E-02	8.700E-03	-0.9	-27
22	$2s^1 2p^4 \ ^2D_{5/2} - 2s^1 2p^4 \ ^4P_{5/2}$	M1	9.246E-02	9.180E-02	8.800E-02	-0.7	-5

TABLE 7—Continued

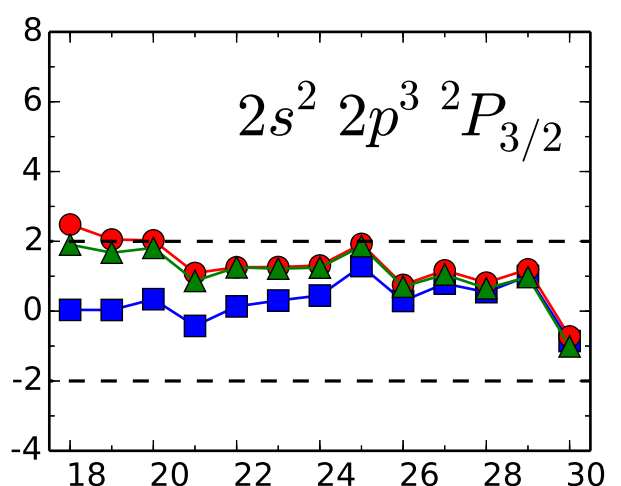
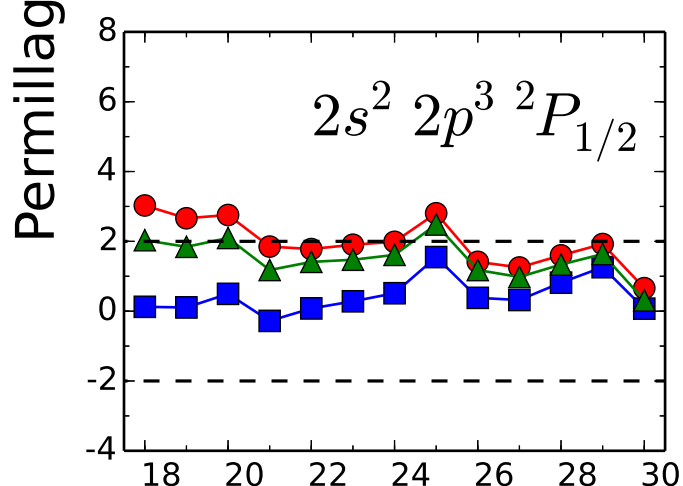
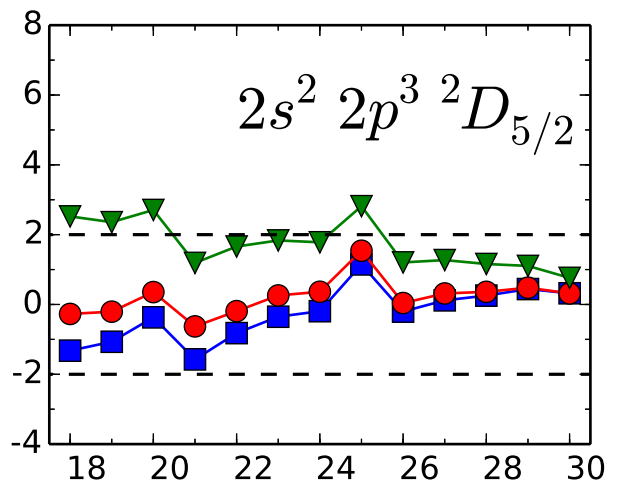
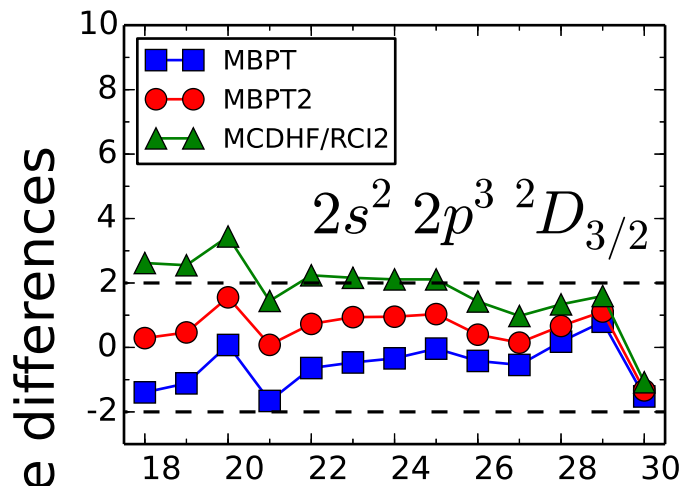
Z	Transition	Type	Line strengths			Difference (%)	
			MBPT	MCDHF/RCI2	NIST	MBPT&MCDHF/RCI2	MBPT&NIST
22	$2s^1 2p^4 \ ^2D_{5/2} - 2s^1 2p^4 \ ^4P_{3/2}$	M1	1.341E-02	1.336E-02	1.300E-02	-0.4	-3
22	$2s^1 2p^4 \ ^2D_{5/2} - 2s^1 2p^4 \ ^2D_{3/2}$	M1	2.345E+00	...	2.400E+00	...	2
22	$2s^1 2p^4 \ ^2S_{1/2} - 2s^1 2p^4 \ ^4P_{3/2}$	M1	4.768E-02	4.751E-02	4.800E-02	-0.4	1
22	$2s^1 2p^4 \ ^2S_{1/2} - 2s^1 2p^4 \ ^2D_{5/2}$	E2	1.194E-02	1.203E-02	1.300E-02	0.8	9
22	$2s^1 2p^4 \ ^2P_{3/2} - 2s^1 2p^4 \ ^2D_{3/2}$	M1	7.558E-02	7.576E-02	7.100E-02	0.2	-6
22	$2s^1 2p^4 \ ^2P_{3/2} - 2s^1 2p^4 \ ^2D_{5/2}$	M1	3.885E-02	3.897E-02	3.700E-02	0.3	-5
22	$2s^1 2p^4 \ ^2P_{3/2} - 2s^1 2p^4 \ ^2S_{1/2}$	M1	1.895E-01	1.904E-01	1.600E-01	0.5	-16
22	$2s^1 2p^4 \ ^2P_{1/2} - 2s^1 2p^4 \ ^2D_{3/2}$	M1	2.085E-02	2.091E-02	2.100E-02	0.3	1
22	$2s^1 2p^4 \ ^2P_{1/2} - 2s^1 2p^4 \ ^2D_{5/2}$	E2	1.800E-03	1.810E-03	1.800E-03	0.6	0
22	$2s^1 2p^4 \ ^2P_{1/2} - 2s^1 2p^4 \ ^2S_{1/2}$	M1	3.441E-01	3.452E-01	2.800E-01	0.3	-19
22	$2s^1 2p^4 \ ^2P_{1/2} - 2s^1 2p^4 \ ^2P_{3/2}$	M1	1.111E+00	1.118E+00	1.200E+00	0.6	8
22	$2p^5 \ ^2P_{1/2} - 2p^5 \ ^2P_{3/2}$	M1	1.319E+00	1.330E+00	1.330E+00	0.8	1
22	$2p^5 \ ^2P_{1/2} - 2p^5 \ ^2P_{3/2}$	E2	5.552E-03	...	6.200E-03	...	12
23	$2s^2 2p^3 \ ^2D_{3/2} - 2s^2 2p^3 \ ^4S_{3/2}$	M1	2.772E-01	2.763E-01	3.000E-01	-0.3	8
23	$2s^2 2p^3 \ ^2D_{5/2} - 2s^2 2p^3 \ ^4S_{3/2}$	M1	1.227E-02	1.222E-02	1.200E-02	-0.4	-2
23	$2s^2 2p^3 \ ^2D_{5/2} - 2s^2 2p^3 \ ^2D_{3/2}$	M1	1.941E+00	1.949E+00	1.900E+00	0.4	-2
23	$2s^2 2p^3 \ ^2D_{5/2} - 2s^2 2p^3 \ ^2D_{3/2}$	E2	3.084E-03	...	3.400E-03	...	10
23	$2s^2 2p^3 \ ^2P_{1/2} - 2s^2 2p^3 \ ^4S_{3/2}$	M1	5.998E-02	5.992E-02	6.400E-02	-0.1	7
23	$2s^2 2p^3 \ ^2P_{1/2} - 2s^2 2p^3 \ ^2D_{3/2}$	M1	2.166E-01	2.176E-01	2.400E-01	0.5	11
23	$2s^2 2p^3 \ ^2P_{1/2} - 2s^2 2p^3 \ ^2D_{3/2}$	E2	6.780E-03	6.819E-03	6.800E-03	0.6	0
23	$2s^2 2p^3 \ ^2P_{1/2} - 2s^2 2p^3 \ ^2D_{5/2}$	E2	5.504E-03	...	5.700E-03	...	4
23	$2s^2 2p^3 \ ^2P_{3/2} - 2s^2 2p^3 \ ^4S_{3/2}$	M1	1.172E-01	1.175E-01	1.200E-01	0.2	2
23	$2s^2 2p^3 \ ^2P_{3/2} - 2s^2 2p^3 \ ^2D_{3/2}$	M1	7.358E-01	7.374E-01	7.800E-01	0.2	6
23	$2s^2 2p^3 \ ^2P_{3/2} - 2s^2 2p^3 \ ^2D_{3/2}$	E2	3.127E-03	3.140E-03	2.900E-03	0.4	-7
23	$2s^2 2p^3 \ ^2P_{3/2} - 2s^2 2p^3 \ ^2D_{5/2}$	M1	4.352E-01	4.371E-01	4.900E-01	0.5	13
23	$2s^2 2p^3 \ ^2P_{3/2} - 2s^2 2p^3 \ ^2D_{5/2}$	E2	1.495E-02	1.504E-02	1.500E-02	0.6	0
23	$2s^2 2p^3 \ ^2P_{3/2} - 2s^2 2p^3 \ ^2P_{1/2}$	M1	1.048E+00	1.052E+00	1.030E+00	0.4	-2
23	$2s^2 2p^3 \ ^2P_{3/2} - 2s^2 2p^3 \ ^2P_{1/2}$	E2	1.349E-03	...	1.500E-03	...	11
23	$2p^5 \ ^2P_{1/2} - 2p^5 \ ^2P_{3/2}$	M1	1.320E+00	1.329E+00	1.360E+00	0.7	3
23	$2p^5 \ ^2P_{1/2} - 2p^5 \ ^2P_{3/2}$	E2	4.500E-03	...	5.000E-03	...	11
24	$2s^2 2p^3 \ ^2D_{3/2} - 2s^2 2p^3 \ ^4S_{3/2}$	M1	4.234E-01	4.221E-01	4.500E-01	-0.3	6
24	$2s^2 2p^3 \ ^2D_{5/2} - 2s^2 2p^3 \ ^4S_{3/2}$	M1	2.054E-02	2.047E-02	2.100E-02	-0.3	2
24	$2s^2 2p^3 \ ^2D_{5/2} - 2s^2 2p^3 \ ^2D_{3/2}$	M1	1.886E+00	1.893E+00	1.860E+00	0.4	-1
24	$2s^2 2p^3 \ ^2D_{5/2} - 2s^2 2p^3 \ ^2D_{3/2}$	E2	2.690E-03	...	2.800E-03	...	4
24	$2s^2 2p^3 \ ^2P_{1/2} - 2s^2 2p^3 \ ^4S_{3/2}$	M1	7.940E-02	7.927E-02	8.300E-02	-0.2	5
24	$2s^2 2p^3 \ ^2P_{1/2} - 2s^2 2p^3 \ ^2D_{3/2}$	M1	2.306E-01	2.315E-01	2.500E-01	0.4	8
24	$2s^2 2p^3 \ ^2P_{1/2} - 2s^2 2p^3 \ ^2D_{3/2}$	E2	5.401E-03	5.430E-03	5.300E-03	0.5	-2
24	$2s^2 2p^3 \ ^2P_{1/2} - 2s^2 2p^3 \ ^2D_{5/2}$	E2	4.516E-03	...	4.600E-03	...	2
24	$2s^2 2p^3 \ ^2P_{3/2} - 2s^2 2p^3 \ ^4S_{3/2}$	M1	1.259E-01	1.263E-01	1.300E-01	0.3	3

TABLE 7—Continued

Z	Transition	Type	Line strengths			Difference (%)	
			MBPT	MCDHF/RCI2	NIST	MBPT&MCDHF/RCI2	MBPT&NIST
24	$2s^2 2p^3 \ ^2P_{3/2} - 2s^2 2p^3 \ ^2D_{3/2}$	M1	8.295E-01	8.309E-01	8.900E-01	0.2	7
24	$2s^2 2p^3 \ ^2P_{3/2} - 2s^2 2p^3 \ ^2D_{3/2}$	E2	2.247E-03	2.256E-03	2.100E-03	0.4	-7
24	$2s^2 2p^3 \ ^2P_{3/2} - 2s^2 2p^3 \ ^2D_{5/2}$	M1	4.825E-01	4.844E-01	5.200E-01	0.4	8
24	$2s^2 2p^3 \ ^2P_{3/2} - 2s^2 2p^3 \ ^2D_{5/2}$	E2	1.185E-02	1.192E-02	1.200E-02	0.6	1
24	$2s^2 2p^3 \ ^2P_{3/2} - 2s^2 2p^3 \ ^2P_{1/2}$	M1	1.015E+00	1.018E+00	1.000E+00	0.3	-1
24	$2p^5 \ ^2P_{1/2} - 2p^5 \ ^2P_{3/2}$	M1	1.321E+00	1.329E+00	1.300E+00	0.6	-2
24	$2p^5 \ ^2P_{1/2} - 2p^5 \ ^2P_{3/2}$	E2	3.685E-03	...	4.000E-03	...	9
26	$2s^2 2p^3 \ ^2D_{3/2} - 2s^2 2p^3 \ ^4S_{3/2}$	M1	8.729E-01	8.703E-01	8.900E-01	-0.3	2
26	$2s^2 2p^3 \ ^2D_{5/2} - 2s^2 2p^3 \ ^4S_{3/2}$	M1	5.106E-02	5.087E-02	5.170E-02	-0.4	1
26	$2s^2 2p^3 \ ^2D_{5/2} - 2s^2 2p^3 \ ^2D_{3/2}$	M1	1.780E+00	1.785E+00	1.760E+00	0.3	-1
26	$2s^2 2p^3 \ ^2D_{5/2} - 2s^2 2p^3 \ ^2D_{3/2}$	E2	1.909E-03	...	1.900E-03	...	0
26	$2s^2 2p^3 \ ^2P_{1/2} - 2s^2 2p^3 \ ^4S_{3/2}$	M1	1.316E-01	1.314E-01	1.400E-01	-0.1	6
26	$2s^2 2p^3 \ ^2P_{1/2} - 2s^2 2p^3 \ ^2D_{3/2}$	M1	2.373E-01	2.383E-01	2.512E-01	0.4	6
26	$2s^2 2p^3 \ ^2P_{1/2} - 2s^2 2p^3 \ ^2D_{3/2}$	E2	3.518E-03	3.535E-03	3.500E-03	0.5	-1
26	$2s^2 2p^3 \ ^2P_{1/2} - 2s^2 2p^3 \ ^2D_{5/2}$	E2	3.125E-03	...	3.200E-03	...	2
26	$2s^2 2p^3 \ ^2P_{3/2} - 2s^2 2p^3 \ ^4S_{3/2}$	M1	1.273E-01	1.279E-01	1.280E-01	0.5	1
26	$2s^2 2p^3 \ ^2P_{3/2} - 2s^2 2p^3 \ ^2D_{3/2}$	M1	1.020E+00	1.021E+00	1.060E+00	0.1	4
26	$2s^2 2p^3 \ ^2P_{3/2} - 2s^2 2p^3 \ ^2D_{5/2}$	M1	5.600E-01	5.618E-01	5.900E-01	0.3	5
26	$2s^2 2p^3 \ ^2P_{3/2} - 2s^2 2p^3 \ ^2D_{5/2}$	E2	7.691E-03	7.730E-03	7.700E-03	0.5	0
26	$2s^2 2p^3 \ ^2P_{3/2} - 2s^2 2p^3 \ ^2P_{1/2}$	M1	9.556E-01	9.583E-01	9.457E-01	0.3	-1
26	$2p^5 \ ^2P_{1/2} - 2p^5 \ ^2P_{3/2}$	M1	1.321E+00	1.328E+00	1.330E+00	0.6	1
26	$2p^5 \ ^2P_{1/2} - 2p^5 \ ^2P_{3/2}$	E2	2.538E-03	2.555E-03	2.700E-03	0.7	6
27	$2s^2 2p^3 \ ^2D_{3/2} - 2s^2 2p^3 \ ^4S_{3/2}$	M1	1.174E+00	1.171E+00	1.200E+00	-0.3	2
27	$2s^2 2p^3 \ ^2D_{5/2} - 2s^2 2p^3 \ ^4S_{3/2}$	M1	7.538E-02	7.513E-02	7.600E-02	-0.3	1
27	$2s^2 2p^3 \ ^2D_{5/2} - 2s^2 2p^3 \ ^2D_{3/2}$	M1	1.725E+00	1.731E+00	1.700E+00	0.3	-1
27	$2s^2 2p^3 \ ^2D_{5/2} - 2s^2 2p^3 \ ^2D_{3/2}$	E2	1.555E-03	...	1.700E-03	...	9
27	$2s^2 2p^3 \ ^2P_{1/2} - 2s^2 2p^3 \ ^4S_{3/2}$	M1	1.643E-01	1.641E-01	1.700E-01	-0.1	3
27	$2s^2 2p^3 \ ^2P_{1/2} - 2s^2 2p^3 \ ^2D_{3/2}$	M1	2.300E-01	2.310E-01	2.400E-01	0.4	4
27	$2s^2 2p^3 \ ^2P_{1/2} - 2s^2 2p^3 \ ^2D_{3/2}$	E2	2.868E-03	2.881E-03	2.900E-03	0.4	1
27	$2s^2 2p^3 \ ^2P_{1/2} - 2s^2 2p^3 \ ^2D_{5/2}$	E2	2.631E-03	...	2.700E-03	...	3
27	$2s^2 2p^3 \ ^2P_{3/2} - 2s^2 2p^3 \ ^4S_{3/2}$	M1	1.196E-01	1.202E-01	1.200E-01	0.5	0
27	$2s^2 2p^3 \ ^2P_{3/2} - 2s^2 2p^3 \ ^2D_{3/2}$	M1	1.117E+00	1.118E+00	1.200E+00	0.1	7
27	$2s^2 2p^3 \ ^2P_{3/2} - 2s^2 2p^3 \ ^2D_{5/2}$	M1	5.903E-01	5.922E-01	6.300E-01	0.3	7
27	$2s^2 2p^3 \ ^2P_{3/2} - 2s^2 2p^3 \ ^2D_{5/2}$	E2	6.287E-03	6.315E-03	6.200E-03	0.4	-1
27	$2s^2 2p^3 \ ^2P_{3/2} - 2s^2 2p^3 \ ^2P_{1/2}$	M1	9.300E-01	9.327E-01	9.100E-01	0.3	-2
27	$2p^5 \ ^2P_{1/2} - 2p^5 \ ^2P_{3/2}$	M1	1.321E+00	1.328E+00	1.330E+00	0.5	1
27	$2p^5 \ ^2P_{1/2} - 2p^5 \ ^2P_{3/2}$	E2	2.132E-03	2.145E-03	2.300E-03	0.6	8
28	$2s^2 2p^3 \ ^2D_{3/2} - 2s^2 2p^3 \ ^4S_{3/2}$	M1	1.508E+00	1.505E+00	1.600E+00	-0.2	6
28	$2s^2 2p^3 \ ^2D_{5/2} - 2s^2 2p^3 \ ^4S_{3/2}$	M1	1.063E-01	1.060E-01	1.100E-01	-0.3	3

TABLE 7—Continued

Z	Transition	Type	Line strengths			Difference (%)	
			MBPT	MCDHF/RCI2	NIST	MBPT&MCDHF/RCI2	MBPT&NIST
28	$2s^2 2p^3 \ ^2D_{5/2} - 2s^2 2p^3 \ ^2D_{3/2}$	M1	1.670E+00	1.675E+00	1.660E+00	0.3	-1
28	$2s^2 2p^3 \ ^2P_{1/2} - 2s^2 2p^3 \ ^4S_{3/2}$	M1	2.005E-01	2.003E-01	2.100E-01	-0.1	5
28	$2s^2 2p^3 \ ^2P_{1/2} - 2s^2 2p^3 \ ^2D_{3/2}$	M1	2.166E-01	2.177E-01	2.186E-01	0.5	1
28	$2s^2 2p^3 \ ^2P_{1/2} - 2s^2 2p^3 \ ^2D_{3/2}$	E2	2.350E-03	2.360E-03	2.400E-03	0.4	2
28	$2s^2 2p^3 \ ^2P_{1/2} - 2s^2 2p^3 \ ^2D_{5/2}$	E2	2.231E-03	...	2.200E-03	...	-1
28	$2s^2 2p^3 \ ^2P_{3/2} - 2s^2 2p^3 \ ^4S_{3/2}$	M1	1.074E-01	1.080E-01	1.100E-01	0.6	2
28	$2s^2 2p^3 \ ^2P_{3/2} - 2s^2 2p^3 \ ^2D_{3/2}$	M1	1.215E+00	1.216E+00	1.200E+00	0.1	-1
28	$2s^2 2p^3 \ ^2P_{3/2} - 2s^2 2p^3 \ ^2D_{5/2}$	M1	6.155E-01	6.174E-01	6.400E-01	0.3	4
28	$2s^2 2p^3 \ ^2P_{3/2} - 2s^2 2p^3 \ ^2D_{5/2}$	E2	5.186E-03	5.209E-03	5.200E-03	0.5	0
28	$2s^2 2p^3 \ ^2P_{3/2} - 2s^2 2p^3 \ ^2P_{1/2}$	M1	9.069E-01	9.092E-01	9.120E-01	0.3	1
28	$2p^5 \ ^2P_{1/2} - 2p^5 \ ^2P_{3/2}$	M1	1.321E+00	1.327E+00	1.300E+00	0.5	-2
28	$2p^5 \ ^2P_{1/2} - 2p^5 \ ^2P_{3/2}$	E2	1.804E-03	1.814E-03	1.900E-03	0.5	5



Z